

Proteome signature of breast cancer cells treated with fucoidan



UNIVERSITY *of the*
WESTERN CAPE
UNIVERSITY of the
WESTERN CAPE

Fatima Janodien

Student number: 2838093

A thesis submitted in partial fulfilment of the requirements for the degree of Magister Scientiae in the Department of Biotechnology, University of the Western Cape.

Supervisors: Dr. Rolene Bauer and Prof. Mervin Meyer

2016

Declaration

I, Fatima Janodien, hereby declare that the study: “Proteome signature of breast cancer cells treated with fucoidan” is my own work, that it has not been submitted for any degree or examination in any other University, and that all the sources I have used or quoted have been indicated and acknowledged by complete references.

Full name: Fatima Janodien

Date: 21 January 2016



Signed:



Acknowledgements

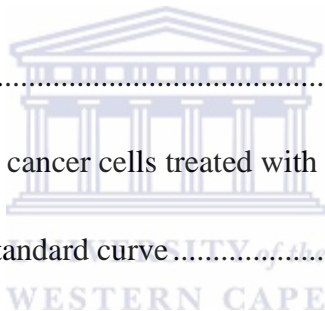
I would like to thank the National Research Foundation for funding this study.



Table of Contents

Declaration.....	ii
Acknowledgements.....	iii
List of abbreviations	vii
List of figures.....	xi
List of tables.....	xiii
Chapter 1.....	1
1.1 Abstract.....	1
1.2 General introduction.....	2
1.3 Aims and objectives	2
Chapter 2.....	4
Potential of proteomics in analysing the action of fucoidan in breast cancer.....	4
2.1 Breast cancer	4
2.2 Cancer treatments.....	6
2.3 Natural products as sources of anticancer drugs	6
2.3.1 Bioactive compounds	6
2.3.2 Bioactive compounds of marine origin	7
2.3.3 Fucoidan mode of action	8
2.3.4 Fucoidan structure and bioactivity	11
2.4 Proteomics approach to study cellular processes.....	21
2.4.1 Quantitative proteomic profiling	22
2.4.2 Stable isotope labelling of amino acids in cell culture	24

2.4.3 Limitations.....	25
References.....	30
Chapter 3.....	42
Investigating proteome changes in breast cancer cells in response to fucoidan	42
3.1 Introduction.....	42
3.2 Materials and methods	43
3.2.1 Mammalian cell culture.....	43
3.2.2 SDS-PAGE and immunoblotting.....	46
3.2.3 SILAC culture.....	48
3.3 Results.....	55
3.3.1 Dose response of breast cancer cells treated with fucoidan	55
3.3.2 Protein quantification standard curve.....	56
3.3.3 Western blot analysis of MCF7 protein extracts	57
3.3.4 SILAC protein quality and equal loading analysis	60
3.3.5 SILAC mass spectrometry analysis.....	61
3.4 Discussion	68
3.4.1 MCF7 cell viability in response to fucoidan treatment	68
3.4.2 Western blot analysis.....	69
3.4.3 SILAC mass spectrometry analysis.....	74
3.5 Conclusion.....	76
References.....	77



Appendix 1.....	86
Materials and suppliers	86
Appendix 2.....	92
Results.....	92



List of abbreviations

°C	degrees celsius
µg/ml	micrograms per millilitre
µm	micrometre
1D SDS-PAGE	one dimensional sodium dodecyl sulfate-polyacrylamide electrophoresis
2D SDS-PAGE	two dimensional sodium dodecyl sulfate-polyacrylamide electrophoresis
A	ampère
ACN	acetonitrile
approx.	approximately
APS	ammonium persulfate
ATCC	American Type Culture Collection
BCA	bicinchoninic acid
BIR	baculoviral IAP repeat
BSA	bovine serum albumin
CPGR	Centre for Proteomic and Genomic Research
DAVID	Database for Visualization and Integrated Discovery
ddH ₂ O	double distilled water
DMEM	Dulbecco's Modified Eagle Medium

DMSO	dimethyl sulfoxide
DNA	deoxyribose nucleic acid
DTT	dithiothreitol
ERK	extracellular signal-regulated
ESI	electrospray ionization
FA	formic acid
FBS	fetal bovine serum
FDR	false discovery rate
<i>g</i>	gravitational acceleration
GO	gene ontology
GSK	glycogen synthase kinase β
h	hour
HCl	hydrochloric acid
HEPES	hydroxyethyl piperazineethanesulfonic acid
HRP	horseradish peroxidase
IAP	inhibitor of apoptosis
IC ₅₀	median inhibition concentration
iCAT	isotope-coded affinity tag
iTRAQ	isobaric tags for relative and absolute quantitation

kDa	kilodaltons
kV	kilovolt
LC-MS	liquid chromatography-mass spectrometry
LC-MS/MS	liquid chromatography-tandem mass spectrometry
<i>m/z</i>	mass/charge
MALDI	matrix-assisted laser desorption/ionization
MAPK	mitogen-activated protein kinase
MCF7	Michigan Cancer Foundation 7 (breast cancer cell line)
mg/ml	milligrams per millilitre
mm	millimetres
MS	mass spectrometry
NAC	N-acetyl-L-cysteine
NADH	nicotinamide adenine dinucleotide (NAD) + hydrogen
nano-HPLC	nano-high-performance liquid chromatography
NCBI	National Center for Biotechnology Information
NMR	nuclear magnetic resonance
PARP	poly(ADP-ribose) polymerase
PBS	phosphate buffered saline
PKB/Akt	protein kinase B/Akt

PSM	peptide spectrum match
PVDF	polyvinylidene difluoride
RIPA	radio immuno precipitation assay
RNA	ribose nucleic acid
ROS	reactive oxygen species
rpm	revolutions per minute
SD	standard deviation
SDS	sodium dodecyl sulfate
SILAC	stable isotope labelling of amino acids in cell culture
STRING	Search Tool for the Retrieval of Interacting Genes
TBS	Tris-buffered saline
TBS-T	Tris-buffered saline-Tween
TEMED	N,N,N',N'-Tetramethylethylenediamine
Trypsin/EDTA	trypsin/ethylenediaminetetraacetic acid
UV	ultra violet
V	volts
VEGF	vascular endothelial growth factor
WST-1	water-soluble tetrazolium salt-1
XIAP	X-linked inhibitor of apoptosis

List of figures

Figure 1: Percentages of incidence and mortality rate of breast cancer in females (Ferlay <i>et al.</i> , 2012).	5
Figure 2: Fucoidan structure depicting repeating disaccharides in extracts from <i>Ascophyllum nodosum</i> and <i>Fucus vesiculosus</i> (Chevolot <i>et al.</i> , 2001).	12
Figure 3: Fucoidan structures found in brown seaweeds. The homofucose backbone chains exist as I) (1→3)-linked α-L-fucopyranose residue repeats, or II) alternating (1→3)- and (1→4)-linked α-L- fucopyranose residues (Cumashi <i>et al.</i> , 2007).	12
Figure 4: Multiple proteomic techniques utilized to determine the proteomics of cancer development in a human fibroblast cell line (Pütz <i>et al.</i> , 2012). (A) Malignant transformation of a primary human fibroblast cell line by successive transduction with retroviral vectors. (B) 2D-PAGE workflow. (C) iTRAQ workflow. (D) SILAC workflow.....	23
Figure 5: Classical SILAC workflow illustrating culture of cells in light (left) and heavy (right) SILAC media and label incorporation over time (Ong, 2012). Label incorporation is followed by cell lysis, protein extraction, tryptic digestion and 1:1 mixing of light and heavy extractions for mass spectrometry analysis.....	25
Figure 6: Characteristics of instrumentation and the related influences on proteome coverage (de Godoy <i>et al.</i> , 2006).	27
Figure 7: Percentage viability of MCF7 breast cancer cells after treatment with fucoidan.	55
Figure 8: Standard curve of BSA standards for BCA protein quantification assay.	56
Figure 9: Coomassie-stained 1D SDS-PAGE acrylamide gel of total lysates produced from MCF7 cells. Twenty µg of protein was loaded per sample. Lanes M: molecular weight marker; Lanes 1-6: untreated cells; Lane 7: empty; Lanes 8-13: fucoidan treated cells.	57
Figure 10: Effect of fucoidan on XIAP expression in MCF7 breast cancer cells over 48h of exposure to fucoidan. (A) Western blot image. Lanes 1-6: untreated cells; Lane 7: empty; Lanes 8-13: fucoidan treated cells. (B) Densitometric analysis of the relative density (fold change) of the signal intensities.	58

Figure 11: Effect of fucoidan on ERK1/2 expression in MCF7 breast cancer cells over 48h exposure to fucoidan. (A) Western blot image. Lanes 1-6: untreated cells; Lane 7: empty; Lanes 8-13: fucoidan treated cells. (B) Densitometric analysis of the relative density (fold changes) of the signal intensities..... 59

Figure 12: Coomassie-stained 1D SDS-PAGE gels of (A) light and (B) heavy SILAC labelled protein extractions from MCF7 cells. Twenty µg of protein was loaded per lane. Lane M: molecular weight marker; Lanes 1-4: untreated samples; Lane 5, empty lane; Lanes 6-9, fucoidan treated samples. 60

Figure 13: Actin Western blot analysis to investigate equal loading and accuracy of protein quantification. (A) Light-labelled SILAC proteins samples. (B) Heavy-labelled SILAC proteins samples. Lanes 1-4, untreated samples; lane 5, empty; lanes 6-9, fucoidan treated samples. 61

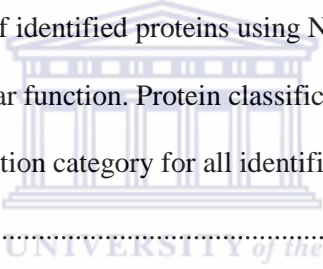
Figure 14: Functional classification of identified proteins using NCBI annotations based on universal Gene Ontology terms for molecular function. Protein classification is shown as percentage proteins expressed for each molecular function category for all identified proteins (adapted from Scaffold).

..... 62

Figure 15: Functional classification of identified proteins using NCBI annotations based on universal Gene Ontology terms for biological process. Protein classification is shown as percentage proteins expressed for each biological process category for all identified proteins (adapted from Scaffold).
..... 62

Figure 16: Functional classification of identified proteins using NCBI annotations based on universal Gene Ontology terms for cell component. Protein classification is shown as percentage proteins expressed for each cellular component category for all identified proteins (adapted from Scaffold).
..... 63

Figure 17: STRING analysis revealed 19 proteins (shown in red) associated with cell death (adapted from STRING)..... 65

Figure A1: STRING analysis revealed 6 proteins (shown in red) associated with cell cycle arrest in up-regulated proteins (adapted from STRING). 111

Figure A2: STRING analysis revealed 5 proteins (shown in red) associated with proteasomal degradation in up-regulated proteins (adapted from STRING).	112
Figure A3: STRING analysis revealed 9 proteins (shown in red) associated with cellular catabolic process in up-regulated proteins (adapted from STRING).	113
Figure A4: STRING analysis revealed 4 proteins (shown in red) associated with the intrinsic apoptotic pathway in down-regulated proteins (adapted from STRING).....	114

List of tables

Table 1: Female breast cancer incidence in South Africa (Vorobiof <i>et al.</i> , 2001).....	5
Table 2: Anticancer effect of fucoidan from in vitro and in vivo studies on various cancers.	15
Table 3: Stock solutions used for preparing SDS-PAGE gels.	46
Table 4: SILAC light and heavy treatments and repeats.....	50
Table 5: SILAC protein extraction mixtures loaded onto SDS-PAGE gel for pair-wise comparisons by mass spectrometry.....	51
Table 6: Parameters for mass spectrometry data acquisition.....	52
Table 7: Absorbance values of BSA standards.....	56
Table 8: Absorbance values for protein samples.	57
Table 9: Protein concentrations calculated from standard curve and absorbance values.	57
Table 10: Functions of 19 cell death-associated proteins.	66
Table A1: Materials and suppliers.	86
Table A2: Antibodies used for Western blot analysis.....	88
Table A3: Media constituents used for stable isotope labelling of amino acids in cell culture (SILAC).	89
Table A4: Solutions and recipes used in the study.	89
Table A5: Differentially regulated proteins and corresponding trends.....	92

Chapter 1

1.1 Abstract

Breast cancer is responsible for a large portion of cancer-related deaths. Worldwide, incidence is increasing. Routinely-used treatments for breast cancer are invasive and are associated with a range of side-effects which may affect quality of life. Fucoidan, a marine bioactive compound, found primarily in brown seaweed, has various medicinal qualities. Among its bioactivities studied, it has potent anticancer activity. Despite numerous studies, the mechanism of action of fucoidan on cancer cells remains unclear. This project aims to shed light on the mechanism of action of fucoidan by studying its effect on the MCF7 breast cancer cell proteome. The IC_{50} obtained for fucoidan treated MCF7 cells was 0.2 mg/ml. Decrease in expression of XIAP and phosphorylation of ERK1/2 was observed, indicating a decrease in inhibition of apoptosis and increased sensitivity to apoptosis, respectively. Literature reports activation of several caspases, including caspase-3, in various cell lines after to fucoidan treatment. Taken together, with data from the current study it can be said that fucoidan treatment led to cell death by apoptosis. SILAC analysis identified over 2000 proteins with more than 1700 at 95% confidence. STRING analysis of enriched proteins revealed 19 cell death related proteins. However, SILAC results were ambiguous with regards to differential protein regulation and should be repeated with lower electrospray ionization flow rates, pairwise and single sample runs, and validation with Western blot analysis of various apoptosis related proteins and biochemical assays.

1.2 General introduction

Conventional chemotherapy and radiotherapy have numerous adverse side effects and indiscriminately cause cell death i.e. these treatments kill both cancerous and non-cancerous cells. This demonstrates the need for the development of anti-cancer drugs or treatments which potentially only target cancerous cells. Fucoïdan, a sulfated polysaccharide found mainly in brown algae has various biological activities including anti-inflammatory, anti-bacterial, anti-viral and anti-cancer properties (Xue *et al.*, 2012). The effect of fucoïdan has been tested *in vitro* and *in vivo* in various cancerous cell lines (Fukahori *et al.*, 2008). It has been found that fucoïdan induces programmed cell death, or apoptosis, in cancerous cells, while having very little or no effect on the non-cancerous lines.

Several studies have been conducted on the effect of fucoïdan on the MCF7 breast cancer cell line and fucoïdan was shown to stimulate apoptosis (Yamasaki-Miyamoto *et al.*, 2009; Zhang *et al.*, 2011; Zhang *et al.*, 2013). A study of global protein expression in MCF7 breast cancer cells treated with fucoïdan may assist in elucidating the pathways and proteins involved in apoptotic cell death. Chapter 2 reviews the anti-cancer effect of fucoïdan and the potential of proteomics in elucidating its mode of action against breast cancer cells. Chapter 3 covers the research performed in this study including the methodology, results, discussion and concluding remarks. Materials used and suppliers are listed in the Appendix.

1.3 Aims and objectives

This study aimed to conduct a global proteome analysis of MCF7 breast cancer cells to examine total protein expression in response to fucoïdan treatment (Chapter 3). Objectives included the (i) determination of the IC₅₀ of fucoïdan for MCF7 breast cancer cells, (ii) Western blot analysis of proteins related to apoptosis, (iii) establishment of light and heavy SILAC-labelled cell

populations of MCF7 cells, and (iv) evaluation of differential protein expression between untreated and treated samples.



Chapter 2

Potential of proteomics in analysing the action of fucoidan in breast cancer

2.1 Breast cancer

Cancer is one of the leading causes of death worldwide with breast cancer having accounted for approximately 521 000 of 8.2 million cancer-related deaths in the year 2012 alone (Ferlay *et al.*, 2013). Percentage incidence and mortality in females are summarized in Figure 1. Breast cancer is the leading cancer among South African women (Schlebusch *et al.*, 2010; Buccimazza, 2015). Findings of a comprehensive study of medical records from 1970 to 1997 in different hospitals in South Africa on breast cancer incidence in South African females are shown in Table 1 (Vorobiof *et al.*, 2001). Roughly half of breast cancer patients have presented at stages I and II, while the rest have presented with more advanced stages III and IV. It has also been estimated that in developed countries about half of the patients diagnosed at stages I and II have a 90% chance of a 5-year survival, whereas developing countries presented lower survival rates. Similar findings were reviewed by Jemal *et al.* (2010) and Unger-Saldaña (2014).

Globally, breast cancer incidence is increasing (Ferlay *et al.*, 2013). Developing countries, however, report higher occurrence of diagnosis in later stages of breast cancer (Unger-Saldaña, 2014). Variability in incidence among different ethnicities has been reported. Vorobiof *et al.* (2001) observed higher incidence in white and Asian females, while black and coloured females more often presented at advanced stages of breast cancer. Socio-economic factors certainly play a role, however, the reasons for variability in incidence amongst difference ethnicities remains largely unexplained (Matatiele & Van den Heever, 2008). Age and sex have been identified as highest risk factors (DeSantis *et al.*, 2013). While reported in males, breast cancer affects mainly women of around pre- and post-menopausal age.

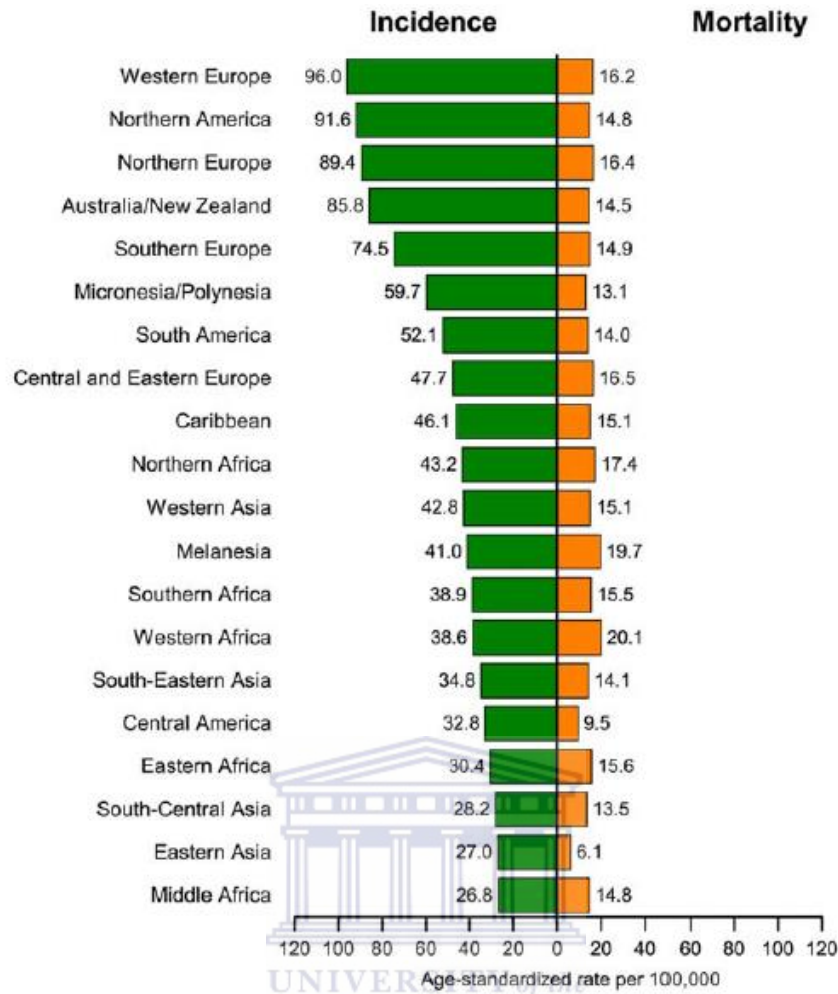


Figure 1: Percentages of incidence and mortality rate of breast cancer in females (Ferlay *et al.*, 2012).

Table 1: Female breast cancer incidence in South Africa (Vorobiof *et al.*, 2001).

	No.	%	Crude	ASIR	Cumulative	Risk
					Risk	
Asian Females	135	24.4	33.2	42.1	4.7	21
Black Females	922	13.4	7.11	11.3	1.2	81
Coloured Females	140	18.2	10.2	14.7	1.6	63
White Females	1733	17.8	85.8	70.2	7.5	13
	3785	16.5	18.5	25.1	2.8	36

Abbreviations: ASIR, age-standardized incidence rate

2.2 Cancer treatments

Most common treatments for breast cancer involve surgical removal of tumours followed by chemotherapy, radiotherapy or endocrine therapy (Eiermann *et al.*, 2001). All treatments are associated with side-effects and health risks which negatively affect quality of life. Chemotherapeutic drugs and radiotherapy are both associated with systemic toxicities which may present as mild to severe (Remesh, 2012; Jagsi, 2014). While side-effects linked to hormonal treatment are generally considered mild, endocrine therapy has been associated with recurrent tumours at different sites, particularly cancers of the uterus or endometrium (Swerdlow & Jones, 2005; Thürlimann *et al.*, 2005; Jones *et al.*, 2012). The development of resistance to hormonal treatment is of concern, in particular patients with estrogen and progesterone receptor positive breast cancers (Sutherland, 2011). Furthermore, non-compliance with administration of hormonal drugs results in poor prognosis (Kemp *et al.*, 2014).

Adverse side-effects caused by current anticancer treatments are a wide-spread concern (Senthilkumar *et al.*, 2013; Moghadamtousi *et al.*, 2014). The discovery of alternative sources for anticancer drugs and chemotherapeutics as well as the development of new methods for cancer treatment are being explored. Increasing interest has been shown in using natural products and bioactive compounds from medicinal plants (Boopathy & Kathiresan, 2010; Moghadamtousi *et al.*, 2014).

2.3 Natural products as sources of anticancer drugs

2.3.1 Bioactive compounds

Bioactive compounds are produced by many organisms including plants, animals and bacteria. These compounds may be produced to stave off predation and infection, and as secondary

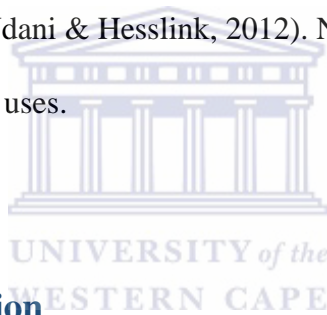
metabolites (Donia & Hamann, 2003). Bioactive compounds may be categorized into different groups, depending on the composition or structure of the compound, such as alkaloids, carbohydrates, peptides, polyketides, terpenes and phenolics (Mayer *et al.*, 2011). Many antibiotics, anticancer drugs, anti-fungal agents and anti-bacterials have been developed from natural sources (Haefner, 2003; Lam, 2007) and drugs derived from natural plant products and their derivatives account for more than 50% of all drugs currently in clinical use (Boopathy & Kathiresan, 2010). Commercially available examples with anticancer activity include doxorubicin (amrubicin hydrochloride), taxol (paclitaxel) and estradiol (fulvestrant) (Lam, 2007).

2.3.2 Bioactive compounds of marine origin

Research involving marine bioactive compounds has become increasingly widespread (Laurienzo, 2010; Vishchuk *et al.*, 2011; Moghadamtousi *et al.*, 2014) due to the discovery of novel marine sources and their compounds having potent bioactivity, showing potential to pioneer new medical treatments (Haefner, 2003). As a large percentage of the world's surface is covered by water with an abundance of diverse marine organisms, marine environments are favourable as a source of bioactive compounds (Wijesekara *et al.*, 2011). Marine bioactive compounds described in literature are largely secondary metabolites (Dixon, 2001; Manilal *et al.*, 2010; Morya *et al.*, 2012). These include polyphenolic compounds, alkaloids and polysaccharides (Boopathy & Kathiresan, 2010). Commercially available anticancer drugs sourced from marine environments are Yondelis, Halaven and Cytosar-U in soft tissue sarcoma, metastatic breast cancer and myeloid leukaemia, respectively (Martins *et al.*, 2014).

Interest in bioactive compounds from seaweeds is gaining momentum due to a range of potent bioactivities such as antibiotic, antiviral, anti-inflammatory, antioxidant, anti-coagulant and

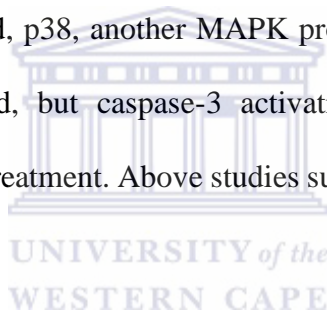
anti-tumour (Kusaykin *et al.*, 2006; Cumashi *et al.*, 2007; Boopathy & Kathiresan, 2010; Boo *et al.*, 2013). Algal bioactives are produced as secondary metabolites and do not appear to play a direct role in growth and development of the organism (Dixon, 2001; Morya *et al.*, 2012). Numerous biologically active compounds from macroalgae have been extracted and studied. Red (Rhodophyceae), green (Chlorophyceae) and brown (Phaeophyceae) seaweeds are respectively known for the production of carrageenans, ulvans and fucans (Patel, 2012). The most prevalent bioactive polysaccharides in algae are the sulfated polysaccharides (Boopathy & Kathiresan, 2010). These are found in abundance in the cell walls of algae (Ale *et al.*, 2011a) and are thought to function through the augmentation of the immune system (Donia & Hamann, 2003). Sulfated polysaccharides are used as food additives, gelling agents (Rupérez *et al.*, 2002) and dietary supplements (Udani & Hesslink, 2012). Numerous studies have reported on its potential for diverse medicinal uses.



2.3.3 Fucoidan mode of action

Fucoidan is a complex sulfated polysaccharide found predominantly in brown macroalgae (Li *et al.*, 2008; Morya *et al.*, 2012). Numerous studies have shown that fucoidan has potent bioactive properties such as antiviral, antibacterial, anti-inflammatory and anticancer activities (Zhang *et al.*, 2011; Morya *et al.*, 2012). Promising findings have been reported by Xue *et al.* (2012) who studied the effect of fucoidan on animal breast cancer cells. Fucoidan was shown to induce apoptosis and inhibit cell growth *in vitro*. *In vivo*, angiogenesis and growth of tumour tissue were inhibited and lung metastasis was suppressed. Fucoidan bioactivities in different cell lines are summarised in Table 2 (Section 2.3.4, page 15). Numerous studies have shown that fucoidan treatment may decrease the expression of key proteins and markers in cancers (Aisa *et al.*, 2005; Hyun *et al.*, 2009; Kim *et al.*, 2010; Xue *et al.*, 2012).

In a study on human lymphoma HS-Sultan cells, Aisa *et al.* (2005) have determined that fucoidan stimulated caspase-dependent apoptosis. Western blot analysis of extracellular stimuli-responsive proteins involved in intracellular signalling pathways was performed. Targeted proteins were extracellular signal-regulated (ERK), glycogen synthase kinase (GSK), protein kinase B (PKB/Akt) and 38-kD mammalian mitogen-activated protein kinase (MAPK) homologous to HOG-1 (p38). Results showed decreased phosphorylation of ERK and GSK, but not of Akt or p38. Dephosphorylation of ERK (deactivation) and GSK (activation) have been described as being linked to induction of apoptosis (Song *et al.*, 2002). The unaltered state of phosphorylation of Akt, an upstream regulator of GSK phosphorylation, revealed that GSK dephosphorylation must have been regulated by another protein in this regard (Aisa *et al.*, 2005). Though ERK was affected, p38, another MAPK protein, was not. It is unclear which apoptotic pathway was involved, but caspase-3 activation was confirmed induction of apoptosis as a result of fucoidan treatment. Above studies suggest that treatment with fucoidan results in apoptosis.



Hyun *et al.* (2009) observed growth inhibition of HCT-15 human colon carcinoma cells when treated with fucoidan. Investigation of mechanism of apoptosis induction was conducted by Western blot analysis. In contrast to the results of previous studies, apoptosis was accompanied by increased phosphorylation of MAPK proteins, ERK and p38 over time. Phosphorylation of Akt was highest at 12 hours (h) but progressively decreased thereafter. Expression of anti-apoptosis protein Bcl-2 decreased over time, while expression of proteins indicative of pro-apoptosis (Bax) and DNA repair protein poly(ADP-ribose) polymerase (PARP) was evident after 12h. Caspase-9 and caspase-3 were activated as a result of fucoidan treatment signifying activation of apoptosis. Fucoidan response has been studied in HT-29 and HCT116 human colon cancer cells (Kim *et al.*, 2010). Western blot analysis revealed an increase in DNA repair protein (PARP) cleavage with increasing fucoidan dose, an indication of apoptosis.

Furthermore, cleavage of caspases-8, -9, -7 and -3 increased, while inhibitors of the apoptosis protein family (XIAP and survivin) decreased with increasing fucoidan concentration. Analysis of mitochondrial proteins has shown an increase in cytoplasmic cytochrome C, Smac/Diablo, pro-apoptotic Bak and truncated Bid in HT-29 cells. Release of cytochrome C and Smac/Diablo from the mitochondria are signs of mitochondrial stress and consequently lead to apoptosis induction. Bak and t-Bid facilitate release of cytochrome C by increasing the mitochondrial membrane permeabilization. Death receptor analysis has shown increases in death receptors (Fas and DR5) and a death receptor ligand (TRAIL). The studies of Hyun *et al.* (2009) and Kim *et al.* (2010) are both indicative of apoptosis induction via both intrinsic and extrinsic apoptotic pathways. Xue *et al.* (2012) have investigated the effect of fucoidan on 4T1 mouse breast cancer cell lines. Expression of anti-apoptotic proteins Bcl-2 and survivin decreased due to fucoidan treatment as well as ERK and vascular endothelial growth factor (VEGF) (Xue *et al.*, 2012). Mitochondrial cytochrome c decreased while cytosolic cytochrome c increased, indicative of mitochondrial membrane permeability and the initial stages of apoptotic induction via a mitochondrial pathway. Additionally, cleaved caspase-3 increased indicating apoptosis induction.

Fucoidan was recently shown to enhance the anticancer activity of commonly used anticancer drugs such as cisplatin, tamoxifen and paclitaxel *in vitro* in MCF7 and MDA-MB-231 breast cancer cell lines (Zhang *et al.*, 2013). The combination of fucoidan with anticancer drugs resulted in increased cytotoxicity, induction of apoptosis and cell cycle arrest as well as decreased expression of anti-apoptotic proteins, Bcl-xl and Mcl-1. Although fucoidan has potent apoptotic or growth inhibitory effects on cancerous cells, it exhibited no effect on non-cancerous cells, including L929 non-cancerous mouse fibroblasts (Xue *et al.*, 2012), MCF10A non-cancerous human mammary epithelial cells (Zhang *et al.*, 2011) and Hs. 677.st. stomach fibroblasts (Kawamoto *et al.*, 2006). Low toxicity are an ideal characteristic for the

development of a new anti-cancer drug or treatment (Queiroz *et al.*, 2006; Xue *et al.*, 2012) and has encouraged studies to elucidate the structure of fucoidan and its mechanism of action.

2.3.4 Fucoidan structure and bioactivity

Although present in marine invertebrates, fucoidan has mainly been isolated from brown macroalgae. The compound is present in cell walls and also extracellular matrix of algae (Li *et al.*, 2008; Ale *et al.*, 2011a). Various brown algae have been studied for fucoidan content in an attempt to clarify the structure and chemical composition (Li *et al.*, 2008). Fucoidan is largely composed of L-fucose and sulfates. Other constituents may be a combination of a variety monosaccharides such as galactose, mannose, xylose (Li *et al.*, 2008), glucuronic acid (Lee *et al.*, 2006) and protein, lending to structural complexity (Morya *et al.*, 2012). The complex, heterogenous and branched nature of fucoidan has made it challenging to elucidate its structure, albeit limited success has been achieved with purified fucoidan of low molecular weight (Chevolot *et al.*, 2001). Chevolot *et al.*, (2001) explored purified low molecular weight fucoidan from *Ascophyllum nodosum* and *Fucus vesiculosus* and found through nuclear magnetic resonance (NMR) spectroscopy the compounds consisted of similar repeating disaccharide units (Figure 2). Fucoidan structure is composed of a homofucose backbone consisting of (1-3) or (1-4) linked α -L-fucopyranose residues (Figure 3) (Cumashi *et al.*, 2007). Fucopyranose residues have been reported to be substituted with 4-sulfate groups (Jiao *et al.*, 2011). The polysaccharide exists mainly as F-fucoidan and U-fucoidan. F-fucoidan represents most fucoidans extracted from seaweeds and consists predominantly of sulfated esters of L-fucose (Morya *et al.*, 2012). U-fucoidan consists roughly of 20% glucuronic acid. Both forms may contain other sugars and even proteins, which make up less than 10% of the compound, while sulfated fucan remains the distinctive feature.

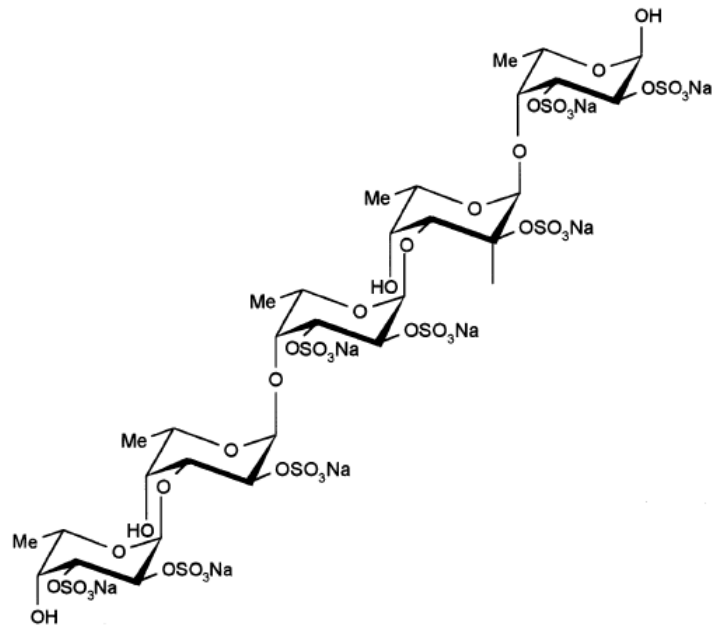


Figure 2: Fucoidan structure depicting repeating disaccharides in extracts from *Ascophyllum nodosum* and *Fucus vesiculosus* (Chevolot *et al.*, 2001).

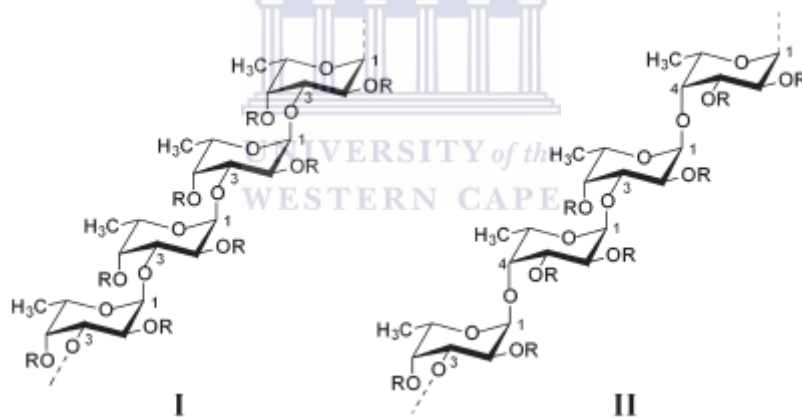


Figure 3: Fucoidan structures found in brown seaweeds. The homofucose backbone chains exist as I) (1→3)-linked α -L-fucopyranose residue repeats, or II) alternating (1→3)- and (1→4)-linked α -L-fucopyranose residues (Cumashi *et al.*, 2007).

Bioactivity of fucoidan is largely governed by structure (Li *et al.*, 2008). Structure is dependent on the source of fucoidan (Queiroz *et al.*, 2006; Cumashi *et al.*, 2007; Ale *et al.*, 2011b). Variables include algal species, climate, and age of the organism at the time of extraction (Skriptsova *et al.*, 2010; Duarte *et al.*, 2001). It has also been found that the method of extraction of fucoidan from seaweeds could influence its structure and therefore its

functionality (Morya *et al.*, 2012). Structural features attributing to bioactivity are degree of sulfation, monosaccharide composition, charge density, purity of fucoidan extract and molecular size (Ale *et al.*, 2011a; Cumashi *et al.*, 2007; Cho *et al.*, 2011). Low molecular weight fucoidan has been reported to display significantly enhanced anticancer activity, endothelial cell migration and anticoagulant efficiency (Morya *et al.*, 2012).

Choi *et al.* (2009) investigated the effect of gamma irradiation on the molecular weight and anti-oxidant activity of seaweed polysaccharides, fucoidan and laminarin. As the gamma irradiation dose increased, the molecular weight decreased and antioxidant activity increased. In a similar study, Choi and Kim (2013) employed gamma irradiation at different doses to obtain low molecular weight fucoidan - each dose resulting in a different molecular weight - and examine the anticancer effect on different cancerous cell lines. It was shown that lower molecular weight fucoidan had increased cytotoxic activity and reduced cell transformation activity. While the reason behind enhanced *in vitro* anticancer activity with smaller sized fucoidan molecules remains to be elucidated (Cho *et al.*, 2011), an explanation for increased activity due to oversulfation may be linked to charge density facilitating association with the cell's surface (Ale *et al.*, 2011c).

Fucoidan has demonstrated anticancer activity against numerous cancerous cell lines *in vitro* and *in vivo* studies. Table 2 presents a summary of these studies. A crude extract of fucoidan from *Fucus vesiculosus* is available commercially and has been widely used in assessing anticancer activity. Cell lines originating from several tissues including stomach (Kawamoto *et al.*, 2006), lung (Ale *et al.*, 2011b; Lee *et al.*, 2012), colon (Hyun *et al.*, 2009; Kim *et al.*, 2010), liver (Hayakawa & Nagamine, 2009), cervix (Zhang *et al.*, 2011) and kidney (Fukahori *et al.*, 2008) were studied. Fucoidan with different structures may have differential inhibitory effects on cell proliferation of various cancers (Cumashi *et al.*, 2007). Different types of cancer cells have distinctive molecular and metabolic characteristics. The effect of fucoidan may

therefore also differ slightly depending on the cell and cancer type. This has been demonstrated by reports on fucoidan displaying varying degrees of bioactivity on various cancers using fucoidan from the same source (Fukahori *et al.*, 2008; Kim *et al.*, 2010). This has been noted on different and similar cancer cell types.



Table 2: Anticancer effect of fucoidan from in vitro and in vivo studies on various cancers.

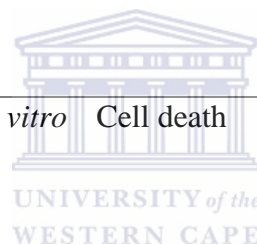
Cell line	Type of cell / tissue	Type of cancer	Type of study	Effect of fucoidan treatment	Source of fucoidan	Ref.
HS-Sultan	B lymphocyte	Burkitt's lymphoma	<i>in vitro</i>	Growth inhibition / apoptosis	Commercial (Sigma-Aldrich) <i>Fucus vesiculosus</i>	Aisa <i>et al.</i> , 2005
KMC-1	Bile duct	Carcinoma	<i>in vitro</i>	Growth inhibition	<i>Cladosiphon okamuranus tokida</i>	Fukahori <i>et al.</i> , 2008
MCF7	Breast	Invasive ductal carcinoma	<i>in vitro</i>	Growth inhibition, apoptosis	<i>Cladosiphon navae-caledoniae</i> , <i>Undaria pinnatifida</i> , Commercial (Sigma-Aldrich) <i>Fucus vesiculosus</i>	Banafa <i>et al.</i> , 2013, Mak <i>et al.</i> , 2014, Yamasaki-Miyamoto <i>et al.</i> , 2009, Zhang <i>et al.</i> , 2011, Zhang <i>et al.</i> , 2013
MDA-MB-231	Breast	Invasive ductal carcinoma	<i>in vitro</i>	Growth inhibition	<i>Cladosiphon navae-caledoniae</i> , Commercial (Sigma-Aldrich) <i>Fucus vesiculosus</i>	Banafa <i>et al.</i> , 2014, Zhang <i>et al.</i> , 2011, Zhang <i>et al.</i> , 2013
T-47D	Breast	Ductal carcinoma	<i>in vitro</i>	Growth inhibition	<i>Saccharina japonica</i> , <i>Undaria pinnatifida</i>	Vishchuk <i>et al.</i> , 2011

4T1	Breast (mouse)	Carcinoma	<i>in vitro</i> & <i>in vivo</i>	Apoptosis	Commercial (Sigma-Aldrich) <i>Fucus vesiculosus</i>	Xue <i>et al.</i> , 2012
HeLa	Cervix	Uterine carcinoma	<i>in vitro</i>	Angiogenic activity & growth inhibition	<i>Cladosiphon novae-caledoniae</i>	Zhang <i>et al.</i> , 2011
HT-29	Colon	Adenocarcinoma	<i>in vitro</i>	Apoptosis	Commercial (Sigma-Aldrich) <i>Fucus vesiculosus</i>	Kim <i>et al.</i> , 2010
HCT116	Colon	Carcinoma	<i>in vitro</i>	Apoptosis	Commercial (Sigma-Aldrich) <i>Fucus vesiculosus</i>	Kim <i>et al.</i> , 2010
HCT-15	Colon	Duke's type C, adenocarcinoma	<i>in vitro</i>	Growth inhibition & Apoptosis	Commercial (Sigma-Aldrich) <i>Fucus vesiculosus</i>	Hyun <i>et al.</i> , 2009
WiDr	Colon	Adenocarcinoma	<i>in vitro</i>	Growth inhibition	<i>Undaria pinnatifida</i> , Commercial (Sigma-Aldrich) <i>Fucus vesiculosus</i>	Mak <i>et al.</i> , 2014
LoVo	Colon	Adenocarcinoma	<i>in vitro</i>	Growth inhibition	<i>Undaria pinnatifida</i> , Commercial (Sigma-Aldrich) <i>Fucus vesiculosus</i>	Mak <i>et al.</i> , 2014

HT1080	Fibroblast	Fibrosarcoma	<i>in vitro</i>	Invasion & growth inhibition	<i>Cladosiphon novae-caledoniae</i>	Zhang <i>et al.</i> , 2011
KMG-1	Gallbladder	Carcinoma	<i>in vitro</i>	Growth inhibition	<i>Cladosiphon okamuranus tokida</i>	Fukahori <i>et al.</i> , 2008
KURU II	Kidney	Carcinoma	<i>in vitro</i>	Growth inhibition	<i>Cladosiphon okamuranus tokida</i>	Fukahori <i>et al.</i> , 2008
KURM	Kidney	Carcinoma	<i>in vitro</i>	Growth inhibition	<i>Cladosiphon okamuranus tokida</i>	Fukahori <i>et al.</i> , 2008
OSRC2	Kidney	Carcinoma	<i>in vitro</i>	Growth inhibition	<i>Cladosiphon okamuranus tokida</i>	Fukahori <i>et al.</i> , 2008
Huh-6	Liver	Blastoma	<i>in vitro</i>	Growth inhibition	<i>Cladosiphon okamuranus tokida</i>	Fukahori <i>et al.</i> , 2008
KIM-1	Liver	Carcinoma	<i>in vitro</i>	Growth inhibition	<i>Cladosiphon okamuranus tokida</i>	Fukahori <i>et al.</i> , 2008
KYN-1	Liver	Carcinoma	<i>in vitro</i>	Growth inhibition	<i>Cladosiphon okamuranus tokida</i>	Fukahori <i>et al.</i> , 2008
KYN-2	Liver	Carcinoma	<i>in vitro</i>	Growth inhibition	<i>Cladosiphon okamuranus tokida</i>	Fukahori <i>et al.</i> , 2008
KYN-3	Liver	Carcinoma	<i>in vitro</i>	Growth inhibition	<i>Cladosiphon okamuranus tokida</i>	Fukahori <i>et al.</i> , 2008

HAK-1A	Liver	Carcinoma	<i>in vitro</i>	Growth inhibition	<i>Cladosiphon okamuranus tokida</i>	Fukahori <i>et al.</i> , 2008
HAK-1	Liver	Carcinoma	<i>in vitro</i>	Growth inhibition	<i>Cladosiphon okamuranus tokida</i>	Fukahori <i>et al.</i> , 2008
Hca-F	Liver (mouse)	Carcinoma	<i>in vitro</i>	Lymphangiogenesis inhibition and lymphatic metastasis	<i>Undaria pinnatifida</i>	Teng <i>et al.</i> , 2015
SMMC-7721	Liver	Carcinoma	<i>in vitro</i>	Apoptosis	<i>Undaria pinnatifida</i>	Yang <i>et al.</i> , 2013
A549	Lung	Carcinoma	<i>in vitro</i>	Apoptosis	Commercial (Sigma-Aldrich) <i>Fucus vesiculosus</i> , <i>Undaria pinnatifida</i>	Lee <i>et a.</i> , 2012, Mak <i>et al.</i> , 2014
Malme-3M	Lung	Melanoma	<i>in vitro</i>	Growth inhibition	<i>Undaria pinnatifida</i> , Commercial (Sigma-Aldrich) <i>Fucus vesiculosus</i>	Mak <i>et al.</i> , 2014
Lewis lung carcinoma	Lung	Carcinoma	<i>in vitro</i> & <i>in vivo</i>	Growth & metastasis inhibition	<i>Sargassum</i> sp. & Commercial (Sigma-Aldrich) <i>Fucus vesiculosus</i>	Ale <i>et al.</i> , 2011a

Namalwa	Lymphoblastoid	Burkitt's Lymphoma	<i>in vitro</i>	Enhanced efficacy of anticancer drug	<i>Fucus evanescens</i>	Philchenkov <i>et al.</i> , 2007
MT4	Lymphocyte	T-acute leukemia	<i>in vitro</i>	Enhanced efficacy of anticancer drug	<i>Fucus evanescens</i>	Philchenkov <i>et al.</i> , 2007
KOC-5C	Ovarian	Carcinoma	<i>in vitro</i>	Growth inhibition	<i>Cladosiphon okamuranus tokida</i>	Fukahori <i>et al.</i> , 2008
U937	Pleura, pleural effusion, lymphocyte, myeloid	Histiocytic lymphoma	<i>in vitro</i>	Apoptosis	Commercial <i>Fucus vesiculosus</i>	Park <i>et al.</i> , 2013
HL60	Peripheral blood leukocytes	Leukemia	<i>in vitro</i>	Cell death	Commercial (Sigma-Aldrich) <i>Fucus vesiculosus</i>	Queiroz <i>et al.</i> , 2006
PC-3	Prostate	Adenocarcinoma	<i>in vitro</i>	Apoptosis	<i>Undaria pinnatifida</i>	Boo <i>et al.</i> , 2013
SK-MEL-28	Skin	Melanoma	<i>in vitro</i>	Growth inhibition	<i>Saccharina japonica</i> , <i>Undaria pinnatifida</i>	Vishchuk <i>et al.</i> , 2011
MC3	Salivary gland	Mucoepidermoid Carcinoma	<i>in vitro</i>	Growth inhibition & Apoptosis	Commercial (Sigma-Aldrich) <i>Fucus vesiculosus</i>	Lee <i>et al.</i> , 2013
B-16	Skin (mouse)	Melanoma	<i>in vitro</i>	Growth inhibition & Apoptosis	Sargassum sp. & Commercial (Sigma-	Ale <i>et al.</i> , 2011a, Ale <i>et al.</i> , 2011b



					Aldrich) <i>Fucus vesiculosus</i>	
AGS	Stomach	Gastric adenocarcinoma	<i>in vitro</i>	Apoptosis & Autophagy	Commercial (Sigma-Aldrich) <i>Fucus vesiculosus</i>	Park <i>et al.</i> , 2011
MKN45	Stomach	Gastric adenocarcinoma	<i>in vitro</i>	Growth inhibition	<i>Cladosiphon okamuranus</i>	Kawamoto <i>et al.</i> , 2006
T24	Urinary bladder	Transitional cell carcinoma	<i>in vitro</i>	Apoptosis	Commercial (Sigma-Aldrich) <i>Fucus vesiculosus</i>	Park <i>et al.</i> , 2014

All cell lines are of human origin unless stated otherwise



2.4 Proteomics approach to study cellular processes

Proteomics involves the study of the proteome of a cell, tissue or biological sample. It allows for the proteins expressed at a given time for a specific set of biological and environmental conditions to be detected and identified (Ong & Mann, 2005). Initially, proteomics studies were limited to observations of up- and down-regulation as well as the presence and absence of proteins between samples using two-dimensional (2D) gel electrophoresis. Proteomics studies were limited to a sub-proteome level such as organelle proteomes and protein complexes, protein-protein interactions and post translation modifications (de Godoy *et al.*, 2006). Development of mass spectrometry and associated proteomics techniques has enabled more extensive, high throughput quantitative study of proteins (Ong & Mann, 2005). Proteomics research has expanded to include the analysis of whole cell and tissue-protein extractions.

Due to the ever-changing nature of proteomes – constant response to stimuli, protein cleavage and post-translational modifications – there is no strong correlation between the transcriptome and the proteome. The proteome is dynamic while the genome is static (Issaq, 2001). Proteomics may provide a more accurate and comprehensive indication as to the cellular functions carried out at a given time, compared to genomic studies (Wulfschlegel *et al.*, 2002; Grønborg *et al.*, 2006). Proteomics may be used for several applications such as identification of an entire proteome, protein expression profiling, protein network mapping and mapping of post-translational modifications (de Godoy *et al.*, 2006; Chandramouli & Qian, 2009). Quantitative proteomics refer to the study of absolute and relative abundance to view global protein expression. Qualitative proteomics is used to ascertain protein abundance of specific target proteins between samples (Ong & Mann, 2005). Both quantitative and qualitative proteomics may therefore involve the study of the effect of certain treatments on protein expression.

2.4.1 Quantitative proteomic profiling

Of the various techniques available for mass spectrometry based protein quantitation, isotopic labelling has become popular (Ong & Mann, 2005; Pütz *et al.*, 2012). Labelling techniques developed for studying relative protein abundance include isotope-coded affinity tags (iCAT), stable isotope labelling of amino acids in cell culture (SILAC), isobaric tags for relative and absolute quantitation (iTRAQ) (McDonagh *et al.*, 2012) and two-dimensional (2D) gel electrophoresis (Pütz *et al.*, 2012). Two-dimensional (2D) gel electrophoresis, the only gel-based technique, is losing popularity due to limitations in comparison with more recent labelling techniques. Limitations include low resolution and abundant proteins overshadowing less abundant proteins (Ong & Mann, 2005). However with labelling techniques like SILAC 1D SDS-polyacrylamide gel electrophoresis (SDS-PAGE) may still be used to fractionate protein mixtures.

The most popular high-throughput labelling methods are iTRAQ and SILAC because technical variation between samples and the number of mass spectrometry runs are reduced (Pütz *et al.*, 2012). SILAC exploits mass differences and is especially useful in determining differential protein expression patterns between two or more samples (Ong & Mann, 2005), for example between treated and untreated cell populations of the same cell line (Ong & Mann, 2006). This would serve to determine any changes in protein expression in reaction to a specific stimulant or substance and thus aid in examining and understanding the cell's response to a particular stimulant (McDonagh *et al.*, 2012). A key feature of SILAC is that labelling occurs in metabolically active cells through the incorporation of specialised light and heavy amino acids (Ong & Mann, 2006). Figure 4 depicts an example of a study on cancer development in a human cell culture model using multiple proteomic techniques (Pütz *et al.*, 2012). In the study, malignant transformation of a primary human fibroblast cell line (BJ) occurred sequentially using retroviral vectors encoding for hTERT, SV40 early region and H-Ras to produce cell

lines BJ-T, BJ-TE and BJ-TER, respectively. Each cell line was then subjected to 2D-PAGE, iTRAQ and SILAC proteomics analysis. The most common and simplest workflow for analysis of complex protein mixtures involves tryptic digestion and chromatographic separation of most abundant peptides by mass spectrometry. Resultant tandem mass spectrometry data is searched against protein databases to identify peptides and compile a list of putative proteins (Ong & Mann, 2006; Cuomo *et al.*, 2011).

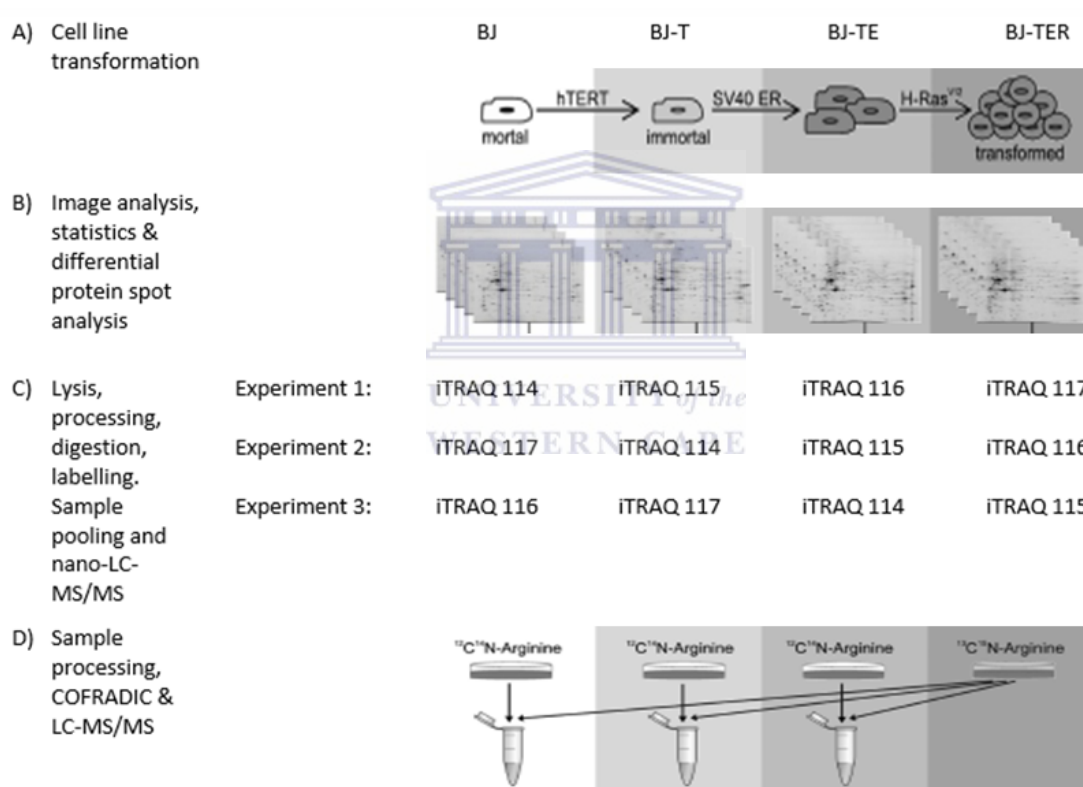


Figure 4: Multiple proteomic techniques utilized to determine the proteomics of cancer development in a human fibroblast cell line (adapted from Pütz *et al.*, 2012). (A) Malignant transformation of a primary human fibroblast cell line by successive transduction with retroviral vectors. (B) 2D-PAGE workflow. (C) iTRAQ workflow. (D) SILAC workflow.

Quantitative proteomics and mass spectrometry play a significant role in the study of disease biomarkers (Trinh *et al.*, 2013). SILAC has become a popular technique for this due to its simplicity (Zhao *et al.*, 2009). Studies on the effect of fucoidan on cancerous cells in vitro have

been limited to specific proteins expressed in specific pathways, especially apoptotic pathways (Aisa *et al.*, 2005; Kim *et al.*, 2010; Xue *et al.*, 2012). A quantitative study on the effect of fucoidan on the entire MCF7 breast cancer cell proteome has yet to be explored.

2.4.2 Stable isotope labelling of amino acids in cell culture

SILAC involves the tagging of proteins on the basis of weight (Ong & Mann, 2006; Fenselau, 2007). It differs from other labelling techniques in that “tags” are incorporated in live cells during cellular growth and protein synthesis. Heavy amino acids are labelled with ^2H , ^{13}C and/or ^{15}N stable isotopes (Ong, 2012). Arginine and lysine are most commonly used as tryptic cleavage of proteins occurs after these amino acids. This ensures that SILAC labels will be incorporated into each of the resulting peptides (Ong, 2012). Typically, two cell populations are established in cell culture medium containing dialyzed fetal bovine serum (FBS) and antibiotics (Figure 5). One population is supplemented with heavy-labelled amino acids and the other with light or normal amino acids. Full incorporation of amino acids requires sufficient culturing and is dependent on the growth rate and doubling time of the cell line in question (Ong & Mann, 2006). Subsequent to culture, cells are lysed and proteins extracted. Light and heavy samples are mixed, subjected to tryptic digestion and resulting peptides analysed by mass spectrometry (Figure 5). SILAC is favoured as it reduces or even eliminates intra-experimental variability introduced by human error and is a robust method for proteomics analysis (Ong, 2012). Mixing of samples prior to analysis reduces variability between mass spectrometry analyses (Lau *et al.*, 2014).

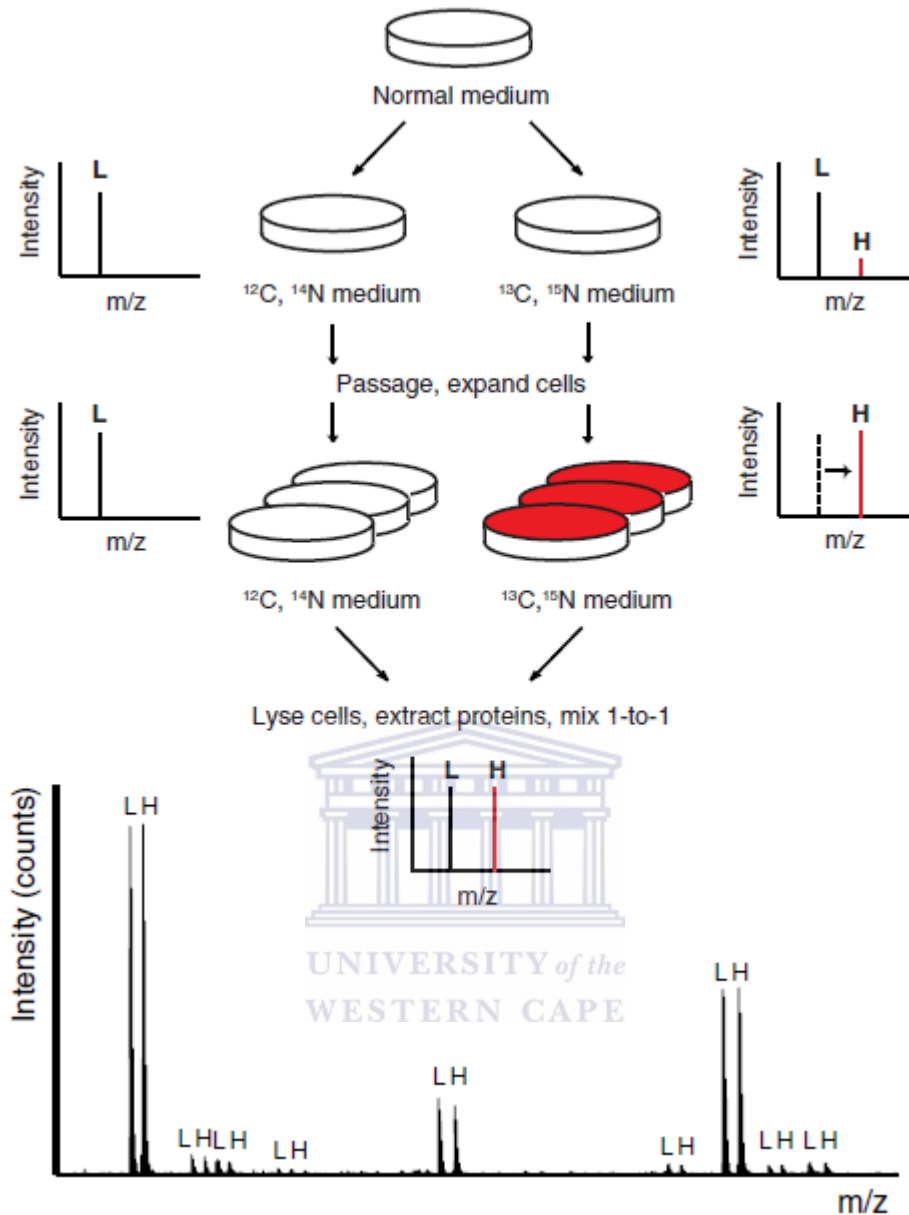


Figure 5: Classical SILAC workflow illustrating culture of cells in light (left) and heavy (right) SILAC media and label incorporation over time (Ong, 2012). Label incorporation is followed by cell lysis, protein extraction, tryptic digestion and 1:1 mixing of light and heavy extractions for mass spectrometry analysis.

2.4.3 Limitations

Mass spectrometers are generally comprised of the ion source, mass analyser and the data processing unit (Yates *et al.*, 2009). Ionisation techniques employed in mass spectrometry (MS) analysis include matrix-assisted laser desorption ionisation (MALDI) and electrospray

ionisation (ESI). Innovation of these soft ionisation techniques allowed for the use of MS to spread to biological sciences (Wilm, 2009). It afforded analysis of protein samples without the risk of considerable degradation of proteins (Yates *et al.*, 2009). To ensure accurate results, molecular concentrations have to match the intensity of the ion signal given off by the mass spectrometer. Discrepancies between molecular concentrations and ion signal intensity may occur in both MALDI and ESI. This is unfavourable but can be prevented by understanding how ionisation occurs in each technique (Wilm, 2009).

For MALDI, an acidic matrix is utilized and ionisation occurs through proton transfer from the matrix (Wilm, 2009). An ion suppression effect occurs when some molecules fail to ionise due to the presence of molecules having a high proton affinity. The discrepancy depends on the size of the peptides being analysed. Peptides larger than 3 kDa have high proton affinity and are not likely to be suppressed by other molecules. When analysing peptides below 3 kDa, a near identical standard should be used for comparison as peptides are likely to be suppressed.

The accuracy of ESI is dependent on the flow rate at which it is operated. Ideally, low flow rates (i.e. 100 nL/min) should be used to most accurately reflect consistent molecular concentrations and mass spectral signal intensities (Wilm, 2009). ESI works by producing ions from droplets less than 1 μm in diameter. With high flow rates, droplets larger than 1 μm are produced resulting in the formation of highly charged secondary droplets. Primary and secondary droplets are hydrophilic and hydrophobic, respectively. Hydrophobic molecules have higher desolvation efficiency. High flow rates therefore results in an ion suppression effect in which the hydrophilic molecules are not detected (Wilm, 2009; Xie *et al.*, 2011).

It is important to note that not all electrospray ionised peptides will be fragmented or lead to successful protein identifications. In the presence of highly abundant peptides, low abundant peptides may not be detected by the mass spectrometer (de Godoy *et al.* 2006). Another

limitation lies in the way liquid chromatography-mass spectrometry (LC-MS) platforms analyse complex mixtures. Since peptides are randomly measured, reproducibility in repeat measurements of the same samples is reduced (de Godoy *et al.*, 2006; Ong, 2012).

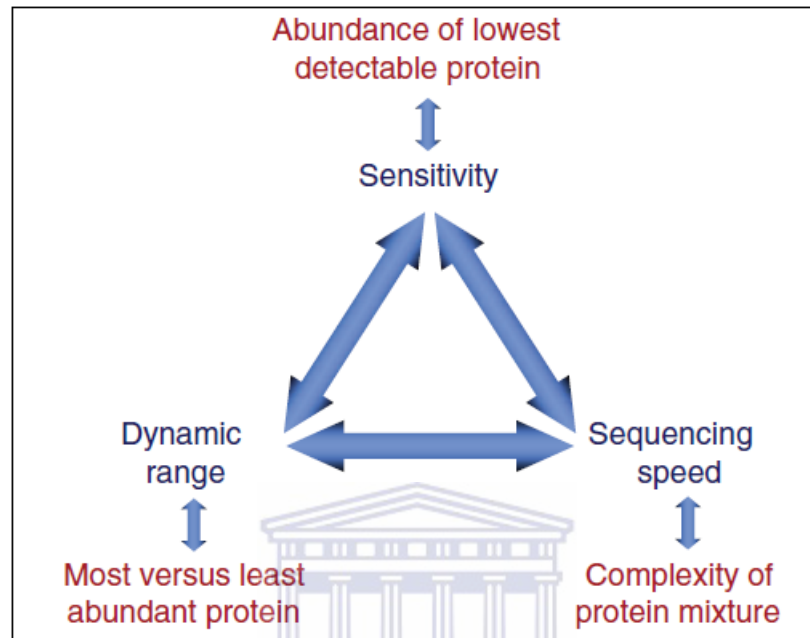


Figure 6: Characteristics of instrumentation and the related influences on proteome coverage (de Godoy *et al.*, 2006).

Achieving full coverage in quantitative proteomics is reliant on three independent but interconnecting characteristics of the mass spectrometer namely sensitivity, speed of sequencing and the dynamic range (Figure 6) (de Godoy *et al.*, 2006). Sensitivity is dictated by the ability to detect low abundant peptides. The sensitivity in quantifying complex peptide mixtures is lower than for single peptides and is restricted if only a small or finite amount of material is available for analysis. Larger samples have an increased likelihood of detecting low abundant peptides (de Godoy *et al.*, 2006). Speed of sequencing refers to the rate peptides are sequenced as they elute from the LC column. If sequencing does not occur rapidly, not all eluted peptides will be sequenced although the signal for the unsequenced peptides will still be detected. Therefore, peptides may be detected but downstream may not be identified. For

SILAC, this could mean that light and heavy peptide pairs are not detected during the same run (de Godoy *et al.*, 2006). Dynamic range denotes the ability to differentiate between high and low abundance signals. A common limitation of dynamic range includes the inability to detect very low abundant signals in the presence of very high abundant signals (de Godoy *et al.*, 2006; Mann & Kelleher, 2008).

Separation science and fractionation minimize limitations of LC-MS and simplifying analysis (Issaq, 2001; de Godoy *et al.*, 2006). The use of a single separation technique will however not be successful in resolving a complex mixture of proteins. Multidimensional separation techniques yield more accurate results and the dynamic range of the protein sample is lowered (Reinders *et al.*, 2006). This is especially evident in the analysis of proteins extracted from whole cell or tissue (Issaq, 2001). It has been established that fractionation prior to MS analysis is beneficial in decreasing the burden on dynamic range and sequencing speed which in turn lower the burden on sensitivity (de Godoy *et al.*, 2006). Common fractionation techniques for proteins and peptides are one-dimensional PAGE (1D PAGE) gels and reversed-phase chromatography, respectively. These techniques are chosen for their robustness and high resolution, and further fractionation is not necessary (de Godoy *et al.*, 2006). While separation is advantageous in allowing full proteome coverage, caution is asserted against extensive fractionation as sampling of the same peptides may occur repeatedly. Also, sample usage and measurement time increases with each separation step.

A limitation of particular concern in SILAC is the conversion of arginine residues to proline in culture (Ong & Mann, 2006). This could be circumvented by reducing the concentration of arginine added to the culture medium. Some cell lines are however negatively affected by arginine starvation (Van Hoof *et al.*, 2007). In cases where less arginine is not an option, manual or mathematical experimental corrections can be made by addition of heavy proline peaks to heavy arginine peaks. This process is labour-intensive, particularly for large data sets

and may result in significantly reduced accuracy. Prevention of arginine to proline conversion or the compensation for this effect has been investigated through computational correction (Park *et al.*, 2009). The addition of unlabelled proline to the SILAC media has also been investigated with favourable results compared to controls without the additional proline and was shown to be cell line independent (Löbner *et al.*, 2011).

Studies have successfully determined proteome changes in cells between non-cancerous and cancer cell lines and in cells as a result of specific treatment using SILAC (Edelmann *et al.*, 2014; Yang *et al.*, 2015). Proteomics would thus be an ideal approach to study proteome changes in MCF7 cells in response to fucoidan treatment.



References

1. Aisa, Y., Miyakawa, Y., Nakazato, T., Shibata, H., Saito, K., Ikedo, Y. & Kizaki, M., 2005. Fucoïdan induces apoptosis of human HS-Sultan cells accompanied by activation of caspase-3 and down-regulation of ERK Pathways. *American Journal of Hematology*, 78, pp.7–14.
2. Ale, M.T., Maruyama, H., Tamauchi, H., Mikkelsen, J.D. & Meyer, A. S., 2011a. Fucoïdan from *Sargassum sp.* and *Fucus vesiculosus* reduces cell viability of lung carcinoma and melanoma cells in vitro and activates natural killer cells in mice in vivo. *International Journal of Biological Macromolecules*, 49, pp.331–336.
3. Ale, M.T., Maruyama, H., Tamauchi, H., Mikkelsen, J.D. & Meyer, A.S., 2011b. Fucose-containing sulfated polysaccharides from brown seaweeds inhibit proliferation of melanoma cells and induce apoptosis by activation of caspase-3 *in vitro*. *Marine Drugs*, 9, pp.2605-2621
4. Ale, M.T., Mikkelsen, J.D. & Meyer, A.S., 2011c. Important determinants for fucoïdan bioactivity: A critical review of structure-function relations and extraction methods for fucose-containing sulfated polysaccharides from brown seaweeds. *Marine Drugs*, 9, pp.2106–2130.
5. Banafa, A.M., Roshan, S., Liu, Y., Zhao, S., Yang, G., He, G., Chen, M., 2014. Fucoïdan induces apoptosis in MDA-MB-231 cells by activating caspase cascade and down-regulating XIAP. *IOSR Journal of Pharmacy and Biological Sciences*, 9, pp.59–64.
6. Banafa, A.M., Roshan, S., Liu, Y., Chen, H., Chen, M., Yang, G., He, G., 2013. Fucoïdan induces G 1 phase arrest and apoptosis through caspase-dependent pathway and ROS induction in human breast cancer MCF-7 cells. *Journal of Huazhong University of Science and Technology-Medical Science*, 33, pp.717–724.

7. Boo, H.J., Hong, J.Y., Kim, S.C., Kang, J.I., Kim, M.K., Kim, E.J., Hyun, J.W, Koh, Y.S., Yoo, E.S., Kwon, J.M. & Kang, H.K., 2013. The anticancer effect of fucoidan in PC-3 prostate cancer cells. *Marine Drugs*, 11, pp.2982–2999.
8. Boopathy, N.S. & Kathiresan, K., 2010. Anticancer drugs from marine flora: An overview. *Journal of Oncology*, 2010, pp.1–18.
9. Buccimazza, I., 2015. Delays in breast cancer: Do they matter ?. *South African Journal of Surgery*, 53, pp.34–36.
10. Chandramouli, K. & Qian, P.Y., 2009. Proteomics: Challenges, techniques and possibilities to overcome biological sample complexity. *Human Genomics and Proteomics*, 2009, pp.1–22.
11. Chevolut, L., Mulloy, B., Ratiskol, J., Foucault, A. & Collic-Jouault, S., 2001. A disaccharide repeat unit is the major structure in fucoidans from two species of brown algae. *Carbohydrate Research*, 330, pp.529–535.
12. Cho, M.L., Lee, B.Y. & You, S.G., 2011. Relationship between oversulfation and conformation of low and high molecular weight fucoidans and evaluation of their in Vitro anticancer activity. *Molecules*, 16, pp.291–297.
13. Choi, J.I. & Kim, H.J., 2013. Preparation of low molecular weight fucoidan by gamma-irradiation and its anticancer activity. *Carbohydrate Polymers*, 97, pp.358–362.
14. Choi, J.I., Kim, H.J., Kim, J.H., Byun, M.W., Chun, B.S., Ahn, D.H., Hwang, Y.J., Kim, D.J., Kim, G.H. & Lee, J.W., 2009. Application of gamma irradiation for the enhanced physiological properties of polysaccharides from seaweeds. *Applied Radiation and Isotopes*, 67, pp.1277–1281.
15. Cumashi, A., Ushakova, N.A., Preobrazhenskaya, M.E., D’Incecco, A., Piccoli, A., Totani, L., Tinari, N., Morozevich, G.E., Berman, A.E., Bilan, M.I., Usov, A.I., Ustyuzhanina, N.E., Grachev, A.A., Sanderson, C.J., Kelly, M., Rabinovich, G.A.,

- Iacobelli, S. & Nifantiev, N.E., 2007. A comparative study of the anti-inflammatory, anticoagulant, antiangiogenic, and antiadhesive activities of nine different fucoidans from brown seaweeds. *Glycobiology*, 17, pp.541–552.
16. Cuomo, A., Moretti, S., Minucci, S. & Bonaldi, T., 2011. SILAC-based proteomic analysis to dissect the “histone modification signature” of human breast cancer cells. *Amino Acids*, 41, pp.387–399.
17. de Godoy, L.M.F., Olsen, J.V., de Souza, G.A., Li, G., Mortensen, P. & Mann, M., 2006. Status of complete proteome analysis by mass spectrometry: SILAC labeled yeast as a model system. *Genome Biology*, 7, pp.R50.
18. DeSantis, C., Ma, J., Bryan, L. & Jemal, A., 2013. Breast cancer statistics, 2013. *CA Cancer Journal for Clinicians*, 64, pp.52–62.
19. Dixon, R.A., 2001. Natural products and plant disease resistance. *Nature*, 411(6839), pp.843–847.
20. Donia, M. & Hamann, M.T., 2003. Marine natural products and their potential applications as anti-infective agents. *THE LANCET Infectious Diseases*, 3, pp.338–348.
21. Duarte, M.E.R., Cardoso, M.A., Nosedá, M.D. & Cerezo, A.S., 2001. Structural studies on fucoidans from the brown seaweed *Sargassum stenophyllum*. *Carbohydrate Research*, 333, pp.281–293.
22. Eiermann, W. Paepke, S., Appfelstaedt, J., Llombart-Cussac, A., Eremin, J., Vinholes, J., Mauriac, L., Ellis, M., Lassus, M., Chaudri-Ross, H. A., Dugan, M., Borgs, M. & Semiglazov, V., 2001. Preoperative treatment of postmenopausal breast cancer patients with letrozole: A randomized double-blind multicenter study. *Annals of Oncology*, 12, pp.1527–1532.
23. Fenselau, C., 2007. A review of quantitative methods for proteomic studies. *Journal of Chromatography B*, 855, pp.14–20.

24. Ferlay J, Soerjomataram I, Ervik M, Dikshit R, Eser S, Mathers C, Rebelo M, Parkin DM, Forman D, Bray, F. GLOBOCAN 2012 v1.0, Cancer Incidence and Mortality Worldwide: IARC CancerBase No. 11 [Internet]. Lyon, France: International Agency for Research on Cancer; 2013. Available from: <http://globocan.iarc.fr>, accessed on 15/July/2015
25. Fukahori, S., Yano, H., Akiba, J., Ogasawara, S., Momosaki, S., Sanada, S., Kuratomi, K., Ishizaki, Y., Moriya, F., Yagi, M. & Kojiro, M., 2008. Fucoidan, a major component of brown seaweed, prohibits the growth of human cancer cell lines in vitro. *Molecular Medicine Reports*, 1, pp.537–542.
26. Haefner, B., 2003. Drugs from the deep: marine natural products as drug candidates. *Drug Discovery Today*, 8, pp.536–544.
27. Hayakawa, K. & Nagamine, T., 2009. Effect of fucoidan on the biotinidase kinetics in human hepatocellular carcinoma. *Anticancer Research*, 29, pp.1211–1218.
28. Hyun, J.H., Kim, S.C., Kang, J.I., Kim, M.K., Boo, H.J., Kwon, J.M., Koh, Y.S., Hyun, J.W., Park, D.B., Yoo, E.S. & Kang, H.K., 2009. Apoptosis inducing activity of fucoidan in HCT-15 colon carcinoma cells. *Biological & Pharmaceutical Bulletin*, 32, pp.1760–1764.
29. Issaq, H.J., 2001. The role of separation science in proteomics research. *Electrophoresis*, 22, pp.3629–3638.
30. Jagsi, R., 2014. Progress and controversies: radiation therapy for invasive breast cancer. *CA: a Cancer Journal for Clinicians*, 64, pp.135–152.
31. Jemal, A., Center, M.M., DeSantis, C. & Ward, E.M., 2010. Global patterns of cancer incidence and mortality rates and trends. *Cancer Epidemiology Biomarkers & Prevention*, 19, pp.1893–1907.

32. Jiao, G., Yu, G., Zhang, J. & Ewart, S., 2011. Chemical structures and bioactivities of sulfated polysaccharides from marine algae. *Marine Drugs*, 9, pp.196–233.
33. Jones, M.E., van Leeuwen, F.E., Hoogendoorn, W.E., Mourtis, M.J.E., Hollema, H., van Boven, H., Press, M.F., Bernstein, L. & Swerdlow, A.J., 2012. Endometrial cancer survival after breast cancer in relation to tamoxifen treatment: pooled results from three countries. *Breast Cancer Research*, 14, pp.R91.
34. Kawamoto, H., Miki, Y., Kimura, T., Tanaka, K., Nakagawa, T., Kawamukai, M. & Matsuda, H., 2006. Effects of fucoidan from Mozuku on human stomach cell lines. *Food Science and Technology Research*, 12, pp.218–222.
35. Kemp, A., Preen, D. B., Saunders, C., Boyle, F., Bulsara, M., Malacova, E. & Roughead, E. E., 2014. Early discontinuation of endocrine therapy for breast cancer: who is at risk in clinical practice? *SpringerPlus*, 3, pp.282.
36. Kim, E.J., Park, S.Y., Lee, J.Y. & Park, J.H.Y., 2010. Fucoidan present in brown algae induces apoptosis of human colon cancer cells. *BMC Gastroenterology*, 10, pp.96.
37. Kusaykin, M.I., Chizhov, A.O., Grachev, A.A., Alekseeva, S.A., Bakunina, I.Y., Nedashkovskaya, O.I., Sova, V.V. & Zvyagintseva, T.N., 2006. A comparative study of specificity of fucoidanases from marine microorganisms and invertebrates. *Journal of Applied Phycology*, 18, pp.369–373.
38. Lam, K.S., 2007. New aspects of natural products in drug discovery. *Trends in Microbiology*, 15, pp.279–289.
39. Lau, H.T., Suh, H.W., Golkowski, M. & Ong, S.E., 2014. Comparing SILAC- and stable isotope dimethyl-labeling approaches for quantitative proteomics. *Journal of Proteome Research*, 13, pp.4164–4174.
40. Laurienzo, P., 2010. Marine polysaccharides in pharmaceutical applications: An overview. *Marine Drugs*, 8, pp.2435–2465.

41. Lee, H., Kim, J.-S. & Kim, E., 2012. Fucoidan from seaweed *Fucus vesiculosus* inhibits migration and invasion of human lung cancer cell via PI3K-Akt-mTOR pathways. *PloS ONE*, 7(11), p.e50624.
42. Lee, H.E., Choi, E.S., Shin, J.A., Lee, S.O., Park, K.S., Cho, N.P. Cho, S.D., 2013. Fucoidan induces caspase-dependent apoptosis in MC3 human mucoepidermoid carcinoma cells. *Experimental and Therapeutic Medicine*, 7, pp. 228-232.
43. Lee, Y.K., Lim, D.J., Lee, Y.H. & Park, Y.I., 2006. Variation in fucoidan contents and monosaccharide compositions of Korean *Undaria pinnatifida* (Harvey) Suringar (Phaeophyta). *Algae*, 21, pp.157–160.
44. Li, B., Lu, F., Wei, X., & Zhao, R., 2008. Fucoidan: structure and bioactivity. *Molecules*, 13, pp.1671–1695.
45. Löbner, C., Warnken, U., Pscherer, A. & Schnölzer, M., 2011. Preventing arginine-to-proline conversion in a cell-line-independent manner during cell cultivation under stable isotope labeling by amino acids in cell culture (SILAC) conditions. *Analytical Biochemistry*, 412, pp.123–125.
46. Mak, W., Wang, S.K., Liu, T., Hamid, N., Li, Y., Lu, J. & White, W.L., 2014. Anti-proliferation potential and content of fucoidan extracted from sporophyll of New Zealand *Undaria pinnatifida*. *Frontiers in Nutrition*, 1, pp.1–10.
47. Manilal, A., Sujith, S., Selvin, J., Kiran, G.S., Shakir, C. & Lipton, A.P., 2010. Antimicrobial potential of marine organisms collected from the southwest coast of India against multiresistant human and shrimp pathogens. *Scientia Marina*, 74, pp.287–296.
48. Mann, M. & Kelleher, N.L., 2008. Precision proteomics: the case for high resolution and high mass accuracy. *PNAS*, 105 pp.18132–18138.

49. Martins, A., Vieira, H., Gaspar, H. & Santos, S., 2014. Marketed marine natural products in the pharmaceutical and cosmeceutical industries: Tips for success. *Marine Drugs*, 12, pp.1066–1101.
50. Matatiele, P. & Van Der Heever, W., 2008. Breast cancer profiles of women presenting with newly diagnosed breast cancer at Universitas Hospital (Bloemfontein, South Africa). *South African Family Practice Journal*, 50, pp.48–49.
51. Mayer, A.M.S., Rodríguez, A.D., Berlinck, R.G.S. & Fusetani, N., 2011. Marine pharmacology in 2007–8: Marine compounds with antibacterial, anticoagulant, antifungal, anti-inflammatory, antimalarial, antiprotozoal, antituberculosis, and antiviral activities; affecting the immune and nervous system, and other miscellaneous mechanisms of action. *Comparative Biochemistry and Physiology Part C: Toxicology & Pharmacology*, 153, pp.191–222.
52. McDonagh, B., Martínez-Acedo, P., Vázquez, J., Padilla, C.A., Sheehan, D. & Bárcena, J. A., 2012. Application of iTRAQ reagents to relatively quantify the reversible redox state of cysteine residues. *WESTERN CAPE International Journal of Proteomics*, 2012, pp.1–9.
53. Moghadamtousi, S.Z., Karimian, H., Khanabdali, R., Razavi, M., Firoozinia, M., Zandi, K. & Kadir, H.A., 2014. Anticancer and antitumor potential of fucoidan and fucoxanthin, two main metabolites isolated from brown algae. *The Scientific World Journal*, 2014, pp.768323.
54. Morya, V.K., Kim, J. & Kim, E.K., 2012. Algal fucoidan: Structural and size-dependent bioactivities and their perspectives. *Applied Microbiology and Biotechnology*, 93, pp.71–82.
55. Ong, S.E. & Mann, M., 2006. A practical recipe for stable isotope labeling by amino acids in cell culture (SILAC). *Nature Protocols*, 1, pp.2650–2660.

56. Ong, S.E., 2012. The expanding field of SILAC. *Analytical and Bioanalytical Chemistry*, 404, pp.967–976.
57. Ong, S.E. & Mann, M., 2005. Mass spectrometry-based proteomics turns quantitative. *Nature Chemical Biology*, 1, pp.252–262.
58. Park, S.K., Liao, L., Kim, J.Y. & Yates, J.R., III, 2009. A computational approach to correct arginine-to-proline conversion in quantitative proteomics, *Nature Methods*, 6, pp.184-185
59. Park, H.S., Kim, G.Y., Nam, T.J., Kim, N.D., Choi, Y.H., 2011. Antiproliferative activity of fucoidan was associated with the induction of apoptosis and autophagy in AGS human gastric cancer cells. *Journal of Food Science*, 76, pp.T77–T83.
60. Park, H.Y., Kim, G.Y., Moon, S.K., Kim, W.J., Yoo, Y.H., Choi, Y.H., 2014. Fucoidan inhibits the proliferation of human urinary bladder cancer T24 cells by blocking cell cycle progression and inducing apoptosis. *Molecules*, 19, pp.5981–5998.
61. Park, H.S., Hwang, H.J., Kim, G.Y., Cha, H.J., Kim, W.J., Kim, N.D., Yoo, Y.H. & Choi, Y.H., 2013. Induction of apoptosis by fucoidan in human leukemia U937 cells through activation of p38 MAPK and modulation of Bcl-2 family. *Marine Drugs*, 11, pp.2347–2364.
62. Patel, S., 2012. Therapeutic importance of sulfated polysaccharides from seaweeds: Updating the recent findings, *3 Biotech*, 2, 171-185
63. Philchenkov, A., Zavelevich, M., Imbs, T., Zvyagintseva, T. & Zaporozhets, T., 2007. Sensitization of human malignant lymphoid cells to etoposide by fucoidan, a brown seaweed polysaccharide. *Experimental Oncology*, 29, pp.181–185.

64. Pütz, S.M., Boehm, A.M., Stiewe, T. & Sickmann, A., 2012. iTRAQ analysis of a cell culture model for malignant transformation, including comparison with 2D-PAGE and SILAC. *Journal of Proteome Research*, 11, pp.2140–2153.
65. Queiroz, K.C.S., Assis, C.F., Medeiros, V.P., Rocha, H.A.O., Aoyama, H., Ferreira, C.V. & Leite, E.L., 2006. Cytotoxicity effect of algal polysaccharides on HL60 cells. *Biochemistry*, 71, pp.1312–1315.
66. Reinders, J., Zahedi, R.P., Pfanner, N., Meisinger, C. & Sickmann, A., 2006. Toward the complete yeast mitochondrial proteome: multidimensional separation techniques for mitochondrial proteomics research articles. *Journal of Proteome Research*, 5, pp.1543–1554.
67. Remesh, A., 2012. Toxicities of anticancer drugs and its management. *International Journal of Basic & Clinical Pharmacology*, 1, pp.2-12.
68. Rupérez, P., Ahrazem, O. & Leal, J.A., 2002. Potential antioxidant capacity of sulfated polysaccharides from the edible marine brown seaweed *Fucus vesiculosus*. *Journal of Agricultural and Food Chemistry*, 50, pp.840–845.
69. Schlebusch, C.M., Dreyer, G., Sluiter, M.D., Yawitch, T.M., van den Berg, H.J. & van Rensburg, E.J., 2010. Cancer prevalence in 129 breast-ovarian cancer families tested for BRCA1 and BRCA2 mutations. *South African Medical Journal*, 100, pp.113–117.
70. Senthilkumar, K., Manivasagan, P., Venkatesan, J. & Kim, S.K., 2013. Brown seaweed fucoidan: Biological activity and apoptosis, growth signaling mechanism in cancer. *International Journal of Biological Macromolecules*, 60, pp.366–374.
71. Skriptsova, A.V., Shevchenko, N.M., Zvyagintseva, T.N. & Imbs, T.I., 2010. Monthly changes in the content and monosaccharide composition of fucoidan from *Undaria pinnatifida* (Laminariales, Phaeophyta). *Journal of Applied Phycology*, 22, pp.79–86.

72. Song, L., Sarno, P. De & Jope, R.S., 2002. Central role of Glycogen Synthase Kinase-3 β in endoplasmic reticulum stress-induced caspase-3 activation *. *The Journal of Biological Chemistry*, 277, pp.44701–44708.
73. Sutherland, R.L., 2011. Endocrine resistance in breast cancer: new roles for ErbB3 and ErbB4. *Breast cancer research : Breast Cancer Research*, 13, pp.106.
74. Swerdlow, A.J. & Jones, M.E., 2005. Tamoxifen treatment for breast cancer and risk of endometrial cancer: A case-control study. *Journal of the National Cancer Institute*, 97, pp.375–384.
75. Teng, H., Yang, Y., Wei, H., Liu, Z., Liu, Z., Ma, Y., Gao, Z., Hou, L. & Zou, X., 2015. Fucoidan suppresses hypoxia-induced lymphangiogenesis and lymphatic metastasis in mouse hepatocarcinoma. *Marine Drugs*, 13, pp.3514–3530.
76. Thürlimann, B., Keshaviah, A., Coates, A. S., Mouridsen, H., Mauriac, L., Forbes, J. F., Paridaens, R., Castiglione-Gertsch, M., Gelber, R. D., Rabaglio, M., Smith, I., Wardly, A., Price, K. N. & Goldhirsch, A. 2005. A comparison of letrozole and tamoxifen in postmenopausal women with early breast cancer, *The New England Journal of Medicine*, 353, pp.2747-2757
77. Trinh, H. V., Grossman, J., Gehrig, P., Roschitzki, B., Schlapbach, R., Greber, U. F. & Hemmi, S., 2013. iTRAQ-based and label-free proteomics approaches for studies of human adenovirus infections. *International journal of proteomics*, 2013, pp.581862.
78. Udani, J. & Hesslink, R., 2012. The potential use of fucoidans from brown seaweed as a dietary supplement. *Journal of Nutrition & Food Sciences*, 2, pp.1–6.
79. Unger-Saldaña, K., 2014. Challenges to the early diagnosis and treatment of breast cancer in developing countries. *World Journal of Clinical Oncology*, 5, pp.465–477.

80. Van Hoof, D., Pinkse, M.W., Oostwaard, D.W., Mummery, C.L., Heck, A.J. & Krijgsveld, J., 2007. An experimental correction for arginine-to-proline conversion artifacts in SILAC-based quantitative proteomics. *Nature Methods*, 4, pp.677–678.
81. Vishchuk, O.S., Ermakova, S.P. & Zvyagintseva, T.N., 2011. Sulfated polysaccharides from brown seaweeds *Saccharina japonica* and *Undaria pinnatifida*: isolation, structural characteristics, and antitumor activity. *Carbohydrate Research*, 346, pp.2769–2776.
82. Vorobiof, B.D.A., Sitas, F. & Vorobiof, G., 2001. Breast cancer incidence in South Africa. *Journal of Clinical Oncology*, 19, pp.125–127.
83. Wijesekara, I., Pangestuti, R. & Kim, S.K., 2011. Biological activities and potential health benefits of sulfated polysaccharides derived from marine algae. *Carbohydrate Polymers*, 84, pp.14–21.
84. Wilm, M., 2009. Quantitative proteomics in biological research. *Proteomics*, 9, pp.4590–4605.
85. Wulfschlegel, J.D., Sgroi, D.C., Krutzsch, H., McLean, K., McGarvey, K., Knowlton, M., Chen, S., Shu, H., Sahin, A., Kurek, R., Wallweiner, D., Merino, M.J., Petricoin, III, E.F., Zhao, Y. & Steeg, P.S., 2002. Proteomics of human breast ductal carcinoma in situ. *Cancer Research*, 62, pp.6740–6749.
86. Xie, F., Liu, T., Qian, W.J., Petyuk, V.A. & Smith, R.D., 2011. Liquid chromatography-mass spectrometry-based quantitative proteomics. *Journal of Biological Chemistry*, 286, pp.25443–25449.
87. Xue, M., Ge, Y., Zhang, J., Wang, Q., Hou, L., Liu, Y., Sun, L. & Li, Q., 2012. Anticancer properties and mechanisms of fucoidan on mouse breast cancer in vitro and in Vivo. *PLoS ONE*, 7, pp.3–11.

88. Yamasaki-Miyamoto, Y., Yamasaki, M., Tachibana, H. & Yamada, K., 2009. Fucoïdan induces apoptosis through activation of caspase-8 on human breast cancer MCF-7 cells. *Journal of Agricultural and Food Chemistry*, 57, pp.8677–8682.
89. Yang, L., Wang, P., Wang, H., Li, Q., Teng, H., Liu, Z., Yang, W., Hou, L., Zou, X., 2013. Fucoïdan derived from *Undaria pinnatifida* induces apoptosis in human hepatocellular carcinoma SMMC-7721 cells via the ROS-mediated mitochondrial pathway. *Marine Drugs*, 11, pp.1961–1976.
90. Yang, G., Xu, Z., Lu, W., Li, X., Sun, C., Guo, J., Xue, P. & Guan, F. 2015. Quantitative analysis of differential proteome expression in bladder cancer vs. normal bladder cells using SILAC method. *PLoS ONE*, 10, e0134727
91. Yates, J.R., Ruse, C.I. & Nakorchevsky, A., 2009. Proteomics by mass spectrometry: approaches, advances, and applications. *Annual Review of Biomedical Engineering*, 11, pp.49–79.
92. Zhang, Z., Teruya, K., Yoshida, T., Eto, H. & Shirahata, S., 2013. Fucoïdan extract enhances the anti-cancer activity of chemotherapeutic agents in MDA-MB-231 and MCF-7 breast cancer cells. *Marine Drugs*, 11, pp.81–98.
93. Zhang, Z., Teruya, K., Eto, H. & Shirahata, S., 2011. Fucoïdan extract induces apoptosis in MCF-7 cells via a mechanism involving the ROS-dependent JNK activation and mitochondria-mediated pathways. *PloS ONE*, 6, pp.e27441.
94. Zhao, Y., Lee, W. –N. P. & Xiao, G. G. 2009. Quantitative proteomics and biomarker discovery in human cancer, *Expert Review of Proteomics*, 6, 115-118

Chapter 3

Investigating proteome changes in breast cancer cells in response to fucoidan

3.1 Introduction

Fucoidan is a complex sulfated polysaccharide extracted mainly from brown seaweeds (Morya *et al.*, 2012). A range of bioactivities have been reported, including antibacterial, antiviral, anti-inflammatory and anticancer properties. The anticancer effect of fucoidan has been studied in many cancerous cell lines. The polysaccharide displayed potent apoptotic and growth inhibitory effects on cancerous cells, while having little to no effect on non-cancerous cell lines (Xue *et al.*, 2012). Past research has been focused on the determination of the complex structure of fucoidan (Li *et al.*, 2008) and understanding cellular processes as a result of fucoidan treatment (Fukahori *et al.*, 2008; Kim *et al.*, 2010). While the biochemical structure has only been partially elucidated (Chevolot *et al.*, 2001), bioactivity has been largely attributed to the size, degree of sulfation and structure of the molecule (Morya *et al.*, 2012). The effect of fucoidan has been explored in several studies by Western blot analysis of proteins known to be up- or down-regulated in cancer (Kim *et al.*, 2010; Xue *et al.*, 2012). The mechanism of action remains unclear.

Fucoidan displays potent anticancer activity against breast cancer cells and shows promise as an alternative to chemotherapeutic drugs and radiation therapy. Breast cancer incidence is increasing (Ferlay *et al.*, 2012), while current treatments are invasive and have undesirable side effects (Jones *et al.*, 2012; Senthilkumar *et al.*, 2013; Moghadamtousi *et al.*, 2014). This study aimed to examine the global protein expression of MCF7 breast cancer cells treated with fucoidan. A global proteomic study may illuminate the cellular processes involved in

bioactivity and may provide invaluable insight in determining the mechanism of action of the polysaccharide. Materials used and suppliers are listed in the Appendix.

3.2 Materials and methods

3.2.1 Mammalian cell culture

3.2.1.1 Culturing of human breast cancer cells

Human breast cancer cells (MCF7, ATCC® #HTB-22™) were cultured in Dulbecco's Modified Eagle Medium/Nutrient Mixture F-12 (DMEM/F-12) supplemented with 10% fetal bovine serum (FBS) and penicillin/streptomycin (10 U/ml) in 25 cm² flasks unless stated otherwise. Cells were cultured in a humidified incubator at 37°C with 5% CO₂ atmosphere.

Cryovials containing mammalian cells were retrieved from -150°C storage and partially thawed in a water bath at 37°C. Contents were transferred to a sterile 15 ml tube containing 5 ml DMEM/F-12. Cells were collected by centrifugation (Sorvall® TC6 Benchtop centrifuge (DuPont) / rotor serial number H400) at 2000 rpm for 3 minutes, resuspended in 5 ml DMEM/F-12 media, transferred to a 25 cm² flask and cultured. All harvesting of cells was done using a Sorvall® TC6 Benchtop centrifuge (DuPont) / rotor serial number H400 centrifuge at 2000 rpm for 3 minutes unless stated otherwise.

3.2.1.2 Trypsinization, counting and cryopreservation of cells

Media were decanted from flasks when the cells reached 80-100% confluency. Cells were gently washed with 5 ml 1X PBS. A 3ml solution of Trypsin/EDTA (0.25%/0.02%) was added and the culture was incubated at 37°C for 2-3 minutes. Cells were viewed under a phase contrast microscope (Nikon, TMS-F No.301841) to inspect for cell detachment. Media (3 ml)

was added to inactivate trypsin. The mixture was transferred to a sterile 15 ml tube and cells were pelleted by centrifugation.

Cell counts were determined by transferring a 10 µl mixture of cells and Trypan blue exclusion dye (1:1) to Countess chamber slides. Cells were electronically counted using the Countess Automated Cell Counter (Life Technologies).

For cryopreservation, cell pellets were resuspended in DMEM media containing 10% DMSO. Aliquots of 1.5 ml were transferred to cryovials and stored at -150°C.

3.2.1.3 Dose response of human breast cancer cells treated with fucoidan

A working solution of crude fucoidan from *Fucus vesiculosus* (Sigma Aldrich Co.) was prepared in water at 5 mg/ml. Dilutions were prepared in water and UV sterilized using a Stratalinker® UV Crosslinker (Stratagene) for 5 minutes. Trypsinized MCF7 cells were seeded in triplicate into 96-well plates at a density of 1×10^4 cells per well to a final volume of 200 µl. Cells were cultured for 24 h, spent media was removed and cells were washed twice with 100 µl 1X PBS. Fresh media was added to each well (140 µl) followed by 60 µl of fucoidan at different concentrations (0.1 mg/ml – 0.5 mg/ml). After 24 h of culture, media was removed, and 100 µl fresh media and 10 µl of WST-1 were added to each well. Absorbance was measured using a POLARstar Omega microplate reader (BMG Labtech) over a range of wavelengths (430 nm, 440 nm, 450 nm, 460 nm, 470 nm, 480 nm, 490 nm and a reference wavelength of 610 nm). Absorbance readings were taken every 30 minutes over a period of 3 h and 30 minutes to determine the optimum wavelength and incubation time. The IC₅₀ was assessed as the concentration that inhibited 50% of cell growth. Cell viability was calculated using the

equation:
$$\frac{\text{Absorbance of sample} - \text{Absorbance of blank}}{\text{Absorbance of control} - \text{Absorbance of blank}} \times 100$$

Statistical analysis of cell viability data was presented as mean \pm SD.

3.2.1.4 Protein extractions from human breast cancer cells treated with fucoidan

Twelve 25 cm² flasks were seeded and cells were cultured to 60-70% confluency. Cells were treated with 0.2 mg/ml fucoidan. The ratio between media and fucoidan (70:30 v/v) was the same as with dose response assays but in a final volume of 7 ml.

MCF7 cells were treated for 0, 3, 6, 8, 24 and 48 h with fucoidan. Total protein was extracted from the cells following fucoidan treatments. At time of extraction, spent media was decanted with tubes and detached cells were pelleted by centrifugation. The supernatant was discarded. Cells were washed with 5 ml 1X PBS and pelleted by centrifugation. Cell pellets were resuspended in Cytobuster Protein Extraction Reagent and transferred to flasks. Extractions were performed according the manufacturer's instructions. Flasks were placed on a shaker for 5 minutes at room temperature. After incubation, lysed cells were scraped and transferred to a 1.5 ml tube. Cells were collected by centrifugation (Eppendorf Microcentrifuge 5417R) at 16 000 g for 5 minutes at 4°C. Supernatants were analysed for protein content and stored at -20°C.

Protein quantification was performed using the Bicinchoninic Acid (BCA) Protein Assay according to the manufacturer's 96-well assay protocol. Bovine serum albumin (BSA) standards ranging from 0.2-1 mg/ml in 0.2 mg/ml increments were prepared in the same buffer as protein samples. Blanks, standards and protein samples were added to separate wells followed by the BCA working solution (50:1 v/v ratio Bicinchoninic Acid Solution : Copper (II) Sulfate Pentahydrate 4% Solution). All assays were performed in triplicate. The 96-well plate was incubated at room temperature for 30 minutes and absorbance was measured at 562

nm using a POLARstar Omega microplate reader (BMG Labtech). A standard curve of the net absorbance vs. the protein concentration of each protein standard was plotted. The protein concentration was determined with the net absorbance standard curve equation.

3.2.2 SDS-PAGE and immunoblotting

One Dimensional Sodium Dodecyl Sulfate – Poly Acrylamide Gel Electrophoresis (1D SDS-PAGE) gels were prepared using stock solutions for 12% (v/v) separating and 4% (v/v) stacking gels (Table 3). Preparation and electrophoresis was done using Bio-Rad Mini-PROTEAN® Tetra Cell apparatus.

Table 3: Stock solutions used for preparing SDS-PAGE gels.

	12% Separating gel	4% Stacking gel
1.5 M Tris-HCl pH 8.8	2.5 ml	N/A
0.5 M Tris-HCl pH 6.8	N/A	0.5 ml
Acrylamide-Bis (40%)	3 ml	0.4 ml
APS (10%)	0.05 ml	0.025 ml
TEMED	0.01 ml	0.005 ml
Distilled water	4.44 ml	3.07 ml
TOTAL VOLUME	10 ml	4 ml

The 12% (v/v) separating gel was poured between gel plates and overlaid with 1 ml isopropanol. Once the separating gel had solidified, the isopropanol was poured off and the gel washed with dH₂O. The 4% (v/v) stacking gel solution was poured above the separating gel

and a 15-well comb was inserted. Once solidified, the comb was removed. The electrophoresis tank was filled with 1X SDS running buffer before loading of protein samples. Protein samples were diluted to 20 µg and transferred to sterile 0.6 ml Eppendorf tubes. Each sample was mixed with 5X Lane Marker Reducing Sample Buffer, incubated at 95°C for 4 minutes and cooled to room temperature. A protein molecular weight marker and protein sample mixtures were loaded into separate wells of the SDS-PAGE gel. Electrophoresis was carried out at 90 V for 120 minutes.

Immunoblotting (Western blot analysis) was carried out using XIAP and Phospho ERK1/2 antibodies. Protein samples were separated by 1D SDS-PAGE and transferred to a Polyvinylidene Difluoride (PVDF) membrane using a BioRad Mini TransBlot Cell. The semi-dry transfer was conducted using BioRad conditions for 1 mini gel of mixed molecular weight, at 25 V and 1.3 A, for 15 minutes. The membrane was placed in blocking buffer for 1 h with shaking, washed in TBS-T and incubated overnight with shaking in primary antibody (1:2000) at 4°C. The membrane was washed in TBS-T and incubated in secondary antibody (1:4000) for 1 h at room temperature with shaking and washed in TBS-T before visualization. Western Blots were visualized using the UVP BioSpectrum® Imaging System and Western blot substrate solution.

For quantitative band analysis, densitometric analysis was performed using ImageJ densitometry software (Version 1.46r, National Institutes of Health, Bethesda, MD). Bands were quantified based on the relative signal intensities. The densitometry data for the band intensities were used to construct bar graphs. Fold change was calculated relative to the 0 h untreated samples.

3.2.3 SILAC culture

3.2.3.1 SILAC media and labelling

SILAC media was prepared according to manufacturer's instructions. Briefly, the media was supplemented with dialyzed FBS and penicillin/streptomycin (10 U/ml). Dialyzed FBS is added because the small molecules quantities such as amino acids have been significantly reduced to allow for labelling with specific isotopically labelled amino acids. For light and heavy culture medium, 50 mg L-Lysine-2HCl and L-Arginine-HCl were added to 500 ml media resulting in concentrations of 0.46 mM and 0.47 mM, respectively. Media was filter-sterilized using 0.22 µm filters and stored at 4°C. A flask of MCF7 cells was trypsinized and cells split into two 75 cm² flasks, each containing 1.5x10⁵ cells and cultured further in either light or heavy SILAC media (with regular changes) for 13 weeks to achieve full label incorporation.



3.2.3.2 RIPA buffer protein extractions

Following 13 weeks culture in SILAC medium, total protein extractions were carried out using Radio Immuno Precipitation Assay (RIPA) buffer containing 1 U/ml Benzonase nuclease. Floating or detached cells in media were harvested by centrifugation, the cell pellet washed with PBS and again harvested by centrifugation. Cell pellets were resuspended in RIPA buffer, transferred to flasks and kept on ice for 5 minutes with occasional swirling to ensure full coverage of the plate surface. The cell lysate was collected using a cell scraper. The cell debris was pelleted by centrifugation (Eppendorf Centrifuge 5417R) at 14000 g for 15 minutes and resulting supernatant transferred to a sterile 1.5 ml tube and stored at -20°C.

3.2.3.3 Protein quantification

Quantification of protein samples cultured in SILAC media was performed using a Qubit® Protein Assay Kit and a Qubit® 2.0 Fluorometer (Life Technologies). This was performed according to the manufacturer's specifications using 1 µl per sample for quantification.

3.2.3.4 Determination of label incorporation efficiency

Two duplicate 1D SDS-PAGE gels were prepared, each containing 30 µg heavy labelled protein samples extracted from untreated cells. Gels were stained with Coomassie and destained in Destaining solution. Liquid chromatography-tandem mass spectrometry (LC-MS/MS) analysis was conducted at the Centre for Proteomic and Genomics Research (CPGR) to determine labelling efficiency.



3.2.3.5 Lysis of SILAC cultured cells and protein sample preparation

The optimum length of culture time in SILAC media to achieve sufficient label incorporation was achieved as described in Section 3.2.3.1. Cells were cultured in SILAC media for 13 weeks (as determined by label incorporation experiment) and treated with 0.2 mg/ml fucoidan (IC₅₀). The ratio between media and fucoidan (70:30 v/v) was the same as with dose response assays but in a final volume of 9 ml. Distilled water instead of fucoidan solution was added to untreated flasks. The SILAC culture included four biological replicas with four replicas per condition (Table 4).

Table 4: SILAC light and heavy treatments and repeats.

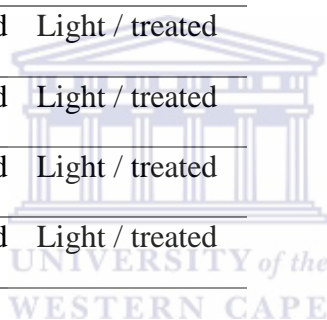
Label	Biological replicas	Treated/ Untreated
Light	1	Untreated
Light	2	Untreated
Light	3	Untreated
Light	4	Untreated
Light	1	Fucoidan treated
Light	2	Fucoidan treated
Light	3	Fucoidan treated
Light	4	Fucoidan treated
Heavy	1	Untreated
Heavy	2	Untreated
Heavy	3	Untreated
Heavy	4	Untreated
Heavy	1	Fucoidan treated
Heavy	2	Fucoidan treated
Heavy	3	Fucoidan treated
Heavy	4	Fucoidan treated

After 24 h of treatment, proteins were extracted with RIPA buffer and stored at -20°C. Protein quantification was performed using a Qubit® Protein Assay Kit and the Qubit® 2.0 Fluorometer as the concentration of dithiothreitol (DTT) in the protein extraction buffer was too high to be compatible with the BCA and Bradford protein assays. Protein concentration was determined and 1D SDS-PAGE analysis was performed to assess protein quality. Western blot analysis was performed to determine equal loading and thus protein quantification

accuracy. Protein samples of biological replicas were mixed (as described in Table 5), separated by 1D SDS-PAGE and analysed by mass spectrometry at the CPGR.

Table 5: SILAC protein extraction mixtures loaded onto SDS-PAGE gel for pair-wise comparisons by mass spectrometry.

Biological replicas	Mixture	
1	Light / untreated	Heavy / treated
2	Light / untreated	Heavy / treated
3	Light / untreated	Heavy / treated
4	Light / untreated	Heavy / treated
1	Heavy / untreated	Light / treated
2	Heavy / untreated	Light / treated
3	Heavy / untreated	Light / treated
4	Heavy / untreated	Light / treated



3.2.3.6 Mass spectrometry quantitation and data analysis

The SILAC labelled protein extraction mixtures were separated by SDS-PAGE and the protein bands were excised from the gel after staining using a scalpel. The gel fragments were cut into 1 mm x 1 mm cubes, destained twice and dehydrated. Proteins were reduced, alkylated and washed. Gel pieces were dehydrated again and protein digested by rehydrating the gel pieces in 0.2 mg/ml trypsin prepared in 50 mM ambic. Gel pieces were kept on ice and digested. Extracts were transferred to a sterile tube. Samples were dried by vacuum centrifugation and the buffer replaced by Millipore ddH₂O. Samples were dried again and resuspended in 0.1% formic acid (FA), 2.5% acetonitrile (ACN) prepared in analytical grade water for LC-MS analysis.

The LC–MS/MS analysis was conducted at the CPGR with a Q-Exactive quadrupole-Orbitrap mass spectrometer (Thermo Fisher Scientific, USA) coupled with a Dionex Ultimate 3000 nano-HPLC system. The extracted peptides were dissolved in sample loading buffer (97.5% water, 2.5% ACN, 0.1% FA) and loaded on a C18 trap column (300 μm ×5 mm×5 μm). Chromatographic separation was performed with a C18 column (75 μm ×250 mm×3.5 μm). Solvent A consisted of water and 0.1% FA, while solvent B consisted of ACN and 0.1% FA. The multi-step linear gradient for peptide separation was generated at 400 nL/minute as follows: 3 minutes time change; gradient change with 1 - 6 % Solvent B; 72 minutes time change; gradient change with 6 – 18% Solvent B; 22 minutes time change; gradient change with 18 – 35% Solvent B; 0.1 minutes time change; gradient change with 35 – 80% Solvent B; 10 minutes hold with 80% Solvent B; 10 minutes re-equilibration with 1% Solvent B. The mass spectrometer was operated in positive ion mode with a capillary temperature of 250°C. The applied electrospray voltage was 1.95 kV. Details of data acquisition are presented in Table 6.

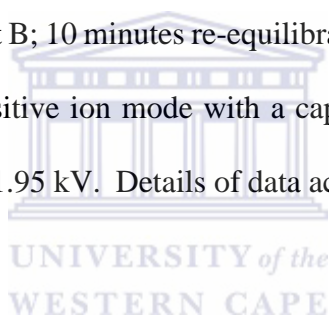


Table 6: Parameters for mass spectrometry data acquisition.

Full Scan	
Resolution	70,000 (@ m/z 200)
AGC target value	3e6
Scan range	320-1750 m/z
Maximal injection time (ms)	125
Data-dependent MS/MS	
Inclusion	Off
Resolution	17,500 (@ m/z 200)
AGC target value	1e5
Maximal injection time (ms)	50
Loop Count	10
Isolation window width (Da)	3
NCE (%)	27
Data-dependent Settings	
Underfill ratio (%)	1
Charge exclusion	Charge states 1,6-8,>8

Peptide match	preferred
Exclusion isotopes	on
Dynamic exclusion (s)	90

SILAC data analysis by MaxQuant quantitation was conducted by loading RAW files into MaxQuant (version 1.5.2.8). Labeling was assigned by setting the multiplicity to 2. Heavy labels were assigned as Arg10 and Lys6. Variable modification selections were acetylation (N-term), deamidation (NQ) and oxidation (M), fixed modification selection was carbamidomethyl (C). Digestion was set to trypsin/p (cleavage even if followed by proline) with 2 missed cleavages. All other parameters were as per default settings except for the inclusion of the re-quantify setting; setting the threshold for false discovery rate (FDR) at the peptide spectrum match (PSM), peptide and protein levels to 1 (i.e. 100%); and setting a minimum number of peptides, razor + unique peptides and unique peptides all to 2. The peptides used for quantitation were also set to unique peptides only. Proteins were searched against the Uniprot Human reference proteome set (Taxon identifier 9606).

The output from MaxQuant was uploaded to Scaffold Q+ (version Scaffold_4.4.0, Proteome Software Inc., Portland, OR) for quantitation of SILAC peptide and protein identifications. Peptide identifications were accepted if they could be established at greater than 9.0% probability to achieve an FDR less than 0.1% by the Scaffold Local FDR algorithm. Protein identifications were accepted if they could be established at greater than 27.0% probability to achieve an FDR less than 1.0% and contained at least 2 identified peptides. Protein probabilities were assigned by the Protein Prophet algorithm (Nesvizhskii *et al.*, 2003). Proteins that contained similar peptides and could not be differentiated based on MS/MS analysis alone were grouped to satisfy the principles of parsimony. Acquired intensities in the experiment were globally normalized across all acquisition runs. Individual quantitative samples were normalized within each acquisition run. Intensities for each peptide identification

were normalized within the assigned protein. The reference channels were normalized to produce a 1:1 fold change. All normalization calculations were performed using medians to multiplicatively normalize data. Differentially expressed proteins were determined using Mann Whitney Test analysis.

3.2.3.7 Functional, network and pathway analysis

Identified proteins were analysed using Scaffold Q+S (version Scaffold_4.4.0, Proteome Software Inc., Portland, OR) and classified by Gene Ontology (GO) terms for molecular function, biological process and cellular component. Proteins with opposing trends between datasets were excluded from further analysis. Statistically significant enriched GO terms were identified using a web-based bioinformatics tool, the Database for Visualization and Integrated Discovery (DAVID) version 6.7 (<http://david.abcc.ncifcrf.gov/>) for gene enrichment. Official gene symbols of differentially regulated proteins were uploaded into DAVID and functional annotation analysis was conducted.

The Search Tool for the Retrieval of Interacting Genes (STRING) version 10 (<http://string-db.org/>) is a web-based database and was used to categorise likely protein interactions (Szkłarczyk *et al.*, 2014) for statistically significant differentially expressed proteins subsequent to DAVID analysis. Separate queries for differentially expressed proteins (up-regulated and down-regulated) were mapped for gene network enrichment and $p < 0.05$ was considered significant for pathway analyses. Interaction analyses were carried out using a confidence score setting of 0.9.

3.3 Results

3.3.1 Dose response of breast cancer cells treated with fucoidan

Dose response is represented as percentage viability of MCF7 cells after 24 h treatment with different concentrations of fucoidan (Figure 7). Cell viability decreased with increasing fucoidan concentrations. The concentration of fucoidan resulting in a 50% reduction in cell viability (IC_{50}) was determined as 0.2 mg/ml.

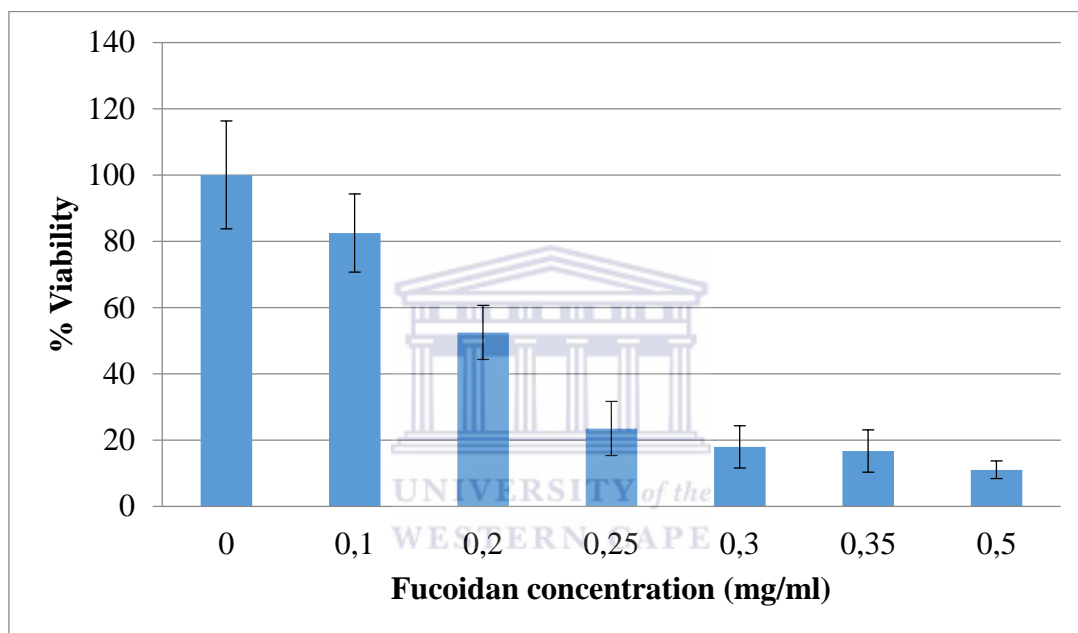


Figure 7: Percentage viability of MCF7 breast cancer cells after treatment with fucoidan. The data shown are the means \pm SD of three experiments.

3.3.2 Protein quantification standard curve

The BCA protein assay standard curve is presented in Figure 8, while the absorbance values for BSA standards are shown in Table 7. The R^2 value for the standard curve was 0.981. Tables 8 and 9 display the absorbance values for the protein samples and the calculated corresponding protein concentrations, respectively. Protein concentrations obtained ranged from 2.083 mg/ml – 3.327 mg/ml.

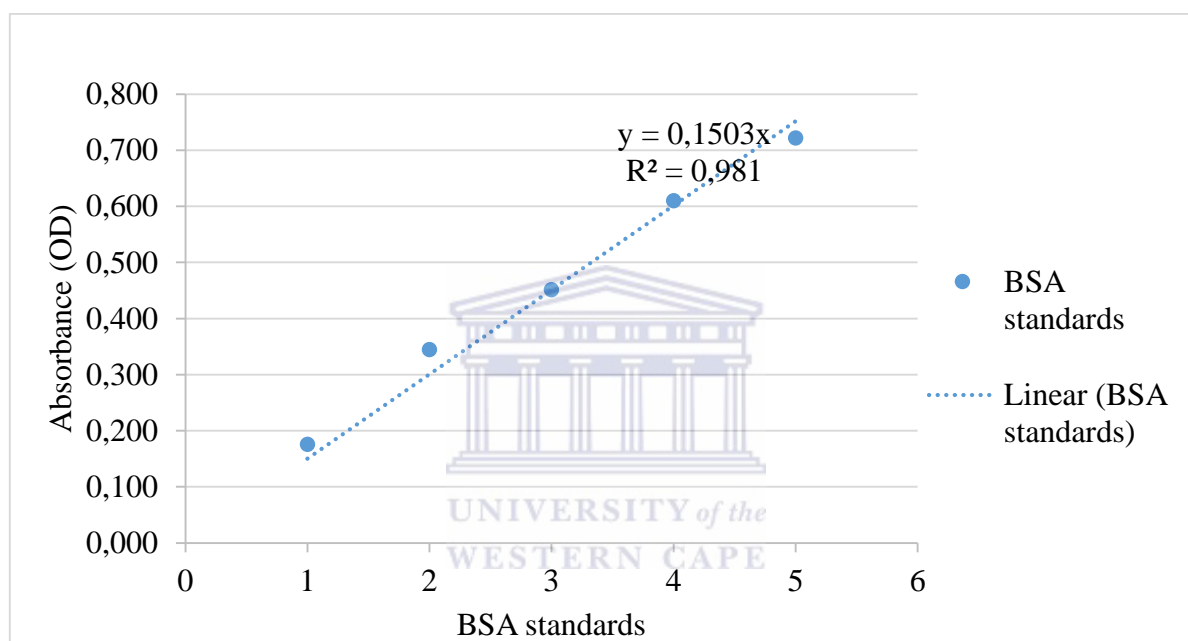


Figure 8: Standard curve of BSA standards for BCA protein quantification assay.

Table 7: Absorbance values of BSA standards.

Absorbance BSA standards					
	1	2	3	4	5
Ave	0.176	0.344	0.451	0.610	0.722
Stdev	0.010	0.033	0.027	0.032	0.009

Table 8: Absorbance values for protein samples.

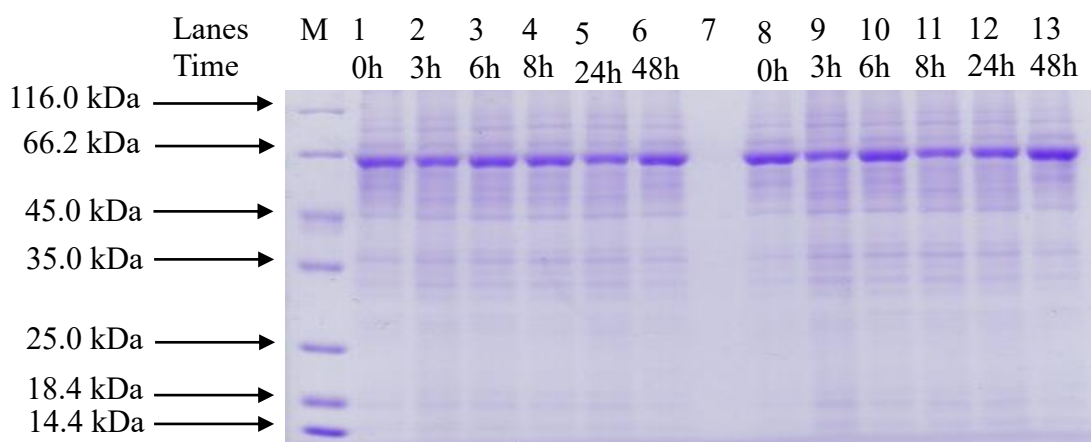
Absorbance protein samples												
	0C	0T	3C	3T	6C	6T	8C	8T	24C	24T	48C	48T
Ave	0.320	0.414	0.407	0.500	0.313	0.335	0.319	0.445	0.319	0.330	0.422	0.363
Stdev	0.004	0.014	0.103	0.034	0.012	0.004	0.034	0.011	0.003	0.064	0.044	0.054

Table 9: Protein concentrations calculated from standard curve and absorbance values.

Protein sample concentrations (mg/ml)												
	0C	0T	3C	3T	6C	6T	8C	8T	24C	24T	48C	48T
Ave	2.129	2.754	2.708	3.327	2.083	2.229	2.122	2.961	2.122	2.196	2.808	2.417

3.3.3 Western blot analysis of MCF7 protein extracts

MCF7 breast cancer cells were treated with fucoidan (0.2 mg/ml) and proteins were extracted at different time points. Control samples were not exposed to fucoidan. The MCF7 protein extractions were well separated by SDS-PAGE as seen by distinct bands (Figure 9). Subsequent Western blot analysis was performed with 2 antibodies: XIAP and Phospho ERK 1/2.

**Figure 9:** Coomassie-stained 1D SDS-PAGE acrylamide gel of total lysates produced from MCF7 cells. Twenty μg of protein was loaded per sample. Lanes M: molecular weight marker; Lanes 1-6: untreated cells; Lane 7: empty; Lanes 8-13: fucoidan treated cells.

3.3.3.1 XIAP Western blot analysis

Protein lysates produced from fucoidan treated cells were investigated for XIAP expression using Western blot analysis. Lysates from untreated cells revealed a gradual increase in expression with a sharp increase between time points 8 h and 24 h and a decrease in expression at 48 h. In the lysates from treated cells the increase in XIAP expression occurred more rapidly with distinct bands at 3 h, 6 h, 8 h and 24 h (Figure 10A). Densitometric analysis of band signal intensities is shown as relative density (fold change) in Figure 10B. XIAP expression increased 5-fold after 3 h of exposure with fucoidan and peaked at 6 h with >9-fold increase, followed by a gradual decrease over the next 42 h. Expression in untreated cells peaked at 24 h (19-fold increase).

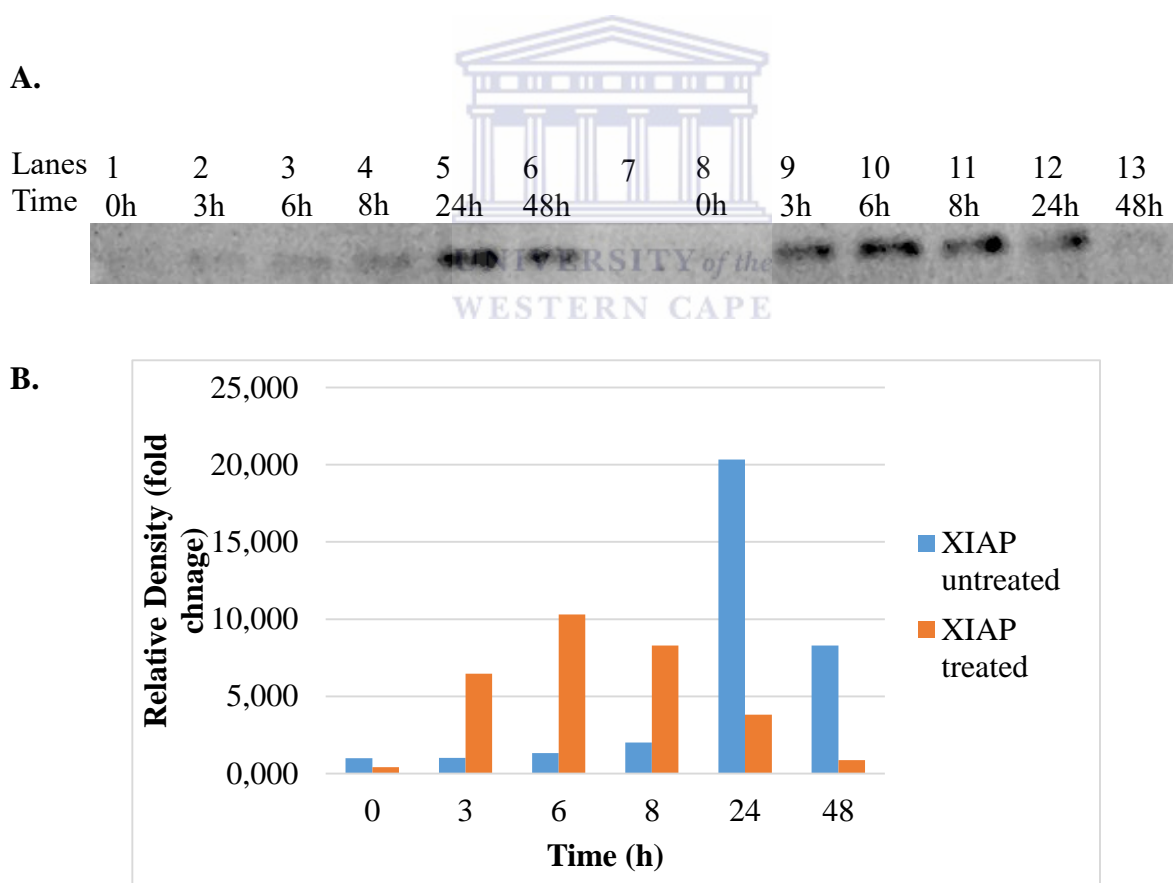


Figure 10: Effect of fucoidan on XIAP expression in MCF7 breast cancer cells over 48h of exposure to fucoidan. (A) Western blot image. Lanes 1-6: untreated cells; Lane 7: empty; Lanes 8-13: fucoidan treated cells. (B) Densitometric analysis of the relative density (fold change) of the signal intensities.

3.3.3.2 Phospho ERK1/2 Western blot analysis

In untreated MCF7 cells, phosphorylation of ERK1/2 gradually increased 26-fold over 48 h (Figure 11). Phosphorylation in fucoidan treated samples peaked at 6 h (8 fold increase) followed by a gradual decrease over time (Figure 11A). Expression over the first 6 h was significantly higher than levels in control cells.

A.

Lanes	1	2	3	4	5	6	7	8	9	10	11	12	13
Time	0h	3h	6h	8h	24h	48h		0h	3h	6h	8h	24h	48h



B.

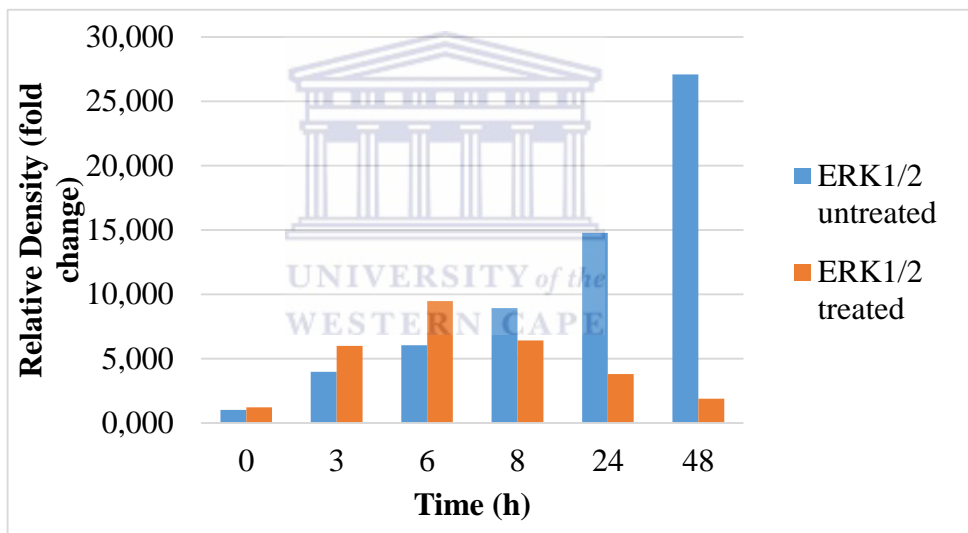
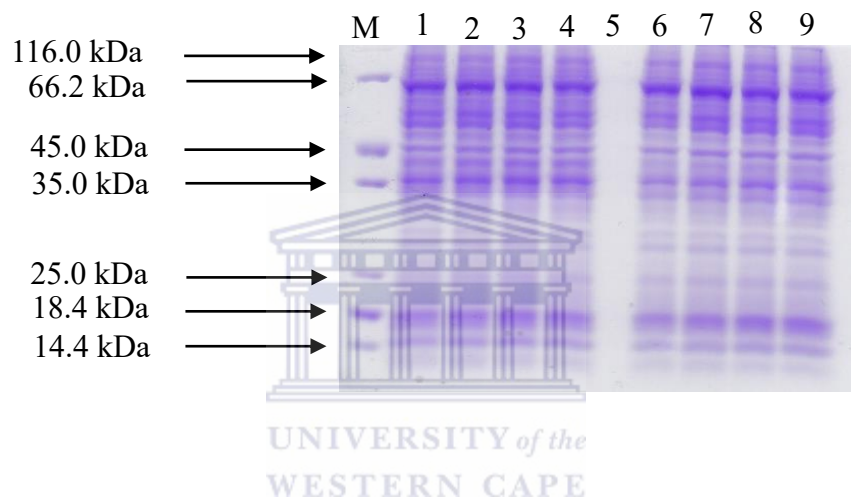


Figure 11: Effect of fucoidan on ERK1/2 expression in MCF7 breast cancer cells over 48h exposure to fucoidan. (A) Western blot image. Lanes 1-6: untreated cells; Lane 7: empty; Lanes 8-13: fucoidan treated cells. (B) Densitometric analysis of the relative density (fold changes) of the signal intensities.

3.3.4 SILAC protein quality and equal loading analysis

SILAC isotope metabolic protein labelling was carried out over a period of 13 weeks as suggested by a pilot SILAC labelling experiment (Section 3.2.3.4). Protein concentrations of SILAC labelled protein extracts were in the range of 2.9 - 3.46 mg/ml. Separation by SDS-PAGE revealed clear, distinct bands indicating good quality protein extracts (Figure 12A and 12B).

A.



B.

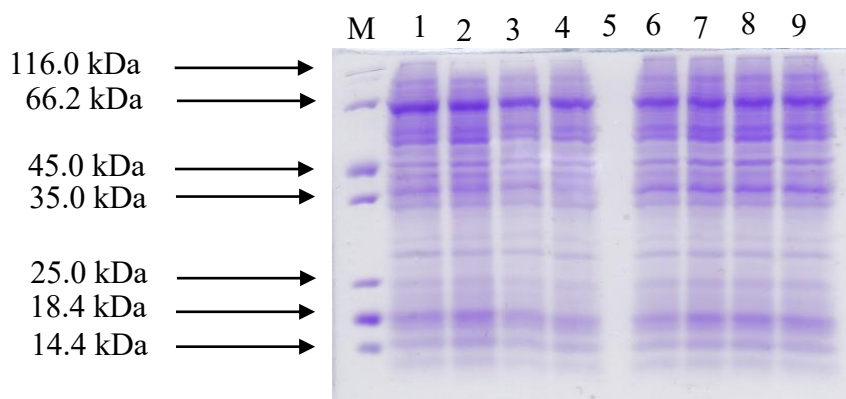
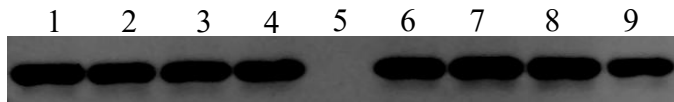


Figure 12: Coomassie-stained 1D SDS-PAGE gels of (A) light and (B) heavy SILAC labelled protein extractions from MCF7 cells. Twenty μg of protein was loaded per lane. Lane M: molecular weight marker; Lanes 1-4: untreated samples; Lane 5, empty lane; Lanes 6-9, fucoidan treated samples.

Confirmation of protein quantification was performed by Western blot analysis with actin, a method commonly used as a loading control (Figures 13A and 13B). Western blot results display that SILAC protein loadings were near equal.

A.



B.

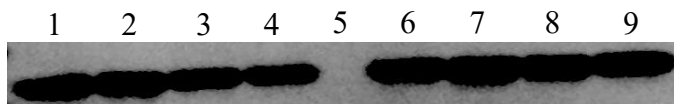


Figure 13: Actin Western blot analysis to investigate equal loading and accuracy of protein quantification. (A) Light-labelled SILAC proteins samples. (B) Heavy-labelled SILAC proteins samples. Lanes 1-4, untreated samples; lane 5, empty; lanes 6-9, fucoidan treated samples.

3.3.5 SILAC mass spectrometry analysis

Mass spectrometry SILAC protein analysis of light labelled fucoidan treated and heavy labelled untreated samples (Data Set 1) resulted in identification of 2098 proteins. Analysis of heavy treated and light untreated samples (Data Set 2) resulted in identification of 2155 proteins. Of these, 1704 and 1776 proteins, respectively, satisfied 95% confidence using Scaffold 4 Q + S Proteomics Software. Proteins were classified by GO terms for molecular function (Figure 14), biological process (Figure 15) and cellular component (Figure 16).

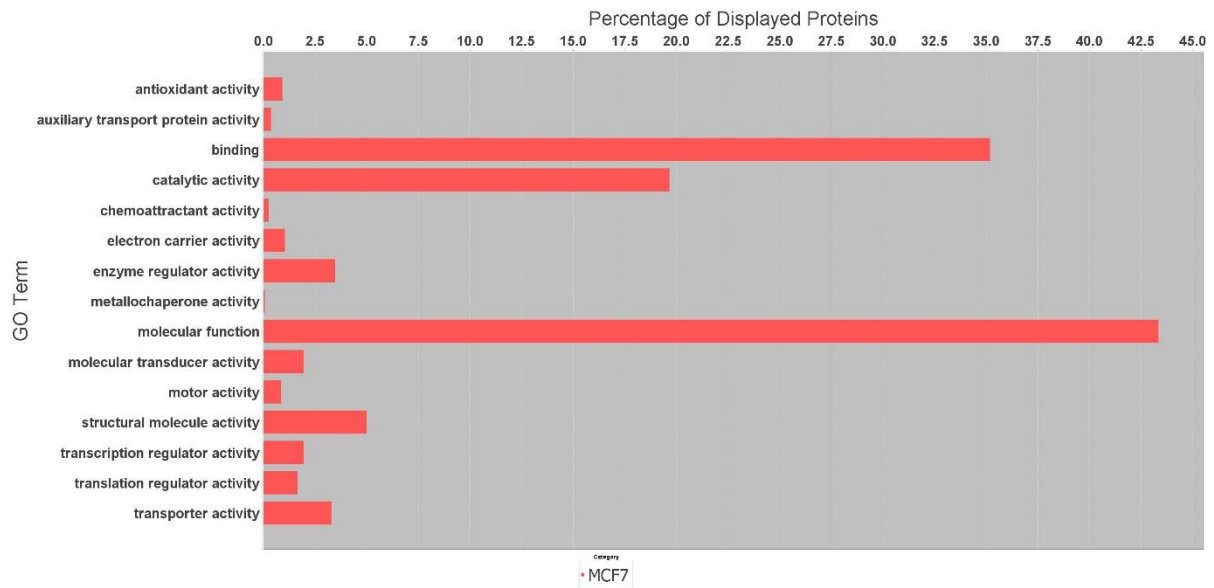


Figure 14: Functional classification of identified proteins using NCBI annotations based on universal Gene Ontology terms for molecular function. Protein classification is shown as percentage proteins expressed for each molecular function category for all identified proteins (adapted from Scaffold).

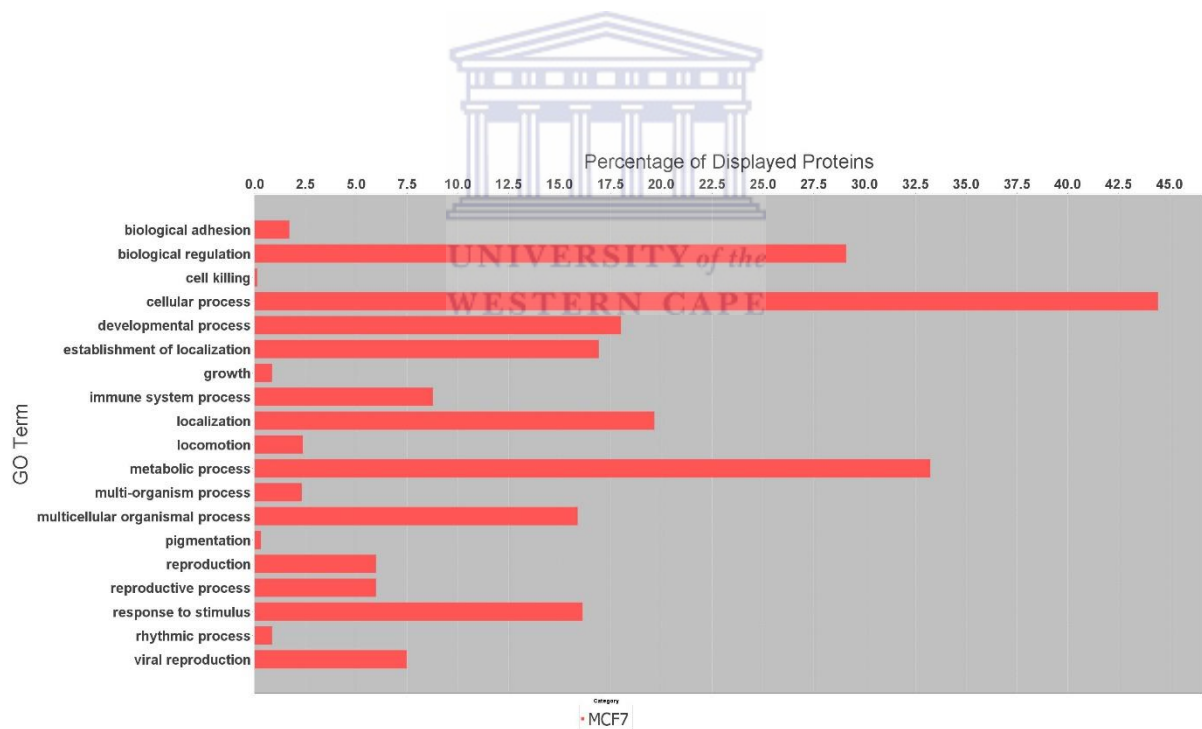


Figure 15: Functional classification of identified proteins using NCBI annotations based on universal Gene Ontology terms for biological process. Protein classification is shown as percentage proteins expressed for each biological process category for all identified proteins (adapted from Scaffold).

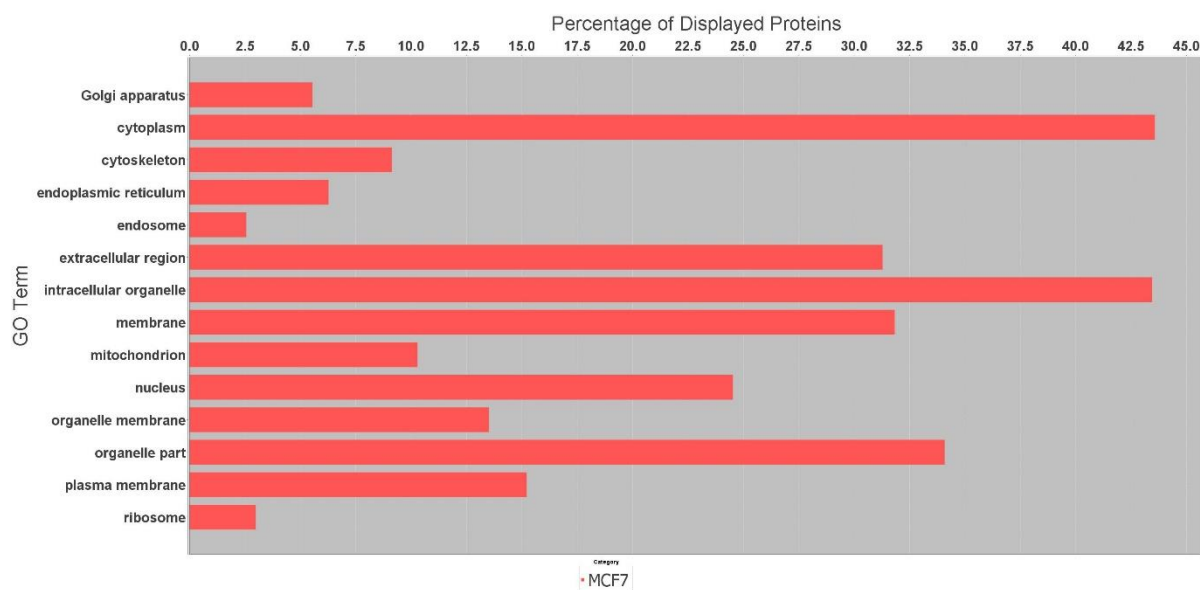


Figure 16: Functional classification of identified proteins using NCBI annotations based on universal Gene Ontology terms for cell component. Protein classification is shown as percentage proteins expressed for each cellular component category for all identified proteins (adapted from Scaffold).

Comparison between data sets revealed discrepancies in differentially regulated proteins (i.e. up-regulated in Data Set 1 and down-regulated in Data Set 2). Proteins which were similarly expressed in both data sets are listed in Table A1 (Appendix). This included a total of 392 proteins of which 201 were up-regulated and 191 down-regulated.

DAVID enrichment analysis revealed 233 proteins (130 up-regulated and 123 down-regulated) with an enrichment score above 1.3. A score above 1.3 concurs with a p-value of 0.05 (Huang *et al.*, 2009). Subsequent STRING interaction analysis was carried out using the highest confidence level (0.9). Significance of pathways was considered for $p < 0.05$. Using STRING, analysis of biological processes for the up-regulated proteins revealed proteins associated with the positive regulation of processes such as cell cycle arrest, ubiquitin-protein ligase activity involved in proteasomal degradation and cellular catabolic process were observed. Moreover, among the up-regulated proteins were 19 proteins related to cell death (Figure 17). Of these,

18 were related to programmed cell death. For down-regulated proteins, proteins involved in positive regulation of intrinsic apoptotic pathway were observed. Figures of the up- and down-regulated proteins involved in the cell cycle arrest (Figure A1), proteasomal degradation (Figure A2), cellular catabolic process (Figure A3) and the intrinsic apoptotic pathway (Figure A4) mentioned are shown in the Appendix. Functions of proteins, high-lighted by STRING for having biological processes which are connected to cell death, are presented in Table 10.



Table 10: Functions of 19 cell death-associated proteins.

Protein	Function	Refs
DSP	Involved in desmosomal cadherin-plakoglobin complex into plasma membrane domains and anchoring intermediate filaments to the desmosomes	Rampazzo <i>et al.</i> , 2002
HTT	Possible role in microtubule-mediated transport or vesicle function	Gauthier <i>et al.</i> , 2004
ALDOC	Glycolytic enzyme that catalyzes the reversible aldol cleavage of fructose-1,6-biphosphate and fructose 1-phosphate to dihydroxyacetone phosphate and either glyceraldehyde-3-phosphate or glyceraldehyde, respectively	Fujita <i>et al.</i> , 2014
GPI	Glycolytic enzyme, can function as tumor-secreted cytokine and angiogenic factor	Knight <i>et al.</i> , 2014
GAPDH	Plays a role in glycolysis. Involved in several functions i.e. transcription, RNA transport, DNA replication and apoptosis	Nicholls <i>et al.</i> , 2012
CSE1L	Possible role in cell proliferation and apoptosis	Lorenzato <i>et al.</i> , 2012
MYBBP1A	May positively or negatively regulate transcription	Mori <i>et al.</i> , 2012
EIF4G2	May be involved in cap-dependent translation to IRES-mediated translation during apoptosis, mitosis and viral infection.	Ghosh & Lasko, 2015
PRKDC	Involved in repair of DNA double strand breaks and recombination	Zhou <i>et al.</i> , 2014
DDX5	Plays a role in transcriptional regulation	Laurent <i>et al.</i> , 2011
PPP2CA	Phosphatase for dephosphorylation of the 20S proteasome	Patil <i>et al.</i> , 2013
PAK2	May play a role in the apoptotic process	Marlin <i>et al.</i> , 2009
PSMA5	Subunit of 20S proteasome complex	Udeshi <i>et al.</i> , 2012
PSMB4	Subunit of 20S proteasome complex	Sánchez-Lanzas <i>et al.</i> , 2014
PSMB5	Subunit of 20S proteasome complex	Vangata <i>et al.</i> , 2014
PSMB6	Subunit of 20S proteasome complex	Sánchez-Lanzas <i>et al.</i> , 2014

PSMC5	Subunit of 19S proteasome complex regulatory particle	Ohnishi <i>et al.</i> , 2015
GNB2L2	May be involved in recruitment, assembly and regulation of signalling molecules	Chang <i>et al.</i> , 2001
SQSTM1	Autophagosome cargo protein. Targets and binds to proteins for selective autophagy	Zhang <i>et al.</i> , 2013a



3.4 Discussion

Fucoidan has been shown to inhibit the growth of cancerous cells (Fukahori *et al.*, 2008; Zhang *et al.*, 2011; Mak *et al.*, 2014) and display an apoptotic effect on various cancerous cell lines (Kim *et al.*, 2010; Lee *et al.*, 2012; Park *et al.*, 2013) with no effect on non-cancerous cells (Kawamoto *et al.*, 2006; Zhang *et al.*, 2011; Xue *et al.*, 2012). Several studies have been conducted on the effect of fucoidan on the mammalian MCF7 breast cancer cell line (Yamasaki-Miyamoto *et al.*, 2002; Xue *et al.*, 2012). The current study investigates the effects of fucoidan treatment on the MCF7 proteome.

Bioactivity of fucoidan is said to be dependent on its structure and molecular weight, correlating with an increase in sulfate to fructose ratio and fucoidan polysaccharides of lower molecular weight (Cho *et al.*, 2011). Although the biochemical structure of fucoidan has not yet been fully elucidated, several factors including species and age of algae, season of sampling, area of sampling and extraction method (Duarte *et al.*, 2001; Skriptsova *et al.*, 2010) have been reported to play a role in its complex structure. This study used a commercially available crude extract of fucoidan from *Fucus vesiculosus* with molecular weight ranging between 20-200 kDa purchased from Sigma-Aldrich.

3.4.1 MCF7 cell viability in response to fucoidan treatment

Colorimetric cell viability assays with tetrazolium salts are routinely used to investigate the effect of compounds on cellular activities of mammalian cells such as cell proliferation and cell death (Berridge *et al.*, 2005). These assays assess the viability of *in vitro* cell cultures following exposure to test compounds. The tetrazolium salt WST-1 (4-[3-(4-Iodophenyl)-2-(4-nitrophenyl)-2H-5-tetrazolio]-1,3-benzene disulfonate) was used to demonstrate cell viability of MCF7 cells in response to fucoidan treatment as described in Section 3.3.1 (page 55). WST-

1 is composed of a tetrazole ring with four nitrogen atoms, surrounded by three aromatic groups that have phenyl moieties. One phenyl moiety is disulfonated, while another contains an iodine residue. Extracellular reduction of WST-1 occurs via electron transport across the plasma membrane by intracellular NADH (Berridge & Tan, 1998). Reduction of tetrazolium occurs via cleavage of the tetrazolium ring to form dark red formazan. Therefore, the amount of formazan produced is directly proportional to the number of viable cells.

In this study, cell viability assays using the WST-1 cell proliferation reagent demonstrated a decrease in viability of MCF7 cells treated with fucoidan at all the fucoidan concentrations tested. The commercial fucoidan sample displayed an IC_{50} of 0.2 mg/ml for MCF7 cells is shown in Figure 7. IC_{50} is defined as the concentration of a substance or drug which exhibits 50% of the maximal inhibitory response (Sebaugh, 2011). The study by Banafa *et al.* (2013) also investigated the cytotoxic effects of fucoidan and found an inhibition of cell proliferation of close to 30% in MCF7 cells treated with fucoidan concentration of 0.2 mg/ml and 60% for 0.3 mg/ml fucoidan concentration. Mak *et al.* (2014) reported an IC_{50} of 0.515 mg/ml for MCF7 cells in response to commercial fucoidan treatment. The IC_{50} value of 0.2 mg/ml for fucoidan in MCF7 cells established in the current study is therefore in agreement with previous studies.

3.4.2 Western blot analysis

Protein extracted from MCF7 cells treated with 0.2mg/ml fucoidan (IC_{50}) yielded concentrations ranging from 2.083 mg/ml – 3.327 mg/ml. Protein extracts were subjected to Western blot analysis to ascertain the effect of fucoidan treatment on expression of specific markers. Antibodies selected as markers were XIAP and Phospho ERK 1/2. These are markers for inhibition of apoptosis (Eckelman *et al.*, 2006) and regulation of cell proliferation, respectively (Meloche & Pouysségur, 2007). Previous studies have reported down-regulation

of several anti-apoptotic or pro-survival proteins, while expression of proteins involved in apoptosis were up-regulated (Atashrazm *et al.*, 2015).

3.4.2.1 XIAP

The inhibitor of apoptosis protein (IAP) family is important as members are pro-survival proteins which are able to inhibit apoptosis via intrinsic and extrinsic apoptotic pathways (Eckelman *et al.*, 2006). XIAP expression was examined by Western blot analysis over time to establish if fucoidan treatment decreases its expression and therefore renders cells more susceptible to apoptosis. Untreated samples showed gradual increase in expression reaching a 7-fold increase by 48 h (Figure 10). In the treated samples, expression peaked at 6 h (9-fold) followed by a steady decrease in expression. Expression of XIAP in the untreated samples indicated that cell survival mechanisms were in place and expression trends could be explained by cells competing for space and nutrients. In the treated samples, the increase in expression XIAP followed by a decrease indicate that cell death mechanisms were activated.

Banafa *et al.* (2014) have reported that fucoidan induced apoptosis and down-regulated XIAP in MDA-MB-231 breast cancer cells. XIAP down-regulation has also been shown to sensitise cells to apoptosis via chemotherapeutic drugs in MCF7 cells (Lima *et al.*, 2004) and gastric cancer cells (Tong *et al.*, 2005). Park *et al.* (2013) examined the induction of apoptosis in human leukemia cells U937. XIAP showed a decrease in signal intensity with increasing concentration of fucoidan (20, 40, 60 and 80 µg/ml). Park *et al.* (2014) also observed a significant decrease in XIAP expression and an inhibition of proliferation in T24 human urinary bladder cancer cells with 100 and 150 µg/ml of fucoidan.

Similar studies with bioactive compounds against a range of cancerous cells (Messmer *et al.*, 2001; Sasaki *et al.*, 2000; Qiao *et al.*, 2008) confirmed that XIAP down-regulation plays a role

in induction of apoptosis. Inhibition of caspase activity by IAP proteins may occur through either proteasomal degradation or enzymatic inhibition. Among the IAP proteins, X-linked inhibitor of apoptosis protein (XIAP) is the most extensively studied (Elmore, 2007). XIAP functions to inhibit apoptosis by direct interaction with caspase proteins (Eckelman *et al.*, 2006). The structure of XIAP consists of three baculoviral IAP repeat (BIR) domains and a ring domain. The BIR2 and BIR3 domains contain binding sites which participate in caspase inhibition. XIAP strongly inhibits caspase activity at the initiator and effector level. IAPs are often found to be overexpressed in cancerous cells (Eckelman *et al.*, 2006; Galbán & Duckett, 2010).

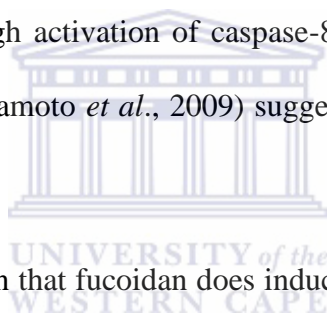
3.4.2.2 Phospho ERK1/2

Phosphorylated Extracellular Signal-Regulated Kinase 1 and 2 (Phospho ERK1/2), proteins in the mitogen-activated protein kinase (MAPK) cascade pathway, is implicated in downstream protein synthesis which plays a role in cell differentiation and proliferation (Lu & Xu, 2006; Roskoski, 2012). Inappropriate activation of ERK1/2 is a common occurrence in human cancers. Phosphorylation of ERK1/2 proteins was studied over time to determine the effect of 0.2 mg/ml commercial fucoidan on activation of the MAPK cascade. In untreated cells, phosphorylation of ERK1/2 appeared to increase over time with high levels of phosphorylated ERK1/2 at 48 h. In contrast, phosphorylation in fucoidan treated samples was characterized by an increase over the first 6h followed by a decrease. This decrease may be due to dephosphorylation or degradation of ERK1/2 and thus a decrease in ERK1/2 activity, which has been associated with an increased sensitivity to apoptosis in cells (Lu & Xu, 2006). Results suggest that fucoidan inhibits inappropriate activation of the Phospho ERK1/2 cascade in cancerous MCF7 cells. Xue *et al.* (2012) also observed decreased expression of ERK1/2 with

increasing concentrations of fucoidan (Sigma-Aldrich) in 4T1 cells (mouse breast cancer). Aisa *et al.* (2005) observed the same effect for fucoidan from Sigma-Aldrich in HS-Sultan cells (human lymphoma). In contrast, Zhang *et al.* (2011 and 2013) have shown that fucoidan extracted from *Cladosiphon novae-caledoniae* Kylin (820 µg/m and 200 µg/ml, respectively) resulted in phosphorylation of ERK1/2 in MCF7 breast cancer cells. However, apoptosis occurred regardless. They stated that activation of ERK1/2 may aid in the induction of apoptosis. ERK1/2-facilitated apoptosis has been reported but is not well-understood (Mebratu & Tesfaigzi, 2009). Hyun *et al.* (2009) also demonstrated activation of ERK1/2 by an increase in Phospho ERK1/2 over time with 100 µg/ml fucoidan.

MAPK cascade proteins take part in extracellular signal transduction and phosphorylation of these proteins signifies activation of cascade. Aberrant regulation of the MAPK cascade may result in a range of diseases (Mebratu & Tesfaigzi, 2009) and up-regulation has been implicated in numerous cancers (Roskoski, 2012). Discrepancies in ERK activation in MCF7 cells (Zhang *et al.*, 2011 and 2013) may be attributed to different fucoidan sources or pre-treatment of cells with N-acetyl-L-cysteine (NAC), a reactive oxygen species (ROS) inhibitor. Studies have shown that treatment of cells with NAC influences protein expression of key proteins linked to apoptosis and survival, including, Mcl-1, p21, caspase-3 (Halasi *et al.*, 2013) and Phospho ERK1/2 (Zhang *et al.*, 2011a). NAC furthermore has a cyto-protective role, protecting cells against ROS-related toxicity (Zhang *et al.*, 2011a). Both studies by Zhang *et al.* (2011 and 2013) acknowledged a reduction in apoptosis in fucoidan treated cells as a result of NAC pre-treatment compared to the control treated with fucoidan only. Furthermore, apoptosis induction regardless of ERK activation for fucoidan treatment could imply that ERK activation does not play a significant or essential role in fucoidan-induced apoptosis. ERK activation as seen in the study on HCT-15 colon cancer cells by Hyun *et al.* (2009) could be a cell line dependent response.

Caspase-3 is an enzyme that plays a key role in programmed cell death, or apoptosis (Plati *et al.*, 2011). In a HCT-15 colon carcinoma cell line, Hyun *et al.* (2009) reported caspase-3 activation after 24 and 48 h incubation with 100 µg/ml fucoidan. Xue *et al.* (2012) observed decreasing levels of pro-caspase-3 and increasing levels of cleaved caspase-3 with increasing concentrations of fucoidan in 4T1 cells, a mouse breast cancer cell line. Park *et al.* (2014) observed the same effect in T24 human urinary bladder cancer cells using 50, 100 and 150 µg/ml fucoidan. Significant decreases in levels of pro-caspases-3, -8 and -9 were reported, while induction of caspase-3, -8 and -9 activities were evident with increasing concentrations of fucoidan. Decrease in levels of pro-caspases-3, -8 and -9 in conjunction with increases in levels caspases-3,-8 and -9 are indicative of caspase activation. In MCF7 cells, apoptosis induction has been shown through activation of caspase-8 (Banafa *et al.*, 2013) as well as caspase-7 and -9 (Yamasaki-Miyamoto *et al.*, 2009) suggestive of induction via the intrinsic and extrinsic pathways.



Consequently, studies have shown that fucoidan does induce apoptosis via caspase activation in various cell lines as well as MCF7 breast cancer cells. Apoptosis, a form of programmed cell death, plays an important role in maintaining homeostasis by removing aging, defective and unnecessary cells. It is characterised by membrane blebbing (cell membrane protrusion) and DNA fragmentation (Portt *et al.*, 2011). The controlled process is mediated by caspase activation and comprises of the extrinsic, intrinsic and the endoplasmic reticulum stress pathways. The extrinsic or death receptor signalling pathway is instigated by death receptors on the cell's surface, whereas the intrinsic or mitochondrial signalling pathway occurs due to mitochondrial stress (Wong *et al.*, 2011). Cysteine aspartic acid-specific proteases or caspases are a family of endoproteases mostly associated with apoptosis, with some implicated in inflammation. Caspases are expressed in an inactive form and are activated through cleavage at aspartic acid amino acid residues (Elmore, 2007), although initial activation occurs through

the formation of dimers with specific protein complexes (Eckelman *et al.*, 2006). They may be classified as either initiator or effector caspases. The initiator caspases are activated early in apoptotic pathways, while the effector caspases are activated downstream in these pathways. As an effector caspase, activation of caspase-3 leads to several downstream processes including cell collapse, chromosomal degradation and expression of ligands for phagocytic recognition.

3.4.3 SILAC mass spectrometry analysis

SILAC labelling of MCF7 cells resulted in identification of more than 2000 proteins of which more than 1700 were identified at 95% confidence. Proteins were grouped by GO terms within molecular function, biological process and cellular component categories. Most common molecular functions were binding (approx. 35%) and catalytic activity (approx. 20%). Foremost biological processes were cellular (approx. 45%), metabolic (approx. 32.5-35%) and biological regulation (approx. 27.5-30%). Major cellular components noted were cytoplasm (approx. 42.5-45%), intracellular organelle (approx. 42.5-45%), organelle part (approx. 32.5-35%), membrane (approx. 30-32.5%) and extracellular region (approx. 30-32.5%).

Data sets generated for light labelled fucoidan treated / heavy labelled untreated and heavy labelled fucoidan treated / light labelled untreated MS analysis were largely not in agreement. Amongst replica experiments, only 392 out of over 2000 proteins were in agreement in terms of direction of expression (up- or down-regulation). Biological processes for up-regulated proteins indicate cell cycle arrest, proteasomal degradation and cellular catabolic processes. Cell cycle arrest is linked to an inhibition in cell proliferation and apoptotic cell death (Park *et al.*, 2014) while proteasomal degradation and cellular catabolism show the cellular break down of proteins and cellular molecules. Together, the biological processes may be suggestive of growth inhibition and cell death. Biological processes for the down-regulated proteins indicate

down-regulation of the intrinsic apoptotic pathway. This, in conjunction with the up-regulated biological processes could suggest that the intrinsic apoptotic pathway is not utilized in favour of other apoptotic pathways.

Nineteen up-regulated proteins were found to be associated with cell death although to date none have been studied with regards to fucoidan treatment. Although not linked to the regulation of specific proteasomal subunits, studies have found that fucoidan treatment leads to proteasomal degradation of certain proteins in several cell lines (Hsu *et al.*, 2014; Kim *et al.*, 2014). Interestingly, of the 19 proteins, GAPDH, was shown in previous studies to be unaffected by fucoidan treatment and therefore was used as a standard or loading control (Lee *et al.*, 2012; Banafa *et al.*, 2013; Yang *et al.*, 2013). Although SILAC is described as a robust and reproducible technique (Ong & Mann, 2006), the discrepancies in data has rendered the analysis inconclusive. While proteins associated with cell death were observed among the up-regulated proteins, SILAC results need to be repeated to ensure reproducibility.

A recent review has reported that labelled and label-free MS proteomics approaches do not out-perform each other and that overall accuracy of either approach is reliant on the experimental setup (Filiou *et al.*, 2012). Concerns regarding SILAC include quantification of proteins only if identified in both samples of the pair-wise comparison. Stochastically occurring protein identifications could result in quantification not always taking place. A proteomic study on human lung cells in response to Copper oxide nanoparticles similarly reported only a total of 186 identified proteins which were in agreement between replica sample runs, although reasons for this effect were unexplained (Edelmann *et al.*, 2014).

Considering all results, it appears that fucoidan-mediated cell death in MCF7 cells occurs via the induction of apoptosis as observed by the down-regulation of apoptosis inhibitory protein, XIAP and cell survival promoting protein, ERK1/2. Although SILAC results did not confirm

expression of these proteins, proteins which were in agreement suggest that cell death mechanisms were up-regulated.

3.5 Conclusion

In conclusion, cell viability assays with WST-1 have shown that MCF7 cell death occurs as a result of fucoidan treatment. Decrease in expression of XIAP and phosphorylation of ERK1/2 supports apoptosis activation. Fucoidan treatment resulted in apoptosis, however, the exact pathway or mechanism remains unclear. SILAC analysis was inconclusive as the vast majority of identified proteins were ambiguous, displaying opposing trends in regulation between data sets for many proteins.

Future work includes a repeat of the SILAC study at lower flow rates. Both pair-wise detection of heavy and light labels as well as single sample analysis should be performed to determine accuracy of pair-wise analysis. Western blot analysis should be expanded to include caspases involved each of the apoptosis pathways and proteins associated with apoptosis to ascertain the exact apoptotic pathway involved and mechanism of action involved in fucoidan-mediated apoptosis. Expression analysis (qRT-PCR and Western blot) could be conducted on the up-regulated proteins identified by STRING analysis for confirmation of differential expression.

References

1. Atashrazm, F., Lowenthal, R. M., Woods, G. M., Holloway, A. F. & Dickinson, J. L., 2015. Fucoidan and cancer: A multifunctional molecule with anti-tumor potential. *Marine Drugs*, 13, pp.2327–2346.
2. Banafa, A.M., Roshan, S., Liu, Y., Zhao, S., Yang, G., He, G., Chen, M., 2014. Fucoidan induces apoptosis in MDA-MB-231 cells by activating caspase cascade and down-regulating XIAP. *Journal of Pharmacy and Biological Sciences*, 9, pp.59–64.
3. Banafa, A.M., Roshan, S., Liu, Y., Chen, H., Chen, M., Yang, G., He, G., 2013. Fucoidan induces G 1 phase arrest and apoptosis through caspase-dependent pathway and ROS induction in human breast cancer MCF-7 cells. *Journal of Huazhong University of Science and Technology-Medical Science*, 33, pp.717–724.
4. Berridge, M.V., Herst, P.M. & Tan, A.S., 2005. Tetrazolium dyes as tools in cell biology: New insights into their cellular reduction. *Biotechnology Annual Review*, 11, pp.127–152.
5. Berridge, M.V. & Tan, A.S., 1998. Trans-plasma membrane electron transport: A cellular assay for NADH- and NADPH-oxidase based on extracellular, superoxide-mediated reduction of the sulfonated tetrazolium salt WST-1. *Protoplasma*, 205, pp.74–82.
6. Chang, B.Y., Chiang, M. & Cartwright, C.A., 2001. The interaction of Src and RACK1 is enhanced by activation of protein kinase C and tyrosine phosphorylation of RACK1. *The Journal of Biological Chemistry*, 276, pp.20346-20356
7. Chevolut, L., Mulloy, B., Ratiskol, J., Foucault, A. & Collic-Jouault, S., 2001. A disaccharide repeat unit is the major structure in fucoidans from two species of brown algae. *Carbohydrate Research*, 330, pp.529–535.

8. Cho, M.L., Lee, B.Y. & You, S.G., 2011. Relationship between oversulfation and conformation of low and high molecular weight fucoidans and evaluation of their in Vitro anticancer activity. *Molecules*, 16, pp.291–297.
9. Duarte, M.E.R., Cardoso, M.A., Nosedá, M.D. & Cerezo, A.S., 2001. Structural studies on fucoidans from the brown seaweed *Sargassum stenophyllum*. *Carbohydrate Research*, 333, pp.281–293.
10. Eckelman, B.P., Salvesen, G.S. & Scott, F.L., 2006. Human inhibitor of apoptosis proteins: why XIAP is the black sheep of the family. *European Molecular Biology Organization Reports*, 7, pp.988–994.
11. Edelmann, M.J., Shack, L.A., Naske, C.D., Walters, K.B. and Nanduri, B., 2014. SILAC-based quantitative proteomic analysis of human lung cell response to copper oxide nanoparticles. *PLoS ONE*, 9, p.e114390.
12. Elmore, S., 2007. Apoptosis: a review of programmed cell death. *Toxicologic Pathology*, 35, pp.495–516.
13. Ferlay J, Soerjomataram I, Ervik M, Dikshit R, Eser S, Mathers C, Rebelo M, Parkin DM, Forman D, Bray, F. GLOBOCAN 2012 v1.0, Cancer Incidence and Mortality Worldwide: IARC CancerBase No. 11 [Internet]. Lyon, France: International Agency for Research on Cancer; 2013. Available from: <http://globocan.iarc.fr>, accessed on 15/July/2015
14. Fukahori, S., Yano, H., Akiba, J., Ogasawara, S., Momosaki, S., Sanada, S., Kuratomi, K., Ishizaki, Y., Moriya, F., Yagi, M. & Kojiro, M., 2008. Fucoidan, a major component of brown seaweed, prohibits the growth of human cancer cell lines in vitro. *Molecular medicine reports*, 1(4), pp.537–542.
15. Fujita, H., Aoki, H., Ajioka, I., Yamazaki, M., Abe, M., Oh-Nishi, A., Sakimura, K. & Sugihara, I., 2014. Detailed expression pattern of Aldolase C (Aldoc) in the cerebellum,

- retina and other areas of the CNS studied in Aldoc-Venus knock-in mice. *PLoS ONE*, 9, p.e86679
16. Galbán, S. & Duckett, C.S., 2010. XIAP as a ubiquitin ligase in cellular signaling. *Cell Death and Differentiation*, 17, pp.54–60.
17. Gauthier, L.R., Charrin, B.C., Borrel-Pagès, M., Dompierre, J.P., Rangone, H., Cordelières, F.P., De Mey, J., MacDonald, M.E., Lessmann, V., Humbert, S. and Saudou, F., 2004. Huntingtin controls neurotrophic support and survival of neurons by enhancing BDNF vesicular transport along microtubules. *Cell*, 118, pp.127-138
18. Ghosh, S. & Lasko, P., 2015. Loss-of-function analysis reveals distinct requirements of the translation initiation factors eIF4E, eIF4E-3, eIF4G and eIFG2 in *Drosophila* spermatogenesis. *PLoS ONE*, 10, p.e0122519
19. Halasi, M., Wang, M., Chavan, T.S., Gaponenko, V., Hay, N. & Gartel, A.L., 2013. ROS inhibitor N-acetyl-L-cysteine antagonizes the activity of proteasome inhibitors. *Biochemical Journal*, 454, pp.201–208.
20. Hsu, H.Y., Lin, T.Y., Wu, Y.C., Tsao, S.M., Hang, P.A., Shih, Y.W. & Hsu, J., 2014. Fucoidan inhibition of lung cancer in vivo and in vitro : role of the Smurf2-dependent ubiquitin proteasome pathway in TGF β receptor degradation. *Oncotarget*, 5, pp.7870-7885
21. Hyun, J.H., Kim, S.C., Kang, J.I., Kim, M.K., Boo, H.J., Kwon, J.M., Koh, Y.S., Hyun, J.W., Park, D.B., Yoo, E.S. & Kang, H.K., 2009. Apoptosis inducing activity of fucoidan in HCT-15 colon carcinoma cells. *Biological & pharmaceutical bulletin*, 32, pp.1760–1764.
22. Jones, M.E., van Leeuwen, F.E., Hoogendoorn, W.E., Mourtis, M.J.E., Hollema, H., van Boven, H., Press, M.F., Bernstein, L. & Swerdlow, A.J., 2012. Endometrial cancer

- survival after breast cancer in relation to tamoxifen treatment: pooled results from three countries. *Breast Cancer Research : BCR*, 14, p.R91.
23. Kim, E.J., Park, S.Y., Lee, J.Y. & Park, J.H.Y., 2010. Fucoïdan present in brown algae induces apoptosis of human colon cancer cells. *BioMed Central Gastroenterology*, 10, pp.96.
24. Kim, Y.W., Baek, S.H., Lee, S.H., Kim, T.H. & Kim, S.Y., 2014. Fucoïdan, a sulfated polysaccharide, inhibits osteoclast differentiation and function by modulating RANKL signaling. *International Journal of Molecular Sciences*, 15, pp.18840–18855.
25. Knight, A.L., Yan, X., Hamamichi, S., Ajjuri, R.R., Mazzulli, J.R., Zhang, M.W., Daigle, J.G., Zhang, S., Borom, A.R., Roberts, L.R., Lee, S.K., DeLeon, S.M., Viollet-Djelassi, C., Krainc, D., O'Donnell, J.M., Caldwell, K.A. & Caldwell, G.A., 2014. The glycolytic enzyme, GPI-1, is a functionally conserved modifier of dopaminergic neurodegeneration in Parkinson's models. *Cell Metabolism*, 20, pp.145-157
26. Laurent, F.X., Sureau, A., Klein, A.F., Trouslard, F., Gasnier, E., Furling, D. and Marie, J., 2011. New function of the RNA helicase p68/DDX5 as a modifier of MBNL1 activity on expanded CUG repeats. *Nucleic Acids Research*, 14, pp.1-13
27. Lee, H., Kim, J.S. & Kim, E., 2012. Fucoïdan from seaweed *Fucus vesiculosus* inhibits migration and invasion of human lung cancer cell via PI3K-Akt-mTOR pathways. *PloS ONE*, 7, p.e50624.
28. Li, B., Lu, F., Wei, X., & Zhao, R., 2008. Fucoïdan: structure and bioactivity. *Molecules*, 13, pp.1671–1695.
29. Lima, R.T., Martins, L.M., Guimarães, J.E., Sambade, C. & Vasconcelos, M.H., 2004. Specific downregulation of bcl-2 and xIAP by RNAi enhances the effects of chemotherapeutic agents in MCF-7 human breast cancer cells. *Cancer Gene Therapy*, 11, pp.309–16.

30. Lorenzato, A., Martino, C., Dani, N., Oligschläger, Y., Ferrero, A.M., Biglia, N., Calogero, R., Olivero, M. & Di Renzo, M.F., 2012. The cellular susceptibility *CAS/CSEIL* gene protects ovarian cancer cells from death by suppressing RASSF1C. *The Federation of American Societies for Experimental Biology Journal*, 26, pp.1-11
31. Lu, Z. & Xu, S., 2006. Critical review ERK1 / 2 MAP kinases in cell survival and apoptosis. *International Union of Biochemistry and Molecular Biology Life*, 58, pp.621–631.
32. Mak, W., Wang, S.K., Liu, T., Hamid, N., Li, Y., Lu, J. & White, W.L., 2014. Anti-proliferation potential and content of fucoidan extracted from sporophyll of New Zealand *Undaria pinnatifida*. *Frontiers in Nutrition*, 1, pp.1–10.
33. Marlin, J.W., Eaton, A., Montano, G.T., Chang, Y.W. & Jakobi, R., 2009. Elevated p21-activated kinase 2 activity results in anchorage-independent growth and resistance to anticancer drug-induced cell death. *Neoplasia*, 11, pp.286-297
34. McIlwain, D.R., Berger, T. & Mak, T.W., 2013. Caspase functions in cell death and disease. *Cold Spring Harbor Perspectives in Biology*, 5, pp.1–28.
35. Mebratu, Y. and Tesfaigzi, Y., 2009. How ERK1/2 activation controls cell proliferation and cell death is subcellular localization the answer?, *Cell Cycle*, 8, pp.1168-1175
36. Meloche, S. & Pouyssegur, J., 2007. The ERK1/2 mitogen-activated protein kinase pathway as a master regulator of the G1- to S-phase transition. *Oncogene*, 26, pp.3227–3239.
37. Messmer, U.K., Pereda-Fernandez, C., Manderscheid, M. & Pfeilschifter, J., 2001. Dexamethasone inhibits TNF-alpha-induced apoptosis and IAP protein downregulation in MCF-7 cells. *British journal of pharmacology*, 133, pp.467–476.
38. Moghadamtousi, S.Z., Karimian, H., Khanabdali, R., Razavi, M., Firoozinia, M., Zandi, K. & Kadir, H.A., 2014. Anticancer and antitumor potential of fucoidan and

- fucoxanthin, two main metabolites isolated from brown algae. *The Scientific World Journal*, 2014, pp.768323.
39. Mori, S., Bernardi, R., Laurent, A., Resnati, M., Crippa, A., Gabrieli, A., Keough, R., Gonda, T.J. & Blasi, F., 2012. Myb-binding protein 1A (MYBBP1A) is essential for early development, controls cell cycle and mitosis, and acts as a tumor suppressor. *PLoS ONE*, 7, p.e39723
40. Morya, V.K., Kim, J. & Kim, E.K., 2012. Algal fucoidan: Structural and size-dependent bioactivities and their perspectives. *Applied Microbiology and Biotechnology*, 93, pp.71–82.
41. Nesvizhskii, A.I., Keller, A., Kolker, E. and Aebersold, R., 2003. A statistical model for identifying proteins by tandem mass spectrometry. *Analytical Chemistry*, 75, pp.4646–4658.
42. Nicholls, C., Li, H. & Liu, J.P., 2012. GAPDH: a common enzyme with uncommon functions. *Clinical and Experimental Pharmacology and Physiology*, 39, pp.674-679
43. Ohnishi, Y.H., Ohnishi, Y.N., Nakamura, T., Ohno, M., Kennedy, P.J., Yasuyuki, O., Nishi, A., Neve, R., Tsuzuki, T. & Nestler, E.J., 2015. PSMC5, a 19S proteasomal ATPase, regulates cocaine action in the nucleus accumbens. *PLoS ONE*, 10, e0126710
44. Ong, S.E. & Mann, M., 2006. A practical recipe for stable isotope labeling by amino acids in cell culture (SILAC). *Nature Protocols*, 1, pp.2650–2660.
45. Park, H., Kim, G.Y., Moon, S.K., Kim, W.J., Yoo, Y.H. & Choi, Y.H., 2014. Fucoidan inhibits the proliferation of human urinary bladder cancer T24 cells by blocking cell cycle progression and inducing apoptosis. *Molecules*, 19, pp.5981–5998.
46. Park, H.S., Hwang, H.J., Kim, G.Y., Cha, H.J., Kim, W.J., Kim, N.D., Yoo, Y.H. & Choi, Y. H., 2013. Induction of apoptosis by fucoidan in human leukemia U937 cells

- through activation of p38 MAPK and modulation of Bcl-2 family. *Marine Drugs*, 11, pp.2347–2364.
47. Patil, A., Kumagai, Y., Liang, K.C., Suzuki, Y. & Nakai, K., 2013. Linking transcriptional changes over time in stimulated dendritic cells to identify gene networks activated during the innate immune response. *PLoS Computational Biology*, 9, p.e1003323
48. Plati, J., Bucur, O. & Khosravi-Far, R., 2011. Apoptotic cell signaling in cancer progression and therapy. *Integrative Biology*, 3, pp.279.
49. Portt, L., Norman, G., Clapp, C., Greenwood, M. & Greenwood, M.T., 2011. Anti-apoptosis and cell survival: A review. *Biochimica et Biophysica Acta (BBA) - Molecular Cell Research*, 1813, pp.238–259.
50. Qiao, L., Dai, Y., Gu, Q., Chan, K.W., Zou, B., Ma, J., Wang, J., Lan, H.Y. & Wong, B.C.Y., 2008. Down-regulation of X-linked inhibitor of apoptosis synergistically enhanced peroxisome proliferator-activated receptor gamma ligand-induced growth inhibition in colon cancer. *Molecular Cancer Therapeutics*, 7, pp.2203–2211.
51. Rampazzo, A., Nava, A., Malacrida, S., Beffagna, G., Bauce, B., Rossi, V., Zimbello, R., Simionati, B., Basso, C., Thiene, G., Towbin, J.A. & Danieli, G.A., 2002. Mutation in human desmoplakin domain binding to plakoglobin causes a dominant form of arrhythmogenic right ventricular cardiomyopathy. *American Journal of Human Genetics*, 71, pp.1200-1206
52. Roskoski, R., 2012. ERK1/2 MAP kinases: Structure, function, and regulation. *Pharmacological Research*, 66, pp.105–143.
53. Sánchez-Lanzas, R. & Castaño, J.G., 2014. Proteins directly interacting with mammalian 20S proteasomal subunits and ubiquitin-independent proteasomal degradation. *Biomolecules*, 4, pp.1140-1154

54. Sasaki, H., Sheng, T. & Kotsujil, F., 2000. Down-regulation of X-linked inhibitor of apoptosis protein induces apoptosis in chemoresistant human ovarian cancer cells. *Cancer Research*, 60, pp.5659–5666.
55. Sebaugh, J.L.Ã., 2011. Guidelines for accurate EC50 / IC50 estimation. *Pharmaceutical Statistics*, 10, pp. 128-134.
56. Senthilkumar, K., Manivasagan, P., Venkatesan, J. & Kim, S.K., 2013. Brown seaweed fucoidan: Biological activity and apoptosis, growth signaling mechanism in cancer. *International Journal of Biological Macromolecules*, 60, pp.366–374.
57. Skriptsova, A.V., Shevchenko, N.M., Zvyagintseva, T.N. & Imbs, T.I., 2010. Monthly changes in the content and monosaccharide composition of fucoidan from *Undaria pinnatifida* (Laminariales, Phaeophyta). *Journal of Applied Phycology*, 22, pp.79–86.
58. Tong, Q.S., Zheng, L.D., Wang, L., Zeng, F.Q., Chen, F.M., Dong, J.H. & Lu, G.C., 2005. Downregulation of XIAP expression induces apoptosis and enhances chemotherapeutic sensitivity in human gastric cancer cells. *Cancer Gene Therapy*, 12, pp.509–514.
59. Udeshi, N.D., Mani, D.R., Eisenhaure, T., Mertins, P., Jaffe, J.D., Clauser, K.R., Hacohen, M. & Carr, S.A., 2012. Methods for quantification of *in vivo* changes in protein ubiquitination following proteasome and deubiquitinase inhibition. *Molecular & Cellular Proteomics*, 11, pp.148-159
60. Vangata, J.R., Dudem, S., Jain, N. & Kalivedi, S.V., 2014. Regulation of PSMB5 protein and β subunits of mammalian proteasome by constitutively activated signal transducer and activator of transcription 3 (STAT3). *The Journal of Biological Chemistry*, 289, pp12612-12622
61. Wong, R.S., 2011. Apoptosis in cancer: From pathogenesis to treatment. *Journal of Experimental & Clinical Cancer Research*, 30, pp.87.

62. Xue, M., Ge, Y., Zhang, J., Wang, Q., Hou, L., Liu, Y., Sun, L. & Li, Q., 2012. Anticancer properties and mechanisms of fucoidan on mouse breast cancer *in vitro* and *in vivo*. *PLoS ONE*, 7, pp.3–11.
63. Yamasaki-Miyamoto, Y., Yamasaki, M., Tachibana, H. & Yamada, K., 2009. Fucoidan induces apoptosis through activation of caspase-8 on human breast cancer MCF-7 cells. *Journal of Agricultural and Food Chemistry*, 57, pp.8677–8682.
64. Yang, L., Wang, P., Wang, H., Li, Q., Teng, H., Liu, Z., Yang, W., Hou, L., Zou, X., 2013. Fucoidan derived from *Undaria pinnatifida* induces apoptosis in human hepatocellular carcinoma SMMC-7721 cells via the ROS-mediated mitochondrial pathway. *Marine Drugs*, 11, pp.1961–1976.
65. Zhang, F., Lau, S.S. & Monks, T.J., 2011a. The cytoprotective effect of N-acetyl- L -cysteine against ROS-induced cytotoxicity is independent of its ability to enhance glutathione synthesis. *Toxicological Sciences*, 120, pp.87–97.
66. Zhang, Z., Teruya, K., Eto, H. & Shirahata, S., 2011. Fucoidan extract induces apoptosis in MCF-7 cells via a mechanism involving the ROS-dependent JNK activation and mitochondria-mediated pathways. *PloS ONE*, 6, p.e27441.
67. Zhang, Z., Teruya, K., Yoshida, T., Eto, H. & Shirahata, S., 2013. Fucoidan extract enhances the anti-cancer activity of chemotherapeutic agents in MDA-MB-231 and MCF-7 breast cancer cells. *Marine Drugs*, 11, pp.81–98.
68. Zhang, Y.B., Gong, J.L., Xing, T.Y., Zheng, S.P. and Ding, W., 2013a. Autophagy protein p62/SQSTM1 is involved in HAMLET-induced cell death by modulating apoptosis in U87MG cells. *Cell Death and Disease*, 4, e550
69. Zhou, Z., Patel, M., Ng, N., Hsieh, M.H., Orth, A.P., Walker, J.R., Batalov, S., Harris, J.L. & Liu, J., 2014. Identification of synthetic lethality of PRKDC in MYC-dependent human cancers by pooled shRNA screening. *BioMed Central Cancer*, 14, 1-13

Appendix 1

Materials and suppliers

General materials and chemicals used are listed in Table A1. Antibodies used for immunoblotting techniques are listed in Table A2. Reagents and solutions used for stable isotope labelling of amino acids in cell culture (SILAC) and in the study are listed in Table A3 and Table A4, respectively.

Table A1: Materials and suppliers.

Materials	Suppliers
Acrylamide-Bis Solution (40%)	Promega Corporation
Ammonium Persulfate (APS)	Sigma-Aldrich
Benzonase Nuclease	Sigma-Aldrich
Bicinchoninic Acid Solution	Sigma-Aldrich
Bovine Serum Albumin (BSA)	Roche
Bradford Reagent	Sigma-Aldrich
Casein from Bovine Milk	Sigma-Aldrich
Cell Proliferation Reagent, WST-1	Roche
Clarity™ Western ECL Substrate	Bio-Rad
Coomassie Brilliant Blue R250	Sigma-Aldrich
Copper (II) Sulfate Pentahydrate 4% Solution	Sigma-Aldrich

Cytobuster™ Protein Extraction Reagent	Merck
Dimethyl Sulfoxide (DMSO)	Sigma-Aldrich
Dithiothreitol (DTT)	Roche
Dulbecco's Modified Eagle Medium (DMEM:F12), 1:1 Mixture with 15mM HEPES, L-Glutamine	Lonza
Ethanol	Kimix
Fetal Bovine Serum	The Scientific Group
Fucoidan (<i>Fucus vesiculosus</i>)	Sigma-Aldrich
Glacial Acetic Acid	Merck
Glycine	Merck
Hydrochloric Acid	Merck
Hydroxyethyl piperazineethanesulfonic acid (HEPES)	Sigma-Aldrich
Isopropanol	Merck
5X Lane Marker Reducing Sample Buffer	Thermo Scientific
Penicillin/Streptomycin (5000 U/ml)	Life Technologies
Phosphate Buffered Saline (PBS)	The Scientific Group
Polyvinylidene Difluoride (PVDF) Membrane	Bio-Rad
Qubit® Protein Assay Kit	Life Technologies

Sodium Chloride	Merck
Sodium Deoxycholate	Sigma-Aldrich
Sodium Dodecyl Sulfate (SDS)	Merck
Sodium Hydroxide	Merck
N,N,N',N'-Tetramethylethylenediamine (TEMED)	Sigma-Aldrich
Tris (hydroxymethyl) aminomethane (Tris)	Merck
Trypan Blue Exclusion Dye 0.4%	Life Technologies
Trypsin/EDTA	The Scientific Group
Tween® 20	Merck
Unstained Protein Molecular Weight Marker	Thermo Scientific
Western Protein Standard	Life Technologies

Table A2: Antibodies used for Western blot analysis.

Antibodies	Suppliers
Actin sc-1616 (HRP-conjugated)	Santa Cruz Biotechnology
Phospho-p44/42 MAPK (E1/2) (Thr202/Tyr204) (E10) (Mouse mAb)	Cell Signaling Technology
XIAP (2F1): sc-58537 (Mouse mAb)	Santa Cruz Biotechnology

Goat Anti-Mouse sc-2031 (HRP-conjugated)	Santa Cruz Biotechnology
Goat Anti-Rabbit sc-2004 (HRP-conjugated)	Santa Cruz Biotechnology

Table A3: Media constituents used for stable isotope labelling of amino acids in cell culture (SILAC).

Materials	Suppliers
L-Arginine-HCl	Separations
L-Arginine-HCl, ¹³C₆, ¹⁵N₄	Separations
L-Lysine-2HCl	Separations
L-Lysine-2HCl, ¹³C₆	Separations
DMEM:F12 (1:1) Media for SILAC	Separations
Dialyzed Fetal Bovine Serum	Separations

Table A4: Solutions and recipes used in the study.

Solutions	Recipes
7% Acetic acid	7% Acetic acid, made up with distilled water
10% Ammonium Persulfate	10% prepared in distilled water, filter sterilized and stored at -20°
Complete DMEM/F-12	DMEM/F-12, 10% FBS, 1% Penstrep
Media	

Coomassie Stain Solution	50% Ethanol, 0.05% Coomassie Brilliant Blue, 10% Acetic Acid, made up with distilled water
Destaining Solution	5% Ethanol, 7% Acetic acid, made up with distilled water
HEPES Solution	100 mM HEPES, pH 7.4 made up in distilled water
RIPA Buffer	150 mM NaCl, 50 mM HEPES, pH 7.4, 0.5% Sodium Deoxycholate, 0.25% SDS, 100 mM DTT made up in distilled water
5X SDS Running Buffer	125 mM Tris, 0.96 M Glycine, 17 mM SDS, made up with distilled water
1X SDS Running Buffer	Dilute 5X Running Buffer according to the dilution 1:5 (v/v) in distilled water
SDS-PAGE Separating buffer	1.5 M Tris, pH 8.8 made up in distilled water and autoclaved
SDS-PAGE Stacking buffer	0.5 M Tris, pH 6.8 made up in distilled water and autoclaved
SILAC Complete Light Media	SILAC DMEM/F12, 10% Dialyzed FBS, 1% Penstrep, 0.47 mM L-Arginine-HCl, 0.46 mM L-Lysine-2HCl
SILAC Complete Heavy Media	SILAC DMEM/F12, 10% Dialyzed FBS, 1% Penstrep, 0.47 mM L-Arginine-HCl, $^{13}\text{C}_6$, $^{15}\text{N}_4$, 0.46 mM L-Lysine-2HCl, $^{13}\text{C}_6$
10X TBS	500 mM Tris, 150 mM NaCl, pH 7.4, made up with distilled water and autoclaved

1X TBS	Dilute 10X TBS according to the dilution 1:10 (v/v) in distilled water
TBS-Tween / Wash Buffer	1X TBS, 0.1% Tween® 20, stored at 4°C
1X Transfer Buffer	25 mM Tris, 192 mM Glycine, 20% Ethanol made up with distilled water, stored at 4°C
1X TBS-Tween-Casein / Blocking Buffer	1% Casein Powder in TBS-Tween



Appendix 2

Results

Table A5: Differentially regulated proteins and corresponding trends.

	Gene symbol	Protein name	Accession no.	Molecular weight
Up-regulated				
1	ARL6IP5	PRA1 family protein 3	O75915	22 kDa
2	TCEA1	Transcription elongation factor A protein 1	P23193	34 kDa
3	DLD	Dihydrolipoyl dehydrogenase, mitochondrial	P09622 (+2)	54 kDa
4	MYBBP1A	Myb-binding protein 1A	Q9BQG0 (+1)	149 kDa
5	CCS	Copper chaperone for superoxide dismutase	O14618	29 kDa
6	ANKRD30B	Ankyrin repeat domain-containing protein 30B	Q9BXX2	158 kDa
7	GNPNAT1	Glucosamine 6-phosphate N-acetyltransferase 1	Q96EK6	21 kDa
8	FARSB	Phenylalanine--tRNA ligase beta subunit	Q9NSD9	66 kDa
9	FAF2	FAS-associated factor 2	Q96CS3	53 kDa
10	ITPA	Inosine triphosphate pyrophosphatase	Q9BY32 (+1)	21 kDa
11	PPP2CA	Serine/threonine-protein phosphatase 2A catalytic subunit alpha isoform	P67775	36 kDa
12	PAK2	Serine/threonine-protein kinase PAK 2	Q13177	58 kDa
13	GUSB	Beta-glucuronidase	P08236 (+2)	75 kDa
14	GOLGA2	Golgin subfamily A member 2	Q08379	113 kDa
15	CKMT1A	Creatine kinase U-type, mitochondrial	P12532	47 kDa
16	VASP	Vasodilator-stimulated phosphoprotein	P50552	40 kDa
17	AKR1C3	Aldo-keto reductase family 1 member C3	P42330	37 kDa
18	EIF3G	Eukaryotic translation initiation factor 3 subunit G	O75821	36 kDa

19	AK2	Adenylate kinase 2, mitochondrial	P54819 (+1)	26 kDa
20	CAP1	Adenylyl cyclase-associated protein 1	Q01518	52 kDa
21	PAFAH1 B3	Platelet-activating factor acetylhydrolase IB subunit gamma	Q15102	26 kDa
22	C21orf33	ES1 protein homolog, mitochondrial	P30042	28 kDa
23	NAPG	Gamma-soluble NSF attachment protein	Q99747	35 kDa
24	PRKCSH	Glucosidase 2 subunit beta	P14314 (+1)	59 kDa
25	AP1B1	AP-1 complex subunit beta-1	Q10567 (+2)	105 kDa
26	AP1G1	AP-1 complex subunit gamma-1	O43747 (+1)	91 kDa
27	PSMB6	Proteasome subunit beta type-6	P28072	25 kDa
28	ATP5J2	ATP synthase subunit f, mitochondrial	P56134 (+3)	11 kDa
29	RASIP1	Ras-interacting protein 1	Q5U651	103 kDa
30	PGAM1	Phosphoglycerate mutase 1	P18669	29 kDa
31	PNPO	Pyridoxine-5'-phosphate oxidase	Q9NVS9 (+1)	30 kDa
32	RPL7	60S ribosomal protein L7	P18124	29 kDa
33	PDXDC1	Pyridoxal-dependent decarboxylase domain- containing protein 1	Q6P996 (+3)	87 kDa
34	GAPDH	Glyceraldehyde-3-phosphate dehydrogenase	P04406	36 kDa
35	RPS2	40S ribosomal protein S2	P15880	31 kDa
36	EPCAM	Epithelial cell adhesion molecule	P16422	35 kDa
37	SYNGR2	Synaptogyrin-2	O43760 (+1)	25 kDa
38	NOP56	Nucleolar protein 56	O00567	66 kDa
39	PCNA	Proliferating cell nuclear antigen	P12004	29 kDa
40	COPB1	Coatomer subunit beta	P53618	107 kDa

41	PSMC5	26S protease regulatory subunit 8	P62195 (+1)	46 kDa
42	MCM2	DNA replication licensing factor MCM2	P49736	102 kDa
43	ATP5B	ATP synthase subunit beta, mitochondrial	P06576	57 kDa
44	PBDC1	Protein PBDC1	Q9BVG4	26 kDa
45	PSMA5	Proteasome subunit alpha type-5	P28066	26 kDa
46	ISOC1	Isochorismatase domain-containing protein 1	Q96CN7	32 kDa
47	NDUFB1 0	NADH dehydrogenase [ubiquinone] 1 beta subcomplex subunit 10	O96000	21 kDa
48	REEP5	Receptor expression-enhancing protein 5	Q00765	21 kDa
49	DDB1	DNA damage-binding protein 1	Q16531	127 kDa
50	TRIM28	Transcription intermediary factor 1-beta	Q13263	89 kDa
51	MYL6	Isoform Smooth muscle of Myosin light polypeptide 6	P60660-2	17 kDa
52	RPL10	60S ribosomal protein L10	P27635	25 kDa
53	GRPEL1	GrpE protein homolog 1, mitochondrial	Q9HAV7	24 kDa
54	GLRX3	Glutaredoxin-3	O76003	37 kDa
55	PRPF19	Pre-mRNA-processing factor 19	Q9UMS4	55 kDa
56	TXNDC1 2	Thioredoxin domain-containing protein 12	O95881	19 kDa
57	EIF1AX	Eukaryotic translation initiation factor 1A, X- chromosomal	P47813	16 kDa
58	RSU1	Ras suppressor protein 1	Q15404	32 kDa
59	ATXN2L	Isoform 6 of Ataxin-2-like protein	Q8WWM7 -6	103 kDa
60	GSR	Glutathione reductase, mitochondrial	P00390 (+4)	56 kDa
61	HEXB	Beta-hexosaminidase subunit beta	P07686	63 kDa
62	GMFB	Glia maturation factor beta	P60983	17 kDa
63	RPL22	60S ribosomal protein L22	P35268	15 kDa

64	TOMM40	Mitochondrial import receptor subunit TOM40 homolog	O96008	38 kDa
65	DBN1	Drebrin	Q16643 (+2)	71 kDa
66	RPN2	Dolichyl-diphosphooligosaccharide--protein glycosyltransferase subunit 2	P04844 (+1)	69 kDa
67	DNAJC3	DnaJ homolog subfamily C member 3	Q13217	58 kDa
68	EEF1G	Elongation factor 1-gamma	P26641	50 kDa
69	AK4	Adenylate kinase 4, mitochondrial	P27144	25 kDa
70	PDCD6	Programmed cell death protein 6	O75340 (+1)	22 kDa
71	TMED2	Transmembrane emp24 domain-containing protein 2	Q15363	23 kDa
72	PPP2R5D	Serine/threonine-protein phosphatase 2A 56 kDa regulatory subunit delta isoform	Q14738 (+2)	70 kDa
73	CLDN3	Claudin-3	O15551	23 kDa
74	RRBP1	Ribosome-binding protein 1	Q9P2E9	152 kDa
75	CIRBP	Cold-inducible RNA-binding protein	Q14011	19 kDa
76	PRRC1	Protein PRRC1	Q96M27	47 kDa
77	ATP6V1 C1	V-type proton ATPase subunit C 1	P21283	44 kDa
78	MAP7	Ensconsin	Q14244 (+6)	84 kDa
79	UCHL5	Ubiquitin carboxyl-terminal hydrolase isozyme L5	Q9Y5K5 (+3)	38 kDa
80	AKAP6	A-kinase anchor protein 6	Q13023	257 kDa
81	EIF4G2	Eukaryotic translation initiation factor 4 gamma 2	P78344 (+1)	102 kDa
82	ZYX	Zyxin	Q15942	61 kDa
83	TSG101	Tumor susceptibility gene 101 protein	Q99816	44 kDa
84	HEATR6	HEAT repeat-containing protein 6	Q6AI08	129 kDa
85	LASP1	LIM and SH3 domain protein 1	Q14847	30 kDa

86	ERP44	Endoplasmic reticulum resident protein 44	Q9BS26	47 kDa
87	PSMB4	Proteasome subunit beta type-4	P28070	29 kDa
88	FAM213 A	Redox-regulatory protein FAM213A	Q9BRX8 (+1)	26 kDa
89	TUFM	Elongation factor Tu, mitochondrial	P49411	50 kDa
90	ECHS1	Enoyl-CoA hydratase, mitochondrial	P30084	31 kDa
91	DHX9	ATP-dependent RNA helicase A	Q08211	141 kDa
92	ACLY	ATP-citrate synthase	P53396 (+2)	121 kDa
93	COX7A2	Cytochrome c oxidase subunit 7A2, mitochondrial	P14406	9 kDa
94	LGALS3 BP	Galectin-3-binding protein	Q08380	65 kDa
95	TRANK1	TPR and ankyrin repeat-containing protein 1	O15050	336 kDa
96	NOMO3	Nodal modulator 3	P69849 (+4)	134 kDa
97	COPS6	COP9 signalosome complex subunit 6	Q7L5N1	36 kDa
98	KLC1	Kinesin light chain 1	Q07866 (+9)	65 kDa
99	DDX5	Probable ATP-dependent RNA helicase DDX5	P17844	69 kDa
100	APMAP	Adipocyte plasma membrane-associated protein	Q9HDC9	46 kDa
101	VPS35	Vacuolar protein sorting-associated protein 35	Q96QK1	92 kDa
102	PGM2	Phosphoglucomutase-2	Q96G03	68 kDa
103	SMC1A	Structural maintenance of chromosomes protein 1A	Q14683	143 kDa
104	EIF3B	Eukaryotic translation initiation factor 3 subunit B	P55884 (+1)	92 kDa
105	DPM1	Dolichol-phosphate mannosyltransferase subunit 1	O60762	30 kDa
106	STARD1 0	PCTP-like protein	Q9Y365	33 kDa
107	FLNA	Filamin-A	P21333 (+1)	281 kDa

108	BCAM	Basal cell adhesion molecule	P50895	67 kDa
109	CLTC	Clathrin heavy chain 1	Q00610 (+1)	192 kDa
110	SUCLG2	Succinyl-CoA ligase [GDP-forming] subunit beta, mitochondrial	Q96199	47 kDa
111	AGR3	Anterior gradient protein 3 homolog	Q8TD06	19 kDa
112	LTA4H	Leukotriene A-4 hydrolase	P09960 (+1)	69 kDa
113	SRPRB	Signal recognition particle receptor subunit beta	Q9Y5M8	30 kDa
114	PHGDH	D-3-phosphoglycerate dehydrogenase	O43175	57 kDa
115	ETFA	Electron transfer flavoprotein subunit alpha, mitochondrial	P13804	35 kDa
116	OAT	Ornithine aminotransferase, mitochondrial	P04181	49 kDa
117	PKM	Pyruvate kinase PKM	P14618	58 kDa
118	PCK2	Phosphoenolpyruvate carboxykinase [GTP], mitochondrial	Q16822	71 kDa
119	CSE1L	Exportin-2	P55060 (+1)	110 kDa
120	CAST	Calpastatin	P20810 (+8)	77 kDa
121	SIL1	Nucleotide exchange factor SIL1	Q9H173	52 kDa
123	PTBP1	Polypyrimidine tract-binding protein 1	P26599 (+2)	57 kDa
124	PPIC	Peptidyl-prolyl cis-trans isomerase C	P45877	23 kDa
125	RPS9	40S ribosomal protein S9	P46781	23 kDa
126	ARL1	ADP-ribosylation factor-like protein 1	P40616 (+1)	20 kDa
127	TPM2	Tropomyosin beta chain	P07951	33 kDa
128	C12orf10	UPF0160 protein MYG1, mitochondrial	Q9HB07	42 kDa
129	PABPC1	Polyadenylate-binding protein 1	P11940	71 kDa
130	NDUFAF2	Mimitin, mitochondrial	Q8N183	20 kDa

131	MT-CO2	Cytochrome c oxidase subunit 2	P00403	26 kDa
132	ALDOC	Fructose-bisphosphate aldolase C	P09972	39 kDa
133	PSMB5	Proteasome subunit beta type-5	P28074	28 kDa
134	ACTBL2	Beta-actin-like protein 2	Q562R1	42 kDa
135	ATP1A1	Sodium/potassium-transporting ATPase subunit alpha-1	P05023 (+1)	113 kDa
136	OBSCN	Obscurin	Q5VST9 (+2)	868 kDa
137	ARPC4	Actin-related protein 2/3 complex subunit 4	P59998 (+2)	20 kDa
138	MACF1	Microtubule-actin cross-linking factor 1, isoforms 1/2/3/5	Q9UPN3	838 kDa
139	TACSTD2	Tumor-associated calcium signal transducer 2	P09758	36 kDa
140	RAB14	Ras-related protein Rab-14	P61106	24 kDa
141	KPNA2	Importin subunit alpha-1	P52292	58 kDa
142	LAMA1	Laminin subunit alpha-1	P25391	337 kDa
143	GPI	Glucose-6-phosphate isomerase	P06744	63 kDa
144	TMEM205	Transmembrane protein 205	Q6UW68	21 kDa
145	CD63	CD63 antigen	P08962 (+2)	26 kDa
146	SVIL	Supervillin	O95425 (+3)	248 kDa
147	RAB10	Ras-related protein Rab-10	P61026	23 kDa
148	GAA	Lysosomal alpha-glucosidase	P10253	105 kDa
149	VCL	Vinculin	P18206 (+1)	124 kDa
150	KIAA1324	UPF0577 protein KIAA1324	Q6UXG2 (+1)	111 kDa
151	OSM	Oncostatin-M	P13725	28 kDa
152	EIF4A1	Eukaryotic initiation factor 4A-I	P60842	46 kDa

153	FDPS	Farnesyl pyrophosphate synthase	P14324 (+1)	48 kDa
154	SHMT2	Serine hydroxymethyltransferase, mitochondrial	P34897 (+1)	56 kDa
155	CHD7	Chromodomain-helicase-DNA-binding protein 7	Q9P2D1	336 kDa
156	GNB2L1	Guanine nucleotide-binding protein subunit beta-2-like 1	P63244	35 kDa
157	EIF3A	Eukaryotic translation initiation factor 3 subunit A	Q14152 (+1)	167 kDa
158	MLH3	DNA mismatch repair protein Mlh3	Q9UHC1 (+1)	164 kDa
159	CDK5RA P3	CDK5 regulatory subunit-associated protein 3	Q96JB5 (+1)	57 kDa
160	ARHGAP 1	Rho GTPase-activating protein 1	Q07960	50 kDa
161	S100PBP	S100P-binding protein	Q96BU1 (+1)	46 kDa
162	DPYSL2	Dihydropyrimidinase-related protein 2	Q16555 (+1)	62 kDa
163	ARF5	ADP-ribosylation factor 5	P84085	21 kDa
164	TMED10	Transmembrane emp24 domain-containing protein 10	P49755	25 kDa
165	LDHA	L-lactate dehydrogenase A chain	P00338 (+1)	37 kDa
166	ISOC2	Isochorismatase domain-containing protein 2, mitochondrial	Q96AB3 (+1)	22 kDa
167	RAB25	Ras-related protein Rab-25	P57735	23 kDa
168	CROCC	Rootletin	Q5TZA2	229 kDa
169	CLIC4	Chloride intracellular channel protein 4	Q9Y696	29 kDa
170	TFRC	Transferrin receptor protein 1	P02786	85 kDa
171	MAT2B	Methionine adenosyltransferase 2 subunit beta	Q9NZL9 (+2)	38 kDa

172	FAM186 A	Protein FAM186A	A6NE01	263 kDa
173	TMED10	Transmembrane emp24 domain-containing protein 10	P49755	25 kDa
174	PLS3	Plastin-3	P13797 (+2)	71 kDa
175	EIF3I	Eukaryotic translation initiation factor 3 subunit I	Q13347	37 kDa
176	CSRP1	Cysteine and glycine-rich protein 1	P21291	21 kDa
177	JUP	Junction plakoglobin	P14923	82 kDa
178	MRPS35	28S ribosomal protein S35, mitochondrial	P82673	37 kDa
179	PFKM	ATP-dependent 6-phosphofructokinase, muscle type	P08237 (+1)	85 kDa
180	TIA1	Nucleolysin TIA-1 isoform p40	P31483 (+3)	43 kDa
181	FAM83B	Protein FAM83B	Q5T0W9	115 kDa
182	DSP	Desmoplakin	P15924	332 kDa
183	SQSTM1	Sequestosome-1	Q13501 (+1)	48 kDa
184	RTTN	Rotatin	Q86VV8 (+1)	249 kDa
185	QPRT	Nicotinate-nucleotide pyrophosphorylase [carboxylating]	Q15274	31 kDa
186	KRT6A	Keratin, type II cytoskeletal 6A	P02538 (+1)	60 kDa
187	FILIP1	Filamin-A-interacting protein 1	Q7Z7B0 (+1)	138 kDa
188	PIP4K2C	Phosphatidylinositol 5-phosphate 4-kinase type-2 gamma	Q8TBX8 (+2)	47 kDa
189	EHD1	EH domain-containing protein 1	Q9H4M9	61 kDa
190	ABCF1	ATP-binding cassette sub-family F member 1	Q8NE71 (+1)	96 kDa
191	IFT122	Intraflagellar transport protein 122 homolog	Q9HBG6 (+8)	142 kDa

192	SEC63	Translocation protein SEC63 homolog	Q9UGP8	88 kDa
193	PRKDC	DNA-dependent protein kinase catalytic subunit	P78527 (+1)	469 kDa
194	POLR1C	DNA-directed RNA polymerases I and III subunit RPAC1	O15160 (+1)	39 kDa
195	CCDC88C	Protein Daple C	Q9P219	228 kDa
196	ZSWIM8	Zinc finger SWIM domain-containing protein 8	A7E2V4 (+4)	197 kDa
197	KCNG3	Potassium voltage-gated channel subfamily G member 3	Q8TAE7 (+1)	50 kDa
198	ZNF318	Zinc finger protein 318	Q5VUA4	251 kDa
199	HTT	Huntingtin	P42858	348 kDa
200	PRPF8	Pre-mRNA-processing-splicing factor 8	Q6P2Q9	274 kDa
201	MYO1B	Unconventional myosin-Ib	O43795 (+1)	132 kDa
Down-regulated				
1	PRDX2	Peroxiredoxin-2	P32119	22 kDa
2	PTGES3	Prostaglandin E synthase 3	Q15185 (+1)	19 kDa
3	COPS2	COP9 signalosome complex subunit 2	P61201 (+1)	52 kDa
4	TOP1	DNA topoisomerase 1	P11387	91 kDa
5	ACP1	Low molecular weight phosphotyrosine protein phosphatase	P24666	18 kDa
6	RPS21	40S ribosomal protein S21	P63220	9 kDa
7	USP14	Ubiquitin carboxyl-terminal hydrolase 14	P54578 (+1)	56 kDa
8	TPBG	Trophoblast glycoprotein	Q13641	46 kDa
9	ABRACL	Costars family protein ABRACL1	Q9P1F3	9 kDa
10	SEC31A	Isoform 7 of Protein transport protein Sec31A	O94979-7	106 kDa
11	TOM1L2	TOM1-like protein 2	Q6ZVM7 (+1)	56 kDa

12	HNRNPA2B1	Heterogeneous nuclear ribonucleoproteins A2/B1	P22626	37 kDa
13	ALYREF	THO complex subunit 4	Q86V81	27 kDa
14	LRRC59	Leucine-rich repeat-containing protein 59	Q96AG4	35 kDa
15	ELAVL1	Isoform 2 of ELAV-like protein 1	Q15717-2	39 kDa
16	QARS	Glutamine--tRNA ligase	P47897 (+1)	88 kDa
17	COX5A	Cytochrome c oxidase subunit 5A, mitochondrial	P20674	17 kDa
18	SYCP2	Synaptonemal complex protein 2	Q9BX26	176 kDa
19	PNN	Pinin	Q9H307	82 kDa
20	SH3GL1	Endophilin-A2	Q99961	41 kDa
21	NCL	Nucleolin	P19338	77 kDa
22	ETFB	Electron transfer flavoprotein subunit beta	P38117 (+1)	28 kDa
23	TMPO	Lamina-associated polypeptide 2, isoforms beta/gamma	P42167	51 kDa
24	CAT	Catalase	P04040	60 kDa
25	FIS1	Mitochondrial fission 1 protein	Q9Y3D6	17 kDa
26	ADK	Isoform 3 of Adenosine kinase	P55263-3	34 kDa
27	TBCA	Tubulin-specific chaperone A	O75347	13 kDa
28	UQCRB	Cytochrome b-c1 complex subunit 7	P14927	14 kDa
29	COMT	Catechol O-methyltransferase	P21964 (+1)	30 kDa
30	DCXR	L-xylulose reductase	Q7Z4W1	26 kDa
31	RMDN1	Regulator of microtubule dynamics protein 1	Q96DB5 (+1)	36 kDa
32	TRAPPC3	Trafficking protein particle complex subunit 3	O43617	20 kDa
33	SMAP	Small acidic protein	O00193	20 kDa
34	HSPB11	Intraflagellar transport protein 25 homolog	Q9Y547	16 kDa

35	NME2	Isoform 3 of Nucleoside diphosphate kinase B	P22392-2	30 kDa
36	H2AFZ	Histone H2A.Z	P0C0S5 (+1)	14 kDa
37	CNPY2	Protein canopy homolog 2	Q9Y2B0	21 kDa
38	OGFR	Opioid growth factor receptor	Q9NZT2 (+1)	73 kDa
39	S100A9	Protein S100-A9	P06702	13 kDa
40	ILF3	Interleukin enhancer-binding factor 3	Q12906 (+1)	95 kDa
41	SF3A3	Splicing factor 3A subunit 3	Q12874	59 kDa
42	RBM25	RNA-binding protein 25	P49756	100 kDa
43	LUC7L3	Luc7-like protein 3	O95232	51 kDa
44	CYP8B1	7-alpha-hydroxycholest-4-en-3-one 12-alpha-hydroxylase	Q9UNU6	58 kDa
45	PSME1	Proteasome activator complex subunit 1	Q06323	29 kDa
46	TLN1	Talin-1	Q9Y490	270 kDa
47	LRPAP1	Alpha-2-macroglobulin receptor-associated protein	P30533	41 kDa
48	DDX17	Probable ATP-dependent RNA helicase DDX17	Q92841	80 kDa
49	CRK	Adapter molecule crk	P46108 (+1)	34 kDa
50	LRIG3	Leucine-rich repeats and immunoglobulin-like domains protein 3	Q6UXM1	123 kDa
51	HIST1H4 A	Histone H4	P62805	11 kDa
52	LETM1	LETM1 and EF-hand domain-containing protein 1, mitochondrial	O95202	83 kDa
53	CAPZA2	F-actin-capping protein subunit alpha-2	P47755	33 kDa
54	CHTOP	Chromatin target of PRMT1 protein	Q9Y3Y2 (+2)	26 kDa
55	COPE	Coatomer subunit epsilon	O14579	34 kDa
56	CMPK1	UMP-CMP kinase	P30085	22 kDa

57	RBM14	RNA-binding protein 14	Q96PK6	69 kDa
58	NEB	Nebulin	P20929 (+3)	773 kDa
59	TMPO	Lamina-associated polypeptide 2, isoforms beta/gamma	P42167	51 kDa
60	HMGCL	Hydroxymethylglutaryl-CoA lyase, mitochondrial	P35914	34 kDa
61	PFDN2	Prefoldin subunit 2	Q9UHV9	17 kDa
62	ZC3H15	Zinc finger CCCH domain-containing protein 15	Q8WU90	49 kDa
63	AHNAK2	Protein AHNAK2	Q8IVF2 (+1)	617 kDa
64	NAP1L4	Nucleosome assembly protein 1-like 4	Q99733 (+1)	43 kDa
65	PTMA	Prothymosin alpha	P06454 (+1)	12 kDa
66	STX16	Isoform A of Syntaxin-16	O14662-2	35 kDa
67	RPS26	40S ribosomal protein S26	P62854	13 kDa
68	LYPLA2	Acyl-protein thioesterase 2	O95372	25 kDa
69	ST13	Hsc70-interacting protein	P50502	41 kDa
70	PSMC1	26S protease regulatory subunit 4	P62191	49 kDa
71	RBM8A	RNA-binding protein 8A	Q9Y5S9 (+1)	20 kDa
72	DNAJC8	DnaJ homolog subfamily C member 8	O75937	30 kDa
73	RPL27A	60S ribosomal protein L27a	P46776	17 kDa
74	LCN10	Epididymal-specific lipocalin-10	Q6JVE6 (+1)	21 kDa
75	SOD1	Superoxide dismutase [Cu-Zn]	P00441	16 kDa
76	SUB1	Activated RNA polymerase II transcriptional coactivator p15	P53999	14 kDa
77	SRSF5	Serine/arginine-rich splicing factor 5	Q13243	31 kDa
78	PRKAR1 A	cAMP-dependent protein kinase type I-alpha regulatory subunit	P10644 (+1)	43 kDa

79	KHSRP	Far upstream element-binding protein 2	Q92945	73 kDa
80	RAN	GTP-binding nuclear protein Ran	P62826	24 kDa
81	SNRNP70	U1 small nuclear ribonucleoprotein 70 kDa	P08621	52 kDa
82	PPP2R2A	Serine/threonine-protein phosphatase 2A 55 kDa regulatory subunit B alpha isoform	P63151 (+2)	52 kDa
83	SMNDC1	Survival of motor neuron-related-splicing factor 30	O75940	27 kDa
84	LMNB1	Lamin-B1	P20700	66 kDa
85	PARK7	Protein deglycase DJ-1	Q99497	20 kDa
86	BID	BH3-interacting domain death agonist	P55957 (+1)	22 kDa
87	MTPN	Myotrophin	P58546	13 kDa
88	GOLPH3	Golgi phosphoprotein 3	Q9H4A6	34 kDa
89	AK1	Adenylate kinase isoenzyme 1	P00568	22 kDa
90	EIF4E	Eukaryotic translation initiation factor 4E	P06730 (+2)	25 kDa
91	BAHCC1	BAH and coiled-coil domain-containing protein 1	Q9P281	277 kDa
92	SSB	Lupus La protein	P05455	47 kDa
93	SRSF1	Serine/arginine-rich splicing factor 1	Q07955	28 kDa
94	KTN1	Kinectin	Q86UP2 (+2)	156 kDa
95	CCDC6	Coiled-coil domain-containing protein 6	Q16204	53 kDa
96	DCTPP1	dCTP pyrophosphatase 1	Q9H773	19 kDa
97	PARP1	Poly [ADP-ribose] polymerase 1	P09874	113 kDa
98	RBM39	RNA-binding protein 39	Q14498 (+2)	59 kDa
99	SF1	Splicing factor 1	Q15637 (+6)	68 kDa
100	NUP62	Nuclear pore glycoprotein p62	P37198	53 kDa

101	UBR4	E3 ubiquitin-protein ligase UBR4	Q5T4S7 (+4)	574 kDa
102	HIST1H2 AG	Histone H2A type	P0C0S8 (+6)	14 kDa
103	CRIP2	Cysteine-rich protein 2	P52943	22 kDa
104 105	PPM1G	Protein phosphatase 1G	O15355	59 kDa
106	NSFL1C	NSFL1 cofactor p47	Q9UNZ2 (+2)	41 kDa
107	PRKAR2 A	cAMP-dependent protein kinase type II-alpha regulatory subunit	P13861 (+1)	46 kDa
108	C7orf55	Isoform 2 of UPF0562 protein C7orf55	Q96HJ9-2	54 kDa
109	DARS	Aspartate--tRNA ligase, cytoplasmic	P14868 (+1)	57 kDa
110	NUP205	Nuclear pore complex protein Nup205	Q92621	228 kDa
111	COPA	Coatomer subunit alpha	P53621 (+1)	138 kDa
112	FXYD3	Isoform 3 of FXYD domain-containing ion transport regulator 3	Q14802-3	15 kDa
113	PAFAH1 B2	Platelet-activating factor acetylhydrolase IB subunit beta	P68402	26 kDa
114	TOR1AIP 1	Torsin-1A-interacting protein 1	Q5JTV8 (+1)	66 kDa
115	SEC11A	Signal peptidase complex catalytic subunit SEC11A	P67812 (+2)	21 kDa
116	POLR3A	DNA-directed RNA polymerase III subunit RPC1	O14802	156 kDa
117	AHSA1	Activator of 90 kDa heat shock protein ATPase homolog 1	O95433 (+1)	38 kDa
118	HMGB3	High mobility group protein B3	O15347	23 kDa
119	ANP32E	Acidic leucine-rich nuclear phosphoprotein 32 family member E	Q9BTT0 (+1)	31 kDa
120	MLEC	Malectin	Q14165	32 kDa
121	PRDX4	Peroxiredoxin-4	Q13162	31 kDa

122	TXLNA	Alpha-taxilin	P40222	62 kDa
123	WBP11	WW domain-binding protein 11	Q9Y2W2	70 kDa
124	PEBP1	Phosphatidylethanolamine-binding protein 1	P30086	21 kDa
125	DNAJA1	DnaJ homolog subfamily A member 1	P31689	45 kDa
126	ANP32A	Acidic leucine-rich nuclear phosphoprotein 32 family member A	P39687	29 kDa
127	CTNBL1	Beta-catenin-like protein 1	Q8WYA6 (+1)	65 kDa
128	RBBP7	Histone-binding protein RBBP7	Q16576	48 kDa
129	PGP	Phosphoglycolate phosphatase	A6NDG6	34 kDa
130	RABL6	Rab-like protein 6	Q3YEC7	80 kDa
131	BSG	Basigin	P35613 (+1)	42 kDa
132	SLC9A3R1	Na(+)/H(+) exchange regulatory cofactor NHE-RF1	O14745	39 kDa
133	SH3BGL	SH3 domain-binding glutamic acid-rich-like protein	O75368	13 kDa
134	TFAM	Transcription factor A, mitochondrial	Q00059 (+1)	29 kDa
135	KHDRBS1	KH domain-containing, RNA-binding, signal transduction-associated protein 1	Q07666 (+1)	48 kDa
136	SNRPA	U1 small nuclear ribonucleoprotein A	P09012	31 kDa
137	CSTF2	Cleavage stimulation factor subunit 2	P33240 (+1)	61 kDa
138	REV1	DNA repair protein REV1	Q9UBZ9 (+1)	138 kDa
139	RALA	Ras-related protein Ral-A	P11233	24 kDa
	MKI67	Antigen KI-67	P46013 (+1)	359 kDa
140	CD9	CD9 antigen	P21926	25 kDa
141	ATP1B3	Sodium/potassium-transporting ATPase subunit beta-3	P54709	32 kDa

142	TRIM33	E3 ubiquitin-protein ligase TRIM33	Q9UPN9 (+1)	123 kDa
143	TRPM6	Transient receptor potential cation channel subfamily M member 6	Q9BX84 (+2)	232 kDa
144	TIAM2	T-lymphoma invasion and metastasis-inducing protein 2	Q8IVF5 (+2)	190 kDa
145	BZRAP1	Peripheral-type benzodiazepine receptor-associated protein 1	O95153 (+2)	200 kDa
146	SRSF3	Serine/arginine-rich splicing factor 3	P84103 (+1)	19 kDa
147	CNTRL	Centriolin	Q7Z7A1 (+1)	269 kDa
148	MYO6	Isoform 6 of Unconventional myosin-VI	Q9UM54- 6	149 kDa
149	H1F0	Histone H1.0	P07305	21 kDa
150	MCM5	DNA replication licensing factor MCM5	P33992	82 kDa
151	MRTO4	mRNA turnover protein 4 homolog	Q9UKD2	28 kDa
152	SF3B3	Splicing factor 3B subunit 3	Q15393	136 kDa
153	PABPN1	Polyadenylate-binding protein 2	Q86U42 (+1)	33 kDa
154	CPNE3	Copine-3	O75131	60 kDa
155	INF2	Inverted formin-2	Q27J81 (+1)	136 kDa
156	PDCD4	Programmed cell death protein 4	Q53EL6 (+1)	52 kDa
157	TRIM5	Tripartite motif-containing protein 5	Q9C035 (+3)	56 kDa
158	EFHD2	EF-hand domain-containing protein D2	Q96C19	27 kDa
159	AFF2	AF4/FMR2 family member 2	P51816 (+1)	145 kDa
160	BANF1	Barrier-to-autointegration factor	O75531	10 kDa
161	ANK3	Ankyrin-3	Q12955 (+4)	480 kDa

162	ACSS3	Acyl-CoA synthetase short-chain family member 3, mitochondrial	Q9H6R3	75 kDa
163	NUCKS1	Nuclear ubiquitous casein and cyclin-dependent kinase substrate 1	Q9H1E3	27 kDa
164	HERC1	Probable E3 ubiquitin-protein ligase HERC1	Q15751	532 kDa
165	DCUN1D1	DCN1-like protein 1	Q96GG9	30 kDa
166	PDS5A	Sister chromatid cohesion protein PDS5 homolog A	Q29RF7	151 kDa
167	KIAA0100	Protein KIAA0100	Q14667 (+1)	254 kDa
168	MUC16	Mucin-16	Q8WXI7	2353 kDa
169	DCHS2	Protocadherin-23	Q6V1P9	322 kDa
170	MAST4	Microtubule-associated serine/threonine-protein kinase 4	O15021 (+1)	284 kDa
171	ATAD3A	ATPase family AAA domain-containing protein 3A	Q9NVI7 (+1)	71 kDa
172	SPTBN4	Spectrin beta chain, non-erythrocytic 4	Q9H254	289 kDa
173	DNAH1	Dynein heavy chain 1, axonemal	Q9P2D7 (+2)	494 kDa
174	SEC31B	Protein transport protein Sec31B	Q9NQW1 (+1)	129 kDa
175	ARID2	AT-rich interactive domain-containing protein 2	Q68CP9 (+1)	197 kDa
176	ZNF638	Zinc finger protein 638	Q14966 (+2)	221 kDa
177	IBTK	Inhibitor of Bruton tyrosine kinase	Q9P2D0 (+1)	151 kDa
178	SIPA1L1	Signal-induced proliferation-associated 1-like protein 1	O43166 (+2)	200 kDa
179	FMR1	Fragile X mental retardation protein 1	Q06787 (+8)	71 kDa
180	SZT2	Protein SZT2	Q5T011 (+1)	378 kDa

181	FAT4	Protocadherin Fat 4	Q6V0I7 (+1)	543 kDa
182	UACA	Uveal autoantigen with coiled-coil domains and ankyrin repeats	Q9BZF9 (+1)	163 kDa
183	KMT2D	Histone-lysine N-methyltransferase 2D	O14686 (+1)	593 kDa
184	DNAH11	Dynein heavy chain 11, axonemal	Q96DT5	520 kDa
185	EFCAB5	EF-hand calcium-binding domain-containing protein 5	A4FU69 (+5)	173 kDa
186	NCAM2	Neural cell adhesion molecule 2	O15394	93 kDa
187	ZNF236	Zinc finger protein 236	Q9UL36 (+1)	204 kDa
188	SRPX	Sushi repeat-containing protein SRPX	P78539 (+4)	52 kDa
189	TACC3	Transforming acidic coiled-coil-containing protein 3	Q9Y6A5	90 kDa
190	DNAJA3	DnaJ homolog subfamily A member 3, mitochondrial	Q96EY1 (+1)	52 kDa
191	PES1	Pescadillo homolog	O00541 (+1)	68 kDa

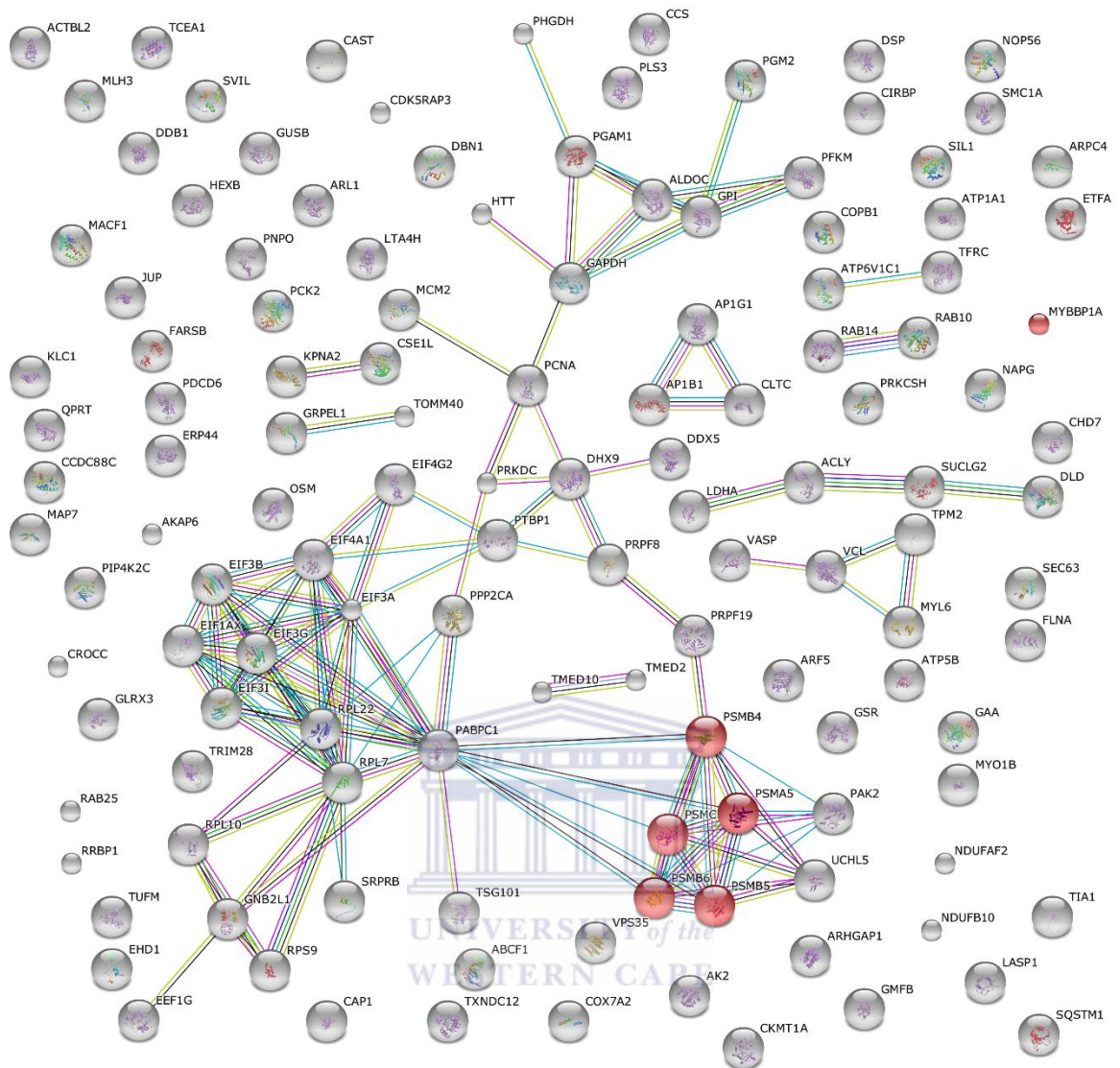


Figure A1: STRING analysis revealed 6 proteins (shown in red) associated with cell cycle arrest in up-regulated proteins (adapted from STRING).

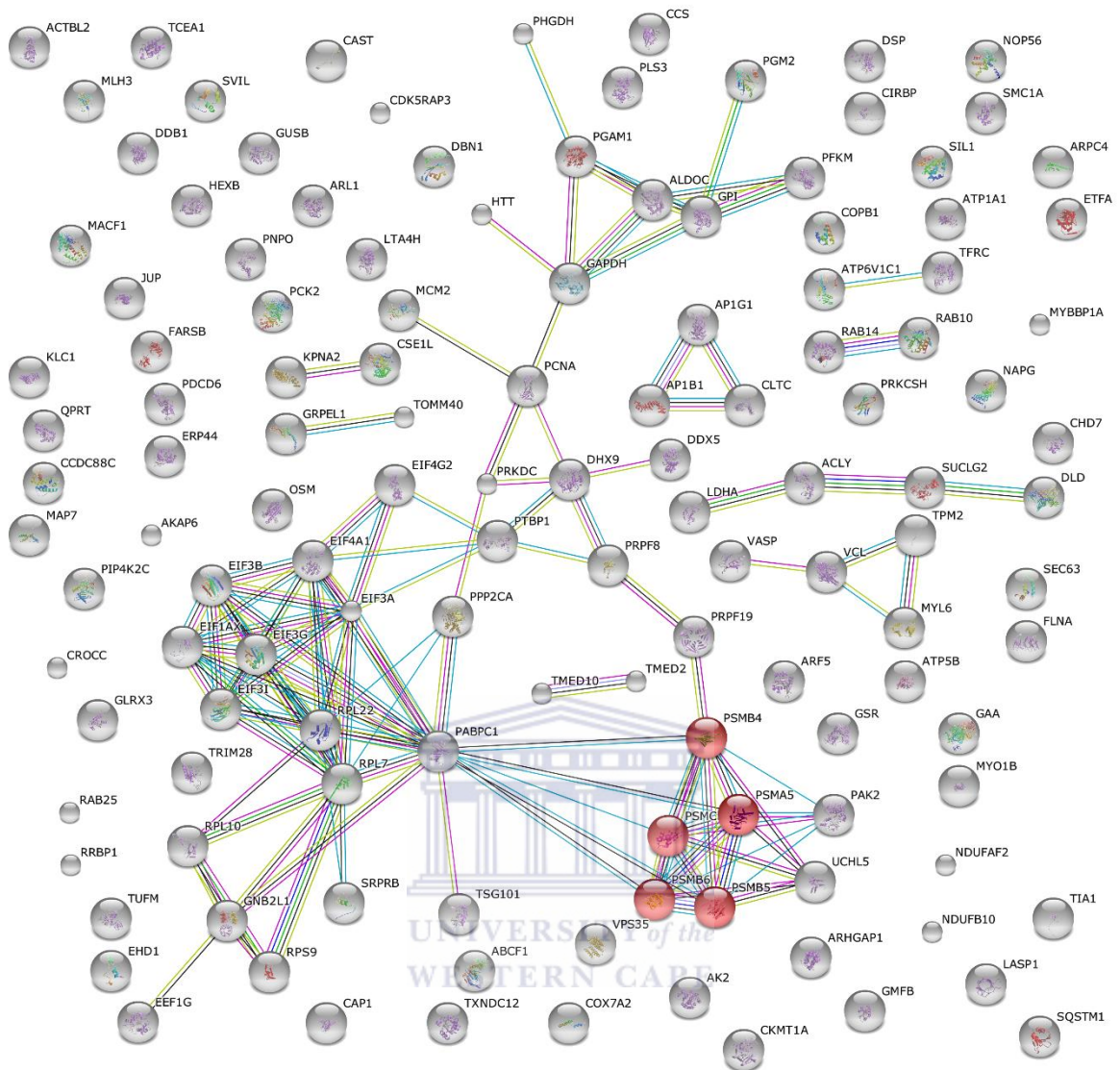


Figure A2: STRING analysis revealed 5 proteins (shown in red) associated with proteasomal degradation in up-regulated proteins (adapted from STRING).

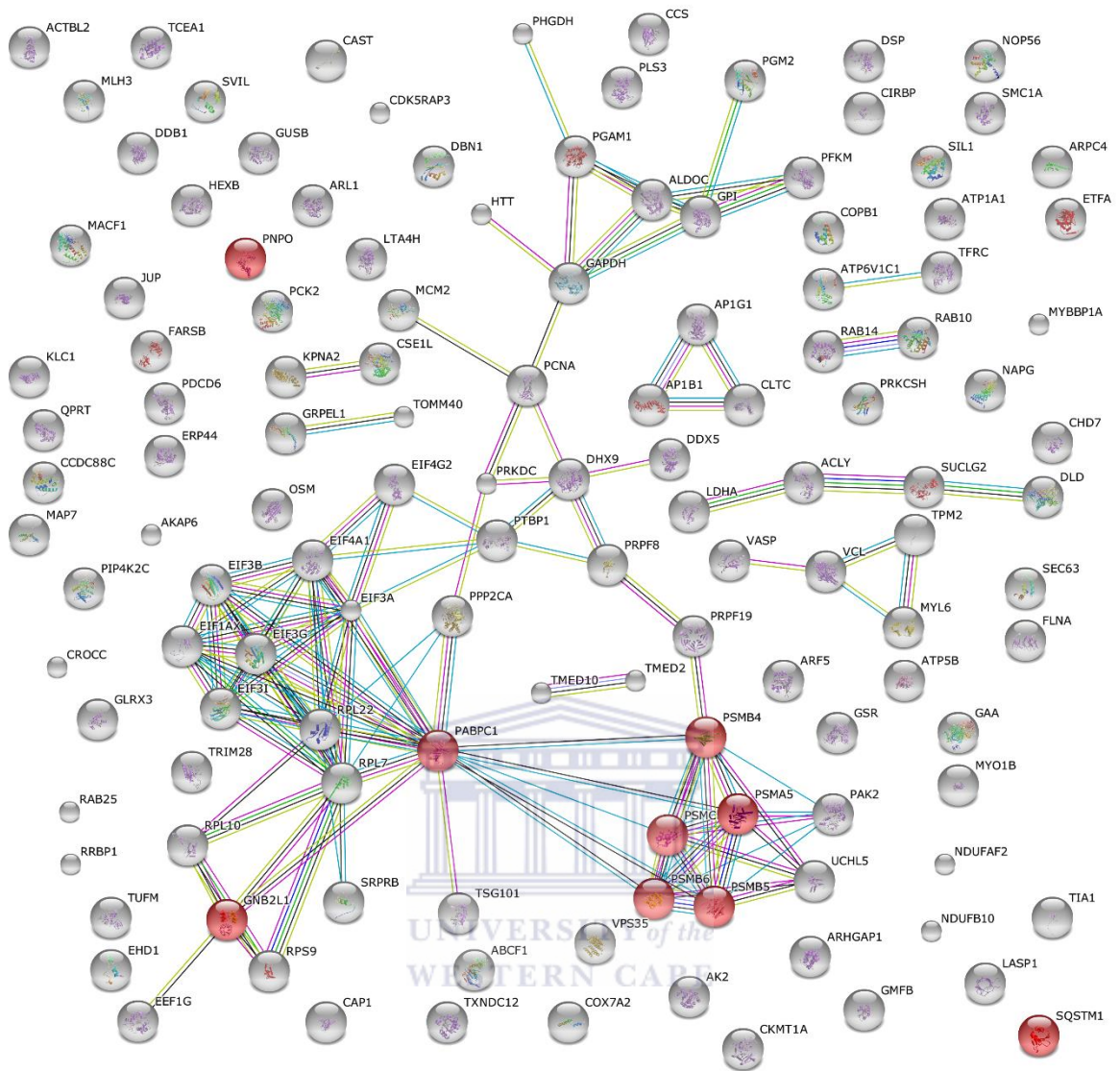


Figure A3: STRING analysis revealed 9 proteins (shown in red) associated with cellular catabolic process in up-regulated proteins (adapted from STRING).

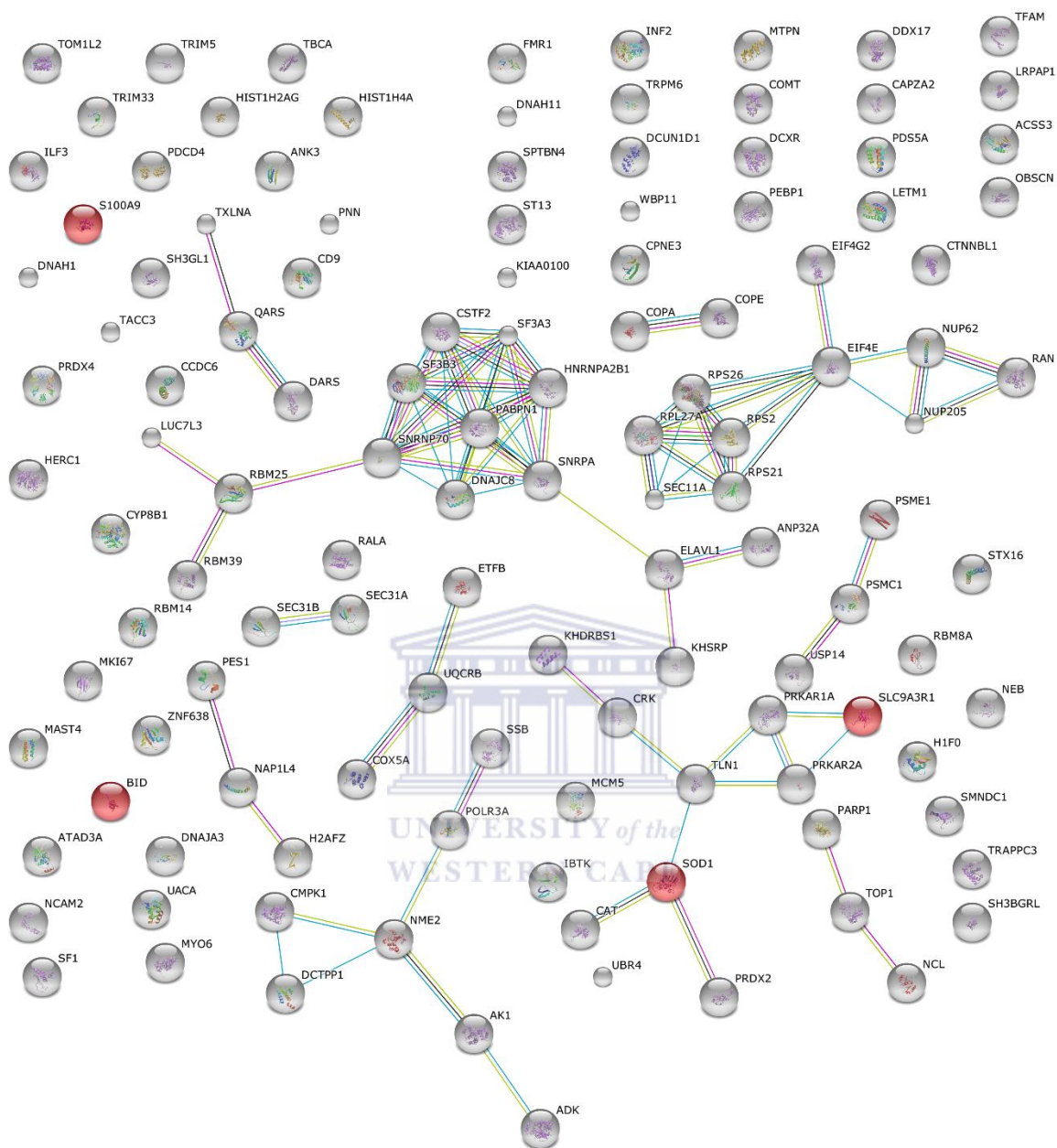


Figure A4: STRING analysis revealed 4 proteins (shown in red) associated with the intrinsic apoptotic pathway in down-regulated proteins (adapted from STRING).